

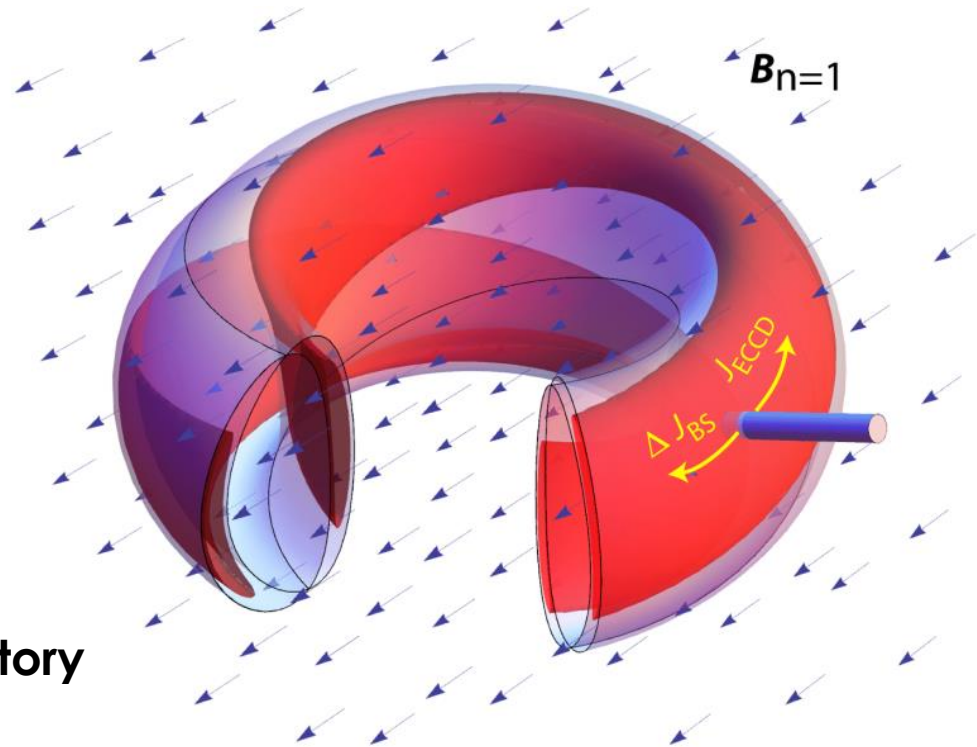
Prediction, Avoidance and Control of Disruptive Locked Modes in DIII-D and ITER

by
Francesco Volpe
Columbia University

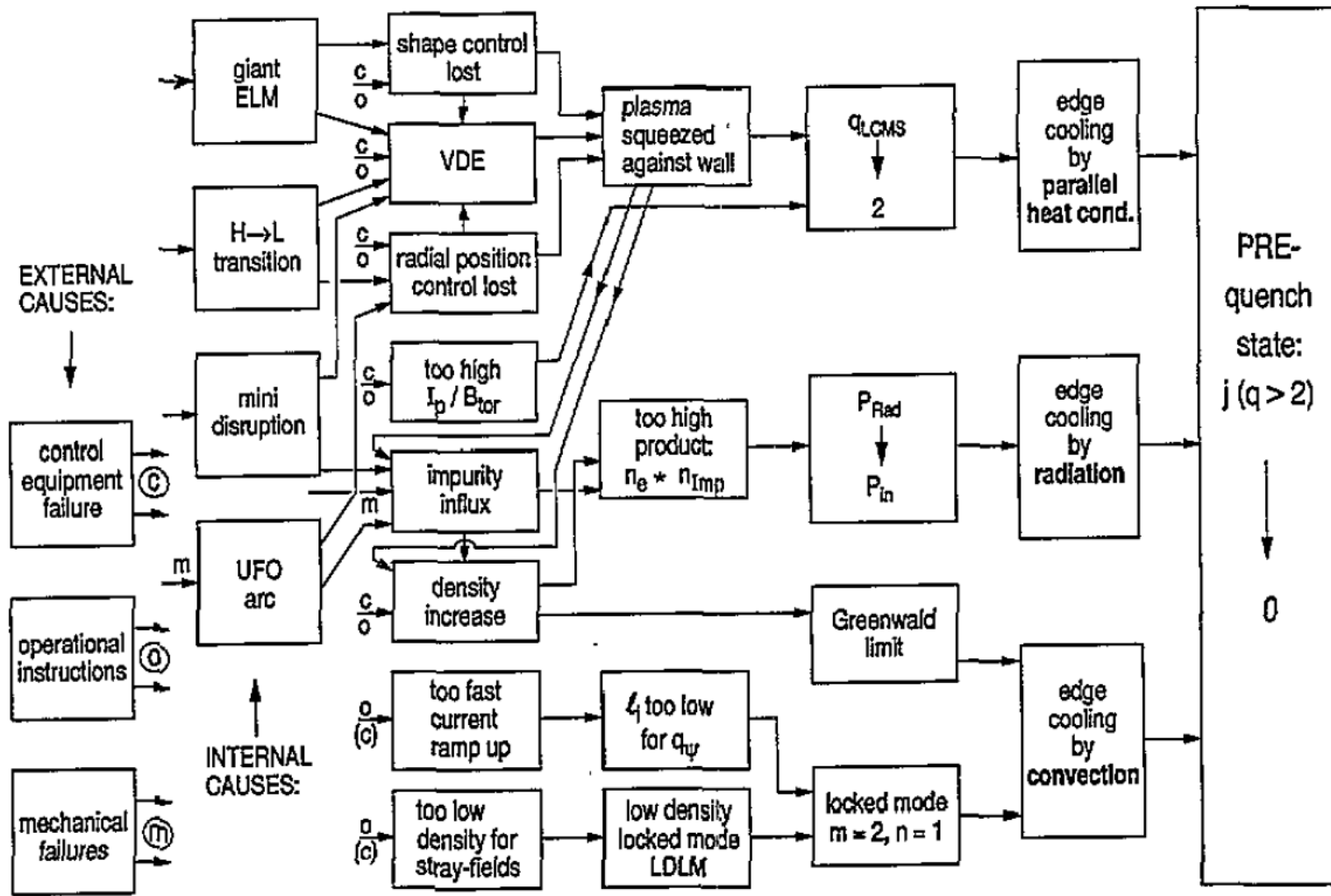
with
W. Choi, R. Sweeney, R.J. La Haye

Presented at the
IEA Theory and Simulation of
Disruptions Workshop

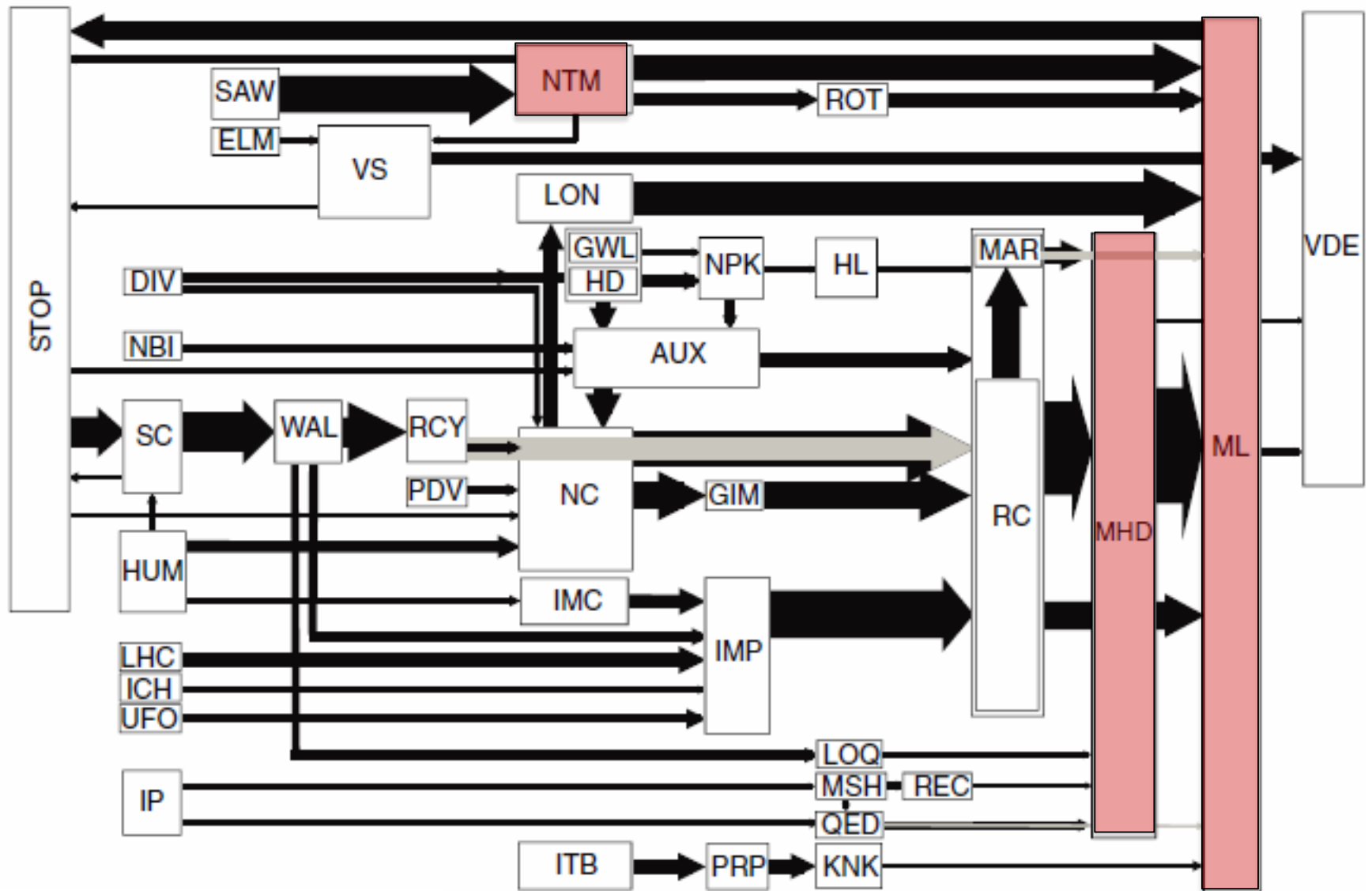
Princeton Plasma Physics Laboratory
Princeton, New Jersey
July 20-22, 2016



Locked islands cool plasma edge mostly by convection



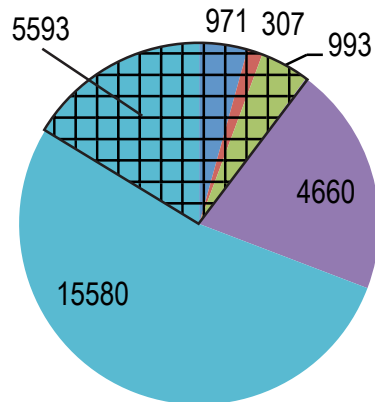
Nearly all JET disruptions eventually exhibit Mode Locking



More than a quarter of high β_N disruptions are due to IRLMs (fraction due to BLMs unknown)

(a)

Survey of 22511 plasma discharges



Shots with IRLM

- excluded IRLM
- non-disruptive IRLMs
- disruptive IRLMs

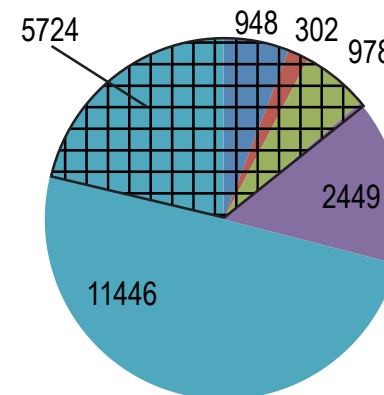
Shots without IRLM

- disruptions without LMs
- normal discharge

▨ 2/1 rotating NTMs

(b)

Survey of 16123 discharges of $\beta_N > 1.5$



Shots with IRLMs

- excluded IRLM
- non-disruptive IRLMs
- disruptive IRLMs

Shots without IRLMs

- disruptions without LMs
- normal discharges

▨ 2/1 rotating NTMs

- Study performed on shots 122000 to 159837 (2005 to 2014)
- 28% of all disruptions in shots with peak $\beta_N > 1.5$ are due to IRLMs, compared with 18% for all peak β_N
- Born locked modes not considered in this work

Outline

- **Prediction**

- Database of Locked Modes at DIII-D
 - Typical evolution, including deceleration, saturation, final growth
 - When do they cause disruptions?
 - How do they cause Thermal Quench?
- When do they lock?
 - Solve Eq. of Motion
 - Future work: couple with Modified Rutherford Eq.

- **Avoidance & Control**

- Static or rotating RMPs + ECCD → disruption avoidance
- Preemptive entrainment → locking avoidance
- Feedback controller of locked mode phase
- Magnetic control in present devices (ITPA, WG-11)
- Modeling for ITER

- **Prediction**

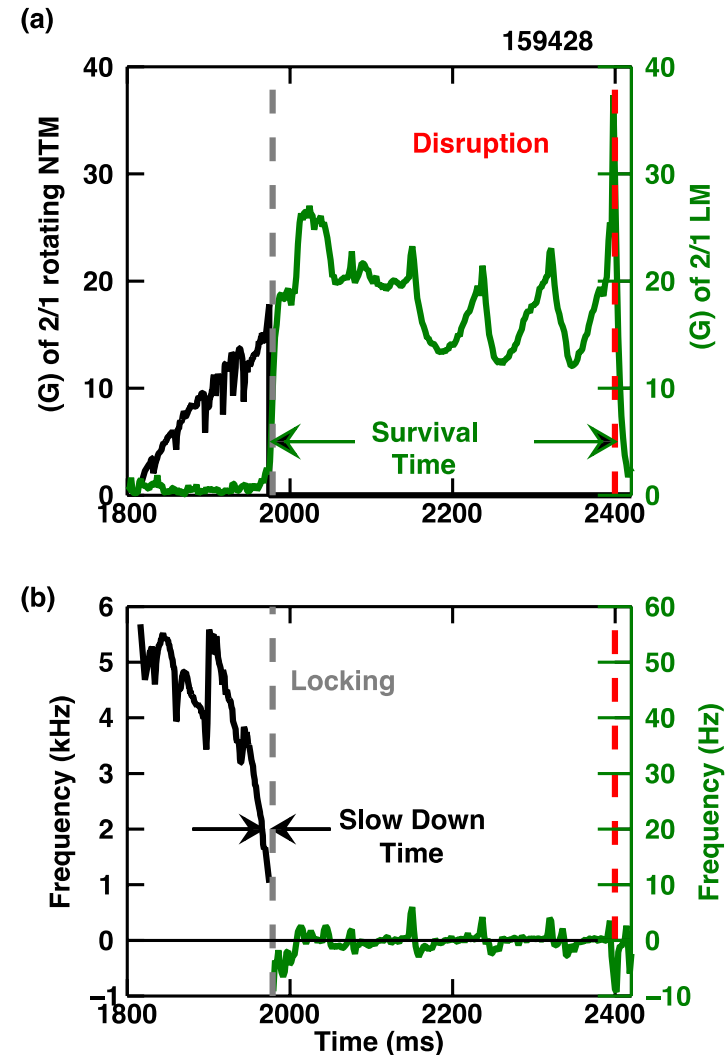
- Database of Locked Modes at DIII-D
 - Typical evolution, including deceleration, saturation, final growth
 - When do they cause disruptions?
 - How do they cause Thermal Quench?
- When do they lock?
 - Solve Eq. of Motion
 - Future work: couple with Modified Rutherford Eq.

- **Avoidance & Control**

- Static or rotating RMPs + ECCD → disruption avoidance
- Preemptive entrainment → locking avoidance
- Feedback controller of locked mode phase
- Magnetic control in present devices (ITPA, WG-11)
- Modeling for ITER

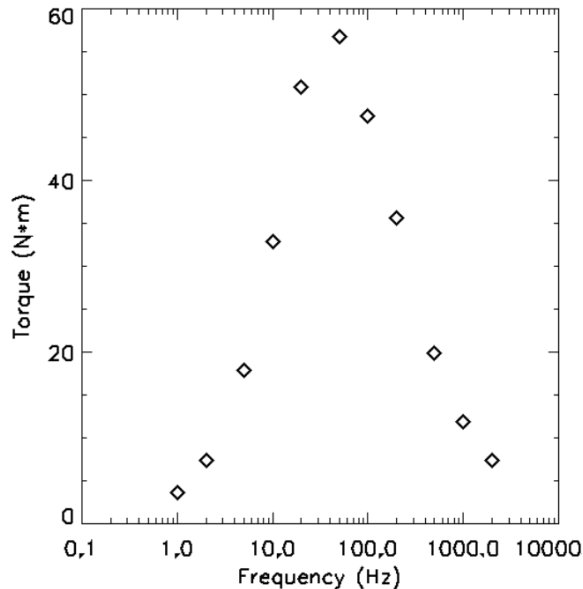
Example of an initially rotating locked mode (IRLM)

1. $m/n = 2/1$ rotating mode
2. Mode locks
3. Exists as locked mode
 - Few to thousands of milliseconds
 - Referred to as **survival time** for disruptive IRLMs
4. Disrupts or...
...ceases to be a locked mode
 - decays
 - or spins up

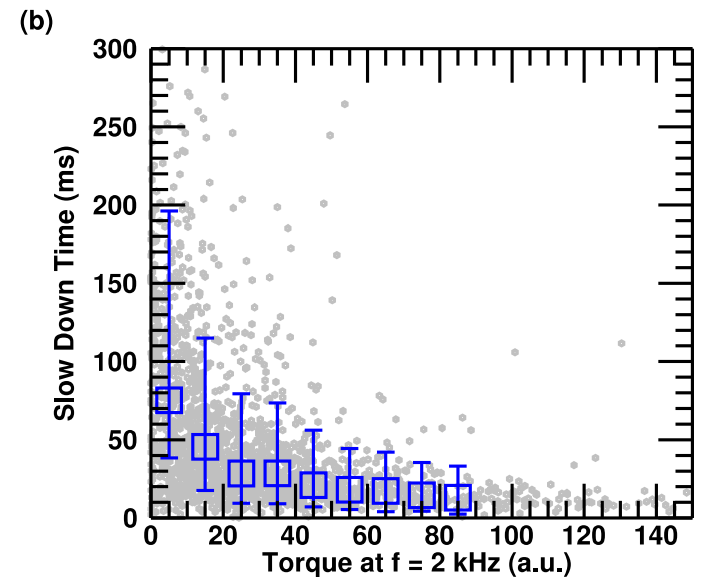
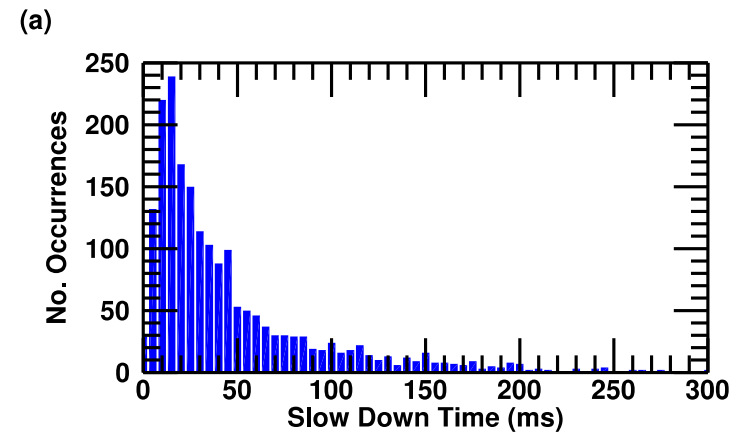


66% of 2/1 NTMs rotating at 2 kHz will lock in 45 ± 10 ms

- **Slow down time = time between 2 kHz rotation and locking**



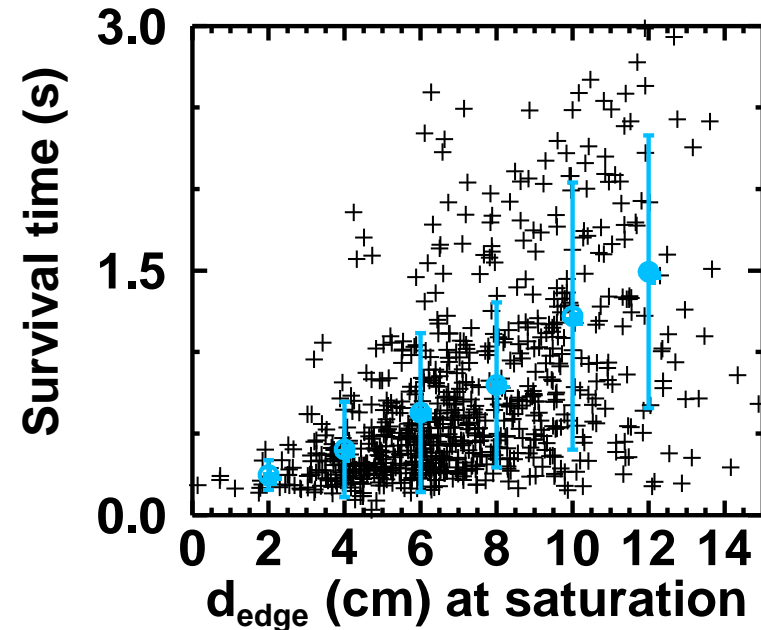
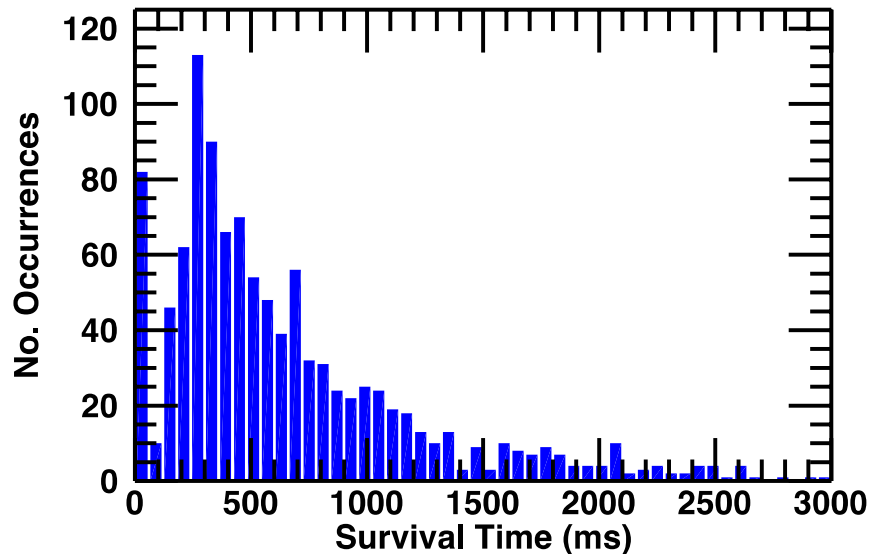
- **Indication of time available to prevent locking**
- **Larger T_{wall} results in shorter slow-down time**



Disruptive IRLMs most frequently survive 270 ± 60 ms

- *Survival time* = time between locking and disruption
- 66% of disruptive modes terminate between 150 to 1010 ms

Distribution of 1011 LM/QSM Events

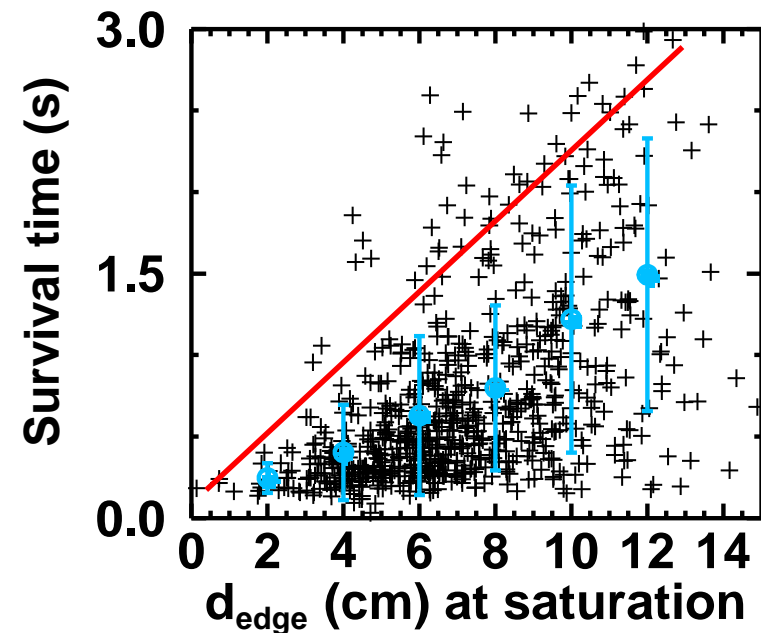


Disruptive IRLMs with small d_{edge} do not survive long

- d_{edge} might pertain to physics of the thermal quench onset

| Parameter | Correlation with t_s |
|-----------------|------------------------|
| d_{edge} | 0.47 |
| ρ_{q2} | -0.42 |
| l_i/q_{95} | -0.39 |
| q_{95} | 0.36 |
| β_p | 0.34 |
| $dq/dr(r_{q2})$ | -0.15 |
| l_i | -0.11 |
| w | 0.10 |
| δI | -0.01 |

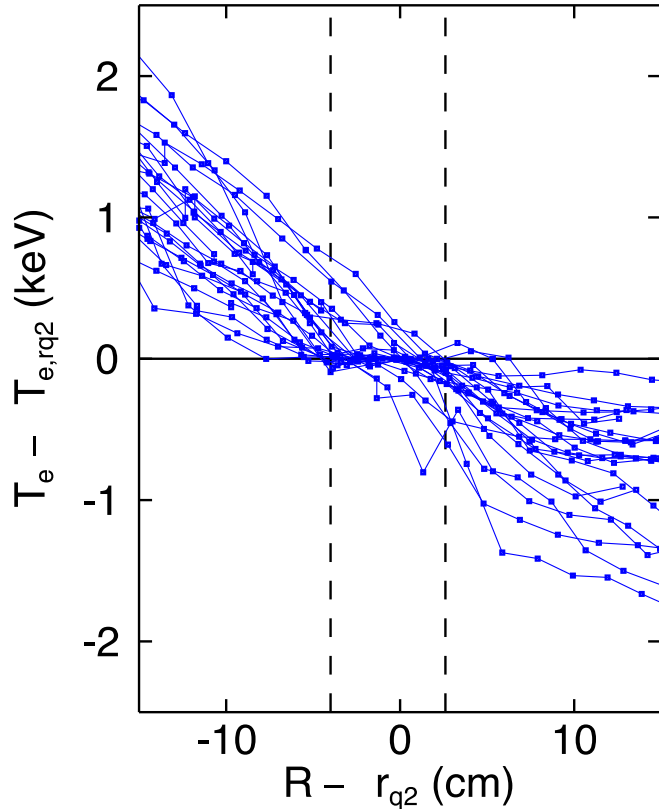
Decreasing abs. value



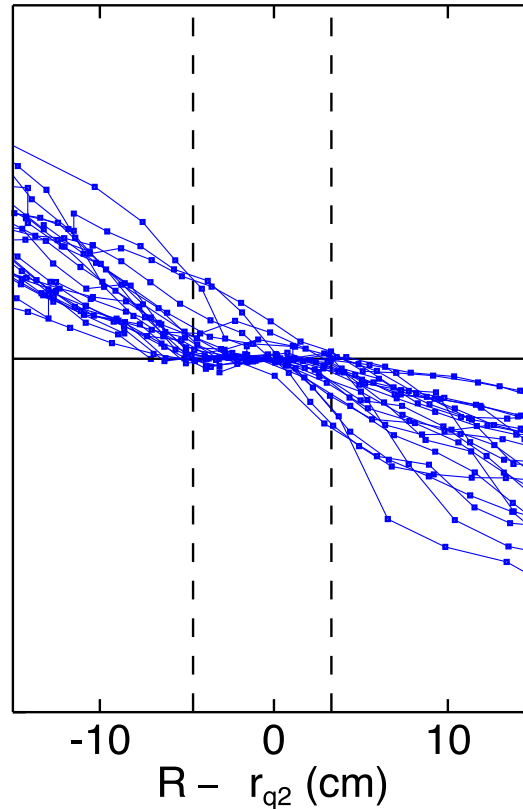
$$\text{IRLM Disruptivity} = \frac{\text{Number of disruptive IRLMs}}{\text{Number of IRLMs}}$$

Disruptive 2/1 widths at ≥ 20 ms prior to the *disruption* are similar to non-disruptive at 100 ms before *decay/spin-up*

24 Disruptive IRLMs

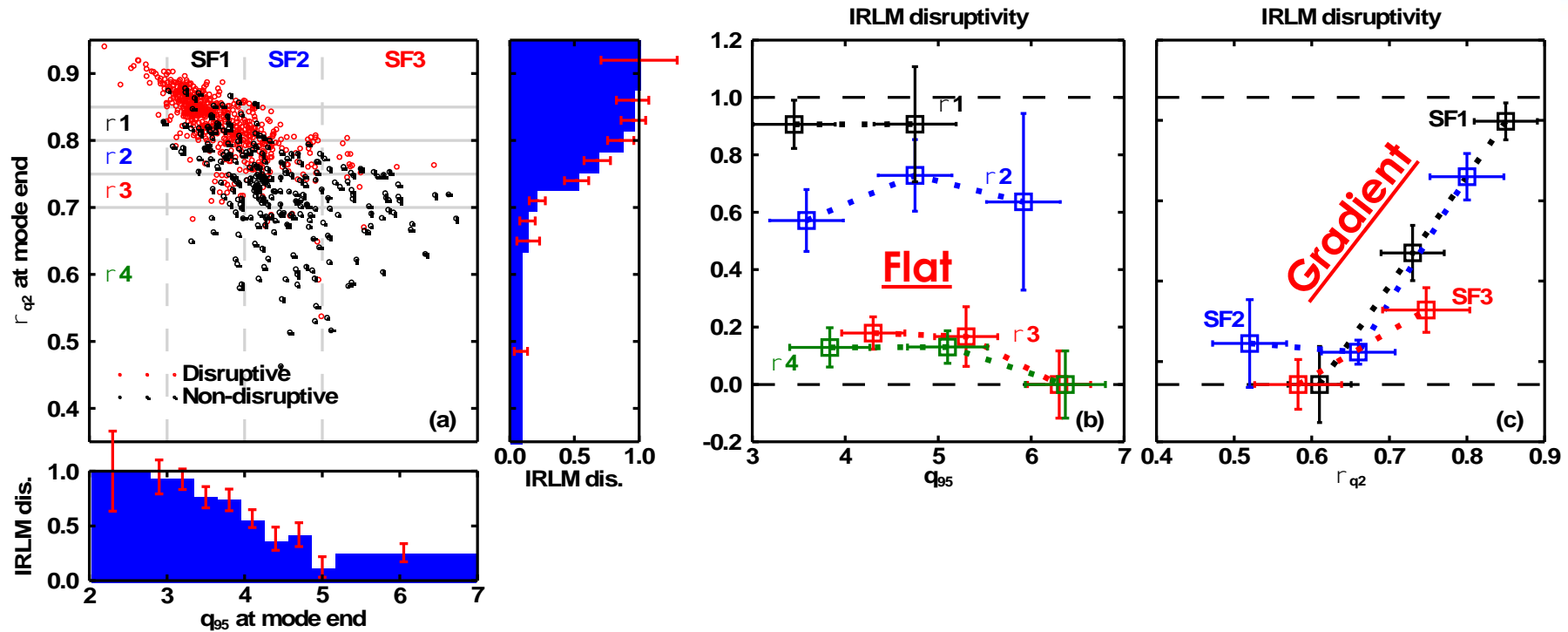


23 Non-disruptive IRLMs



- T_e from Electron Cyclotron Emission (ECE) diagnostic
- Island O-point aligned with ECE in all profiles
- Flattening at $q=2$ shows similar widths

IRLM disruptivity scales strongly with normalized $q=2$ radius ρ_{q2} (fixing q_{95}), and weakly with q_{95} (fixing ρ_{q2})



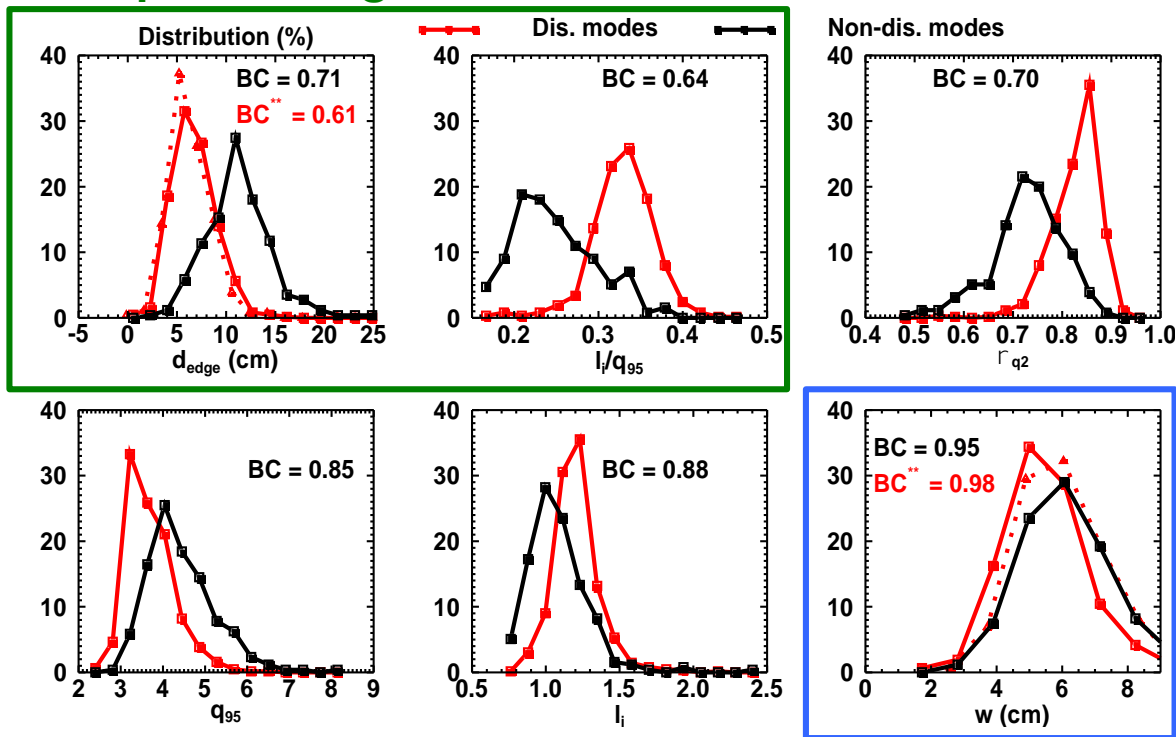
(a) In 1D projections (blue histograms), IRLM disruptivity appears to depend on both ρ_{q2} and q_{95}

(b) Fixing ρ_{q2} shows that IRLM disruptivity scales weakly with q_{95}

(c) Fixing q_{95} shows IRLM disruptivity depends strongly on ρ_{q2}

Bhattacharyya Coefficient informs on best and worst separators

Best performing



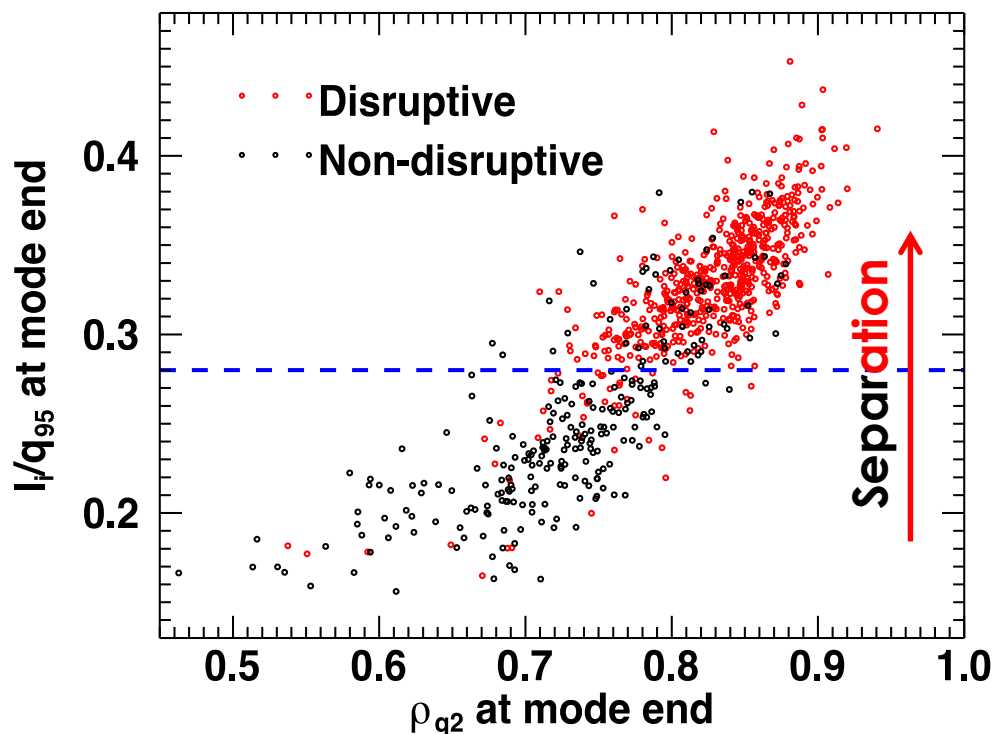
Poor separation (solid is 100 ms prior to disruption, dotted is 20 ms prior)

For discrete probability distributions p and q parameterized by x , the BC value is given by,

$$BC = \sum_{x \in X} \sqrt{p(x)q(x)}$$

- $BC=0$ means p and q do not overlap
- $BC=1$ means p and q are identical (completely overlapping)

ρ_{q2} is highly correlated with l_i/q_{95} , but the latter separates disruptive from non-disruptive IRLMs better



*Mode end here is 100 ms prior to mode termination

$$\frac{l_i}{q_{95}} = \alpha \rho_{q2} + c$$

where $\alpha = 0.67 \pm 0.01$ and $c = -0.23 \pm 0.01$

← Separation is predominantly vertical

- Correlation of $r_c = 0.87$
- l_i/q_{95} is likely a proxy for classical stability (Δ')

IRLM disruptions might be explained by Δ' becoming marginal, or unstable, as a result of the increasing I_i

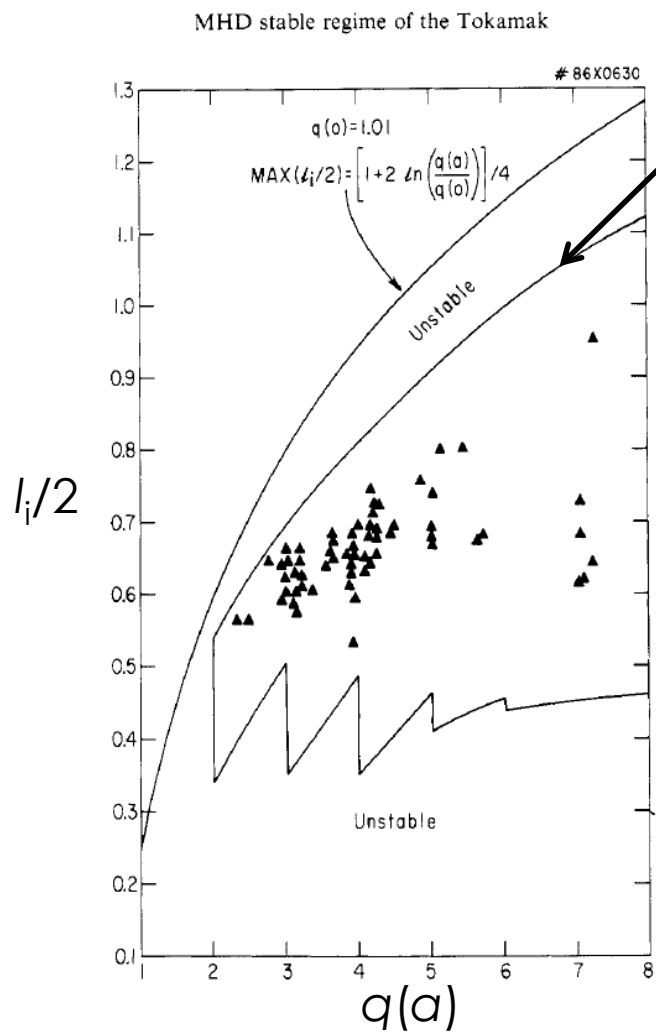
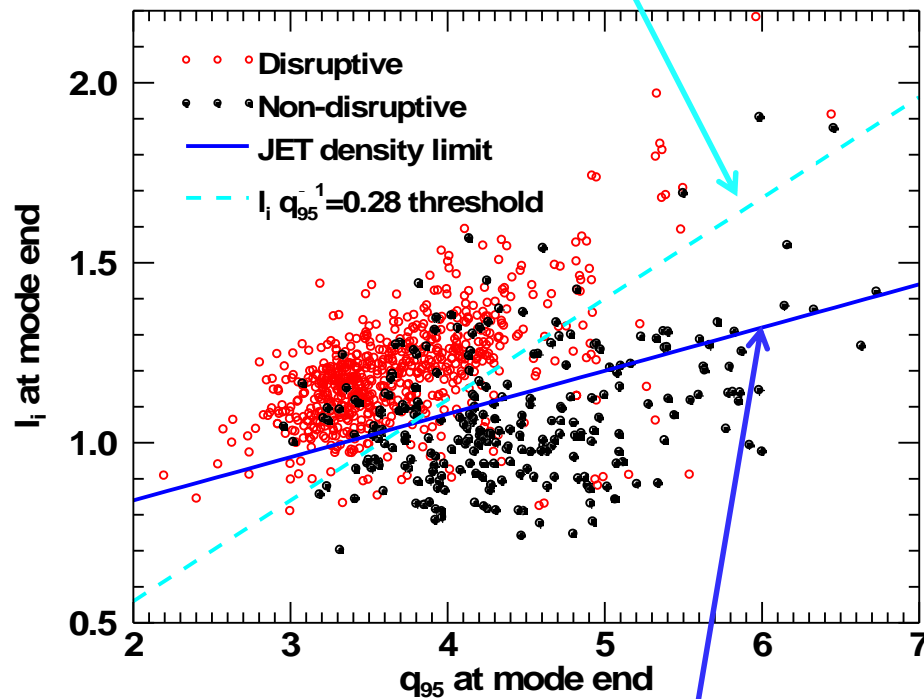


FIG. 4.—The range of permissible internal inductance $I_i/2$ as a function of $q(a)$ for $q(0) = 1.01$ is contained by a jig-saw boundary. The maximum $I_i/2$, which corresponds to a uniform current profile up to $r/a = [q(0)/q(a)]^{1/2}$, is also shown. Steady-state data from TFTR operations are found to fall inside the permissible domain.

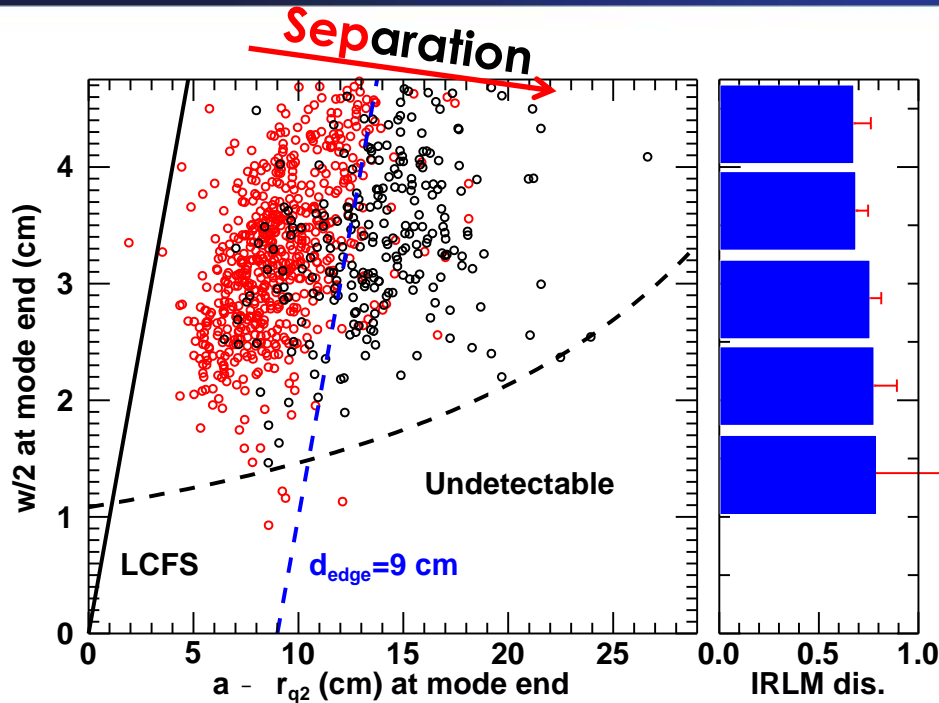
- Theoretical stability limit for tearing mode onset [Cheng, Furth, Boozer PPCF 1987]
- Limit for IRLM disruptions in DIII-D



- Limit for high-density disruptions in JET [Wesson, NF 1989]



A parameter measuring how near the island is to the 2D last closed flux surface also appears disruption relevant



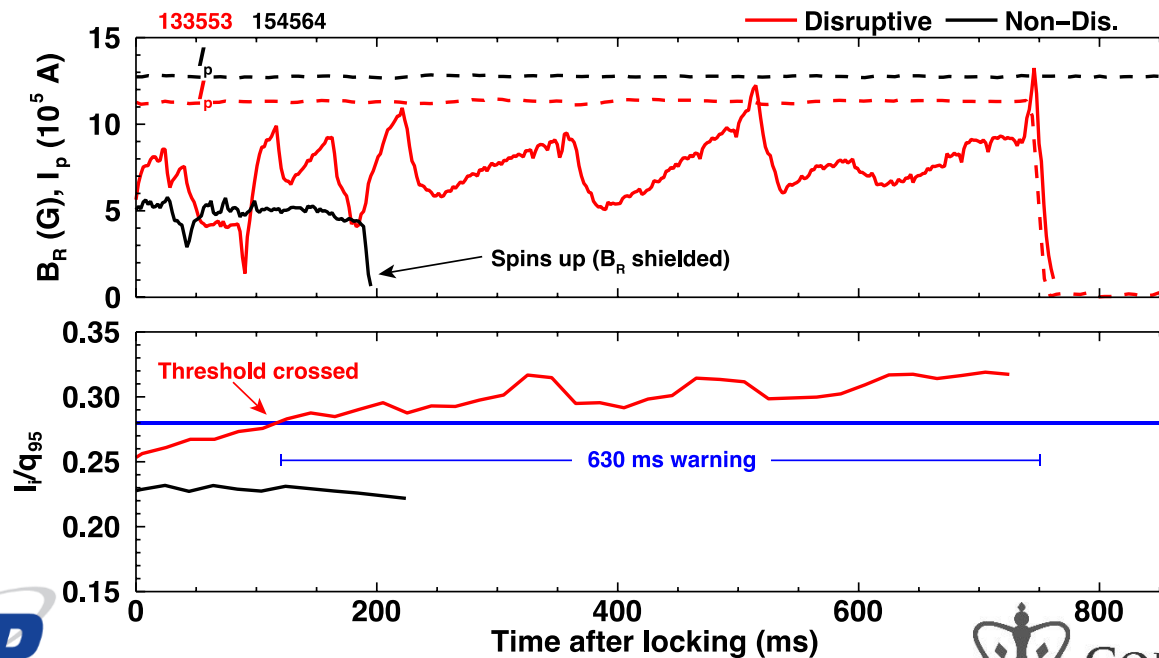
$$d_{edge} = a - (r_{q2} + w/2)$$

- a plasma minor radius
- r_{q2} minor radius of the $q=2$ surface
- w island width
- Mode end 20 ms for disruptive, 100 ms for non-disruptive

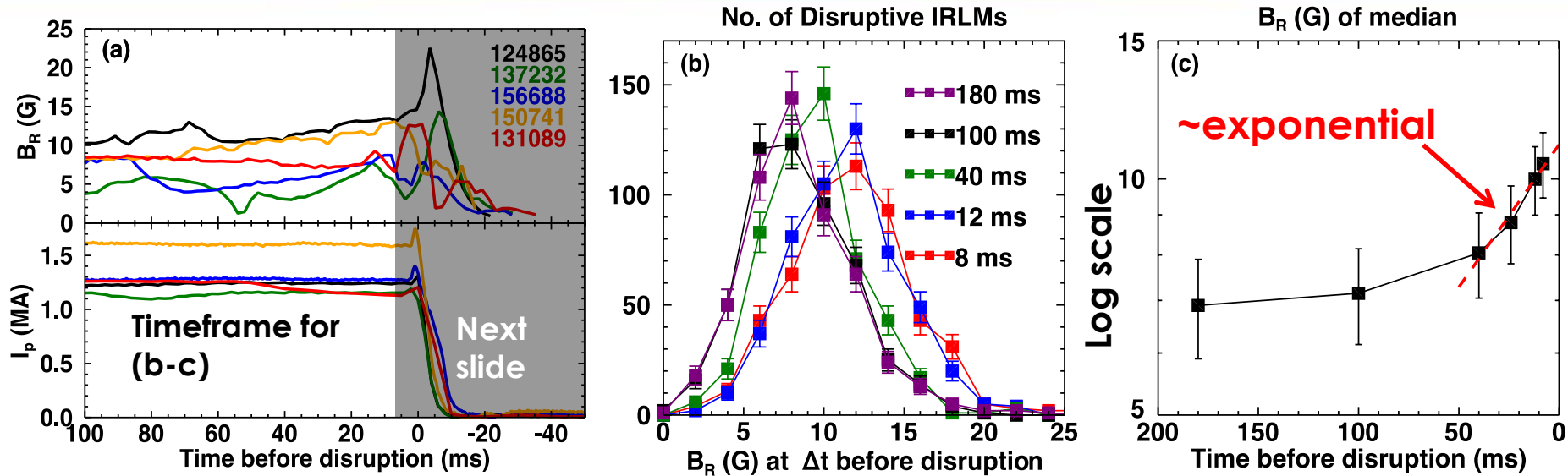
- d_{edge} best separates during the exponential growth; note this assumes the $n=1$ growth is 2/1
- Even assuming 2/1 growth, IRLM disruptivity up to 20 ms before the disruption scales weakly with island width (blue histogram)

I_i/q_{95} and d_{edge} can be used for disruption prediction

| Condition with IRLM | Missed disruptions (%) at 100 [20] ms | False alarms (%) |
|--|---------------------------------------|------------------|
| $\frac{I_i}{q_{95}} > 0.28$ | 6 [6] | 13 |
| $d_{edge} < 9$ cm | 6 [4] | 14 |
| None (i.e. all LMs assumed disruptive) | 0 [0] | 29 |

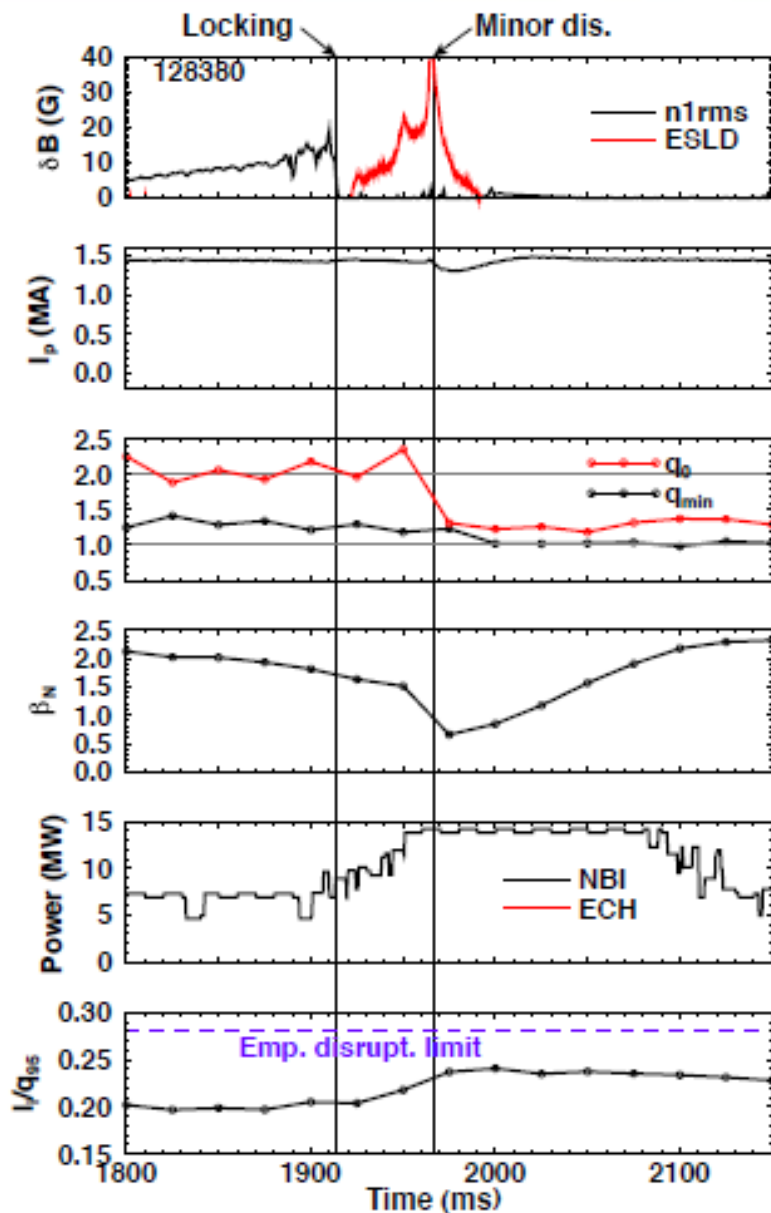


From 100 to a few milliseconds before the thermal quench, the $n=1$ field typically grows



- **(a)** Most IRLMs show increasing $n=1$ field within 100 ms of disruption (5 random IRLMs)
- **(b)** Distributions of $n=1$ field shift higher as disruption approached
- **(c)** Median of (b) grows exponentially in last 50 ms
- Preliminary results suggest m is often even during growth

Some LMs self-stabilize through minor disruptions. Typically high q_{\min} (>2? Double LMs?)



Probably classically stable,
neoclassical unstable.

- ▶ "Hiccup" in I_p
- ▶ q_0 drops at minor disruption
- ▶ Significant drop in β_N
- ▶ Beams appear in feedback
- ▶ I_i/q_{95} below empirical disruption limit

So far, multidimensional scaling confirms I_i/q_{95} as best predictor of LM disruption

| Power law | Technique | Opt. power law | BC Value |
|---|-----------|--|-----------------|
| [current profile] $q_{95}^a \rho_{q2}^b I_p^c q_{min}^d q_0^e I_i^f \left(\frac{dq}{dr}\right)^g$ | discrete | $\left(\frac{I_i}{q_{95}}\right)^2 \left(\frac{q_0}{q_{min}^2}\right) \rho_{q2} I_p$ | 0.62 ± 0.04 |
| same as above | discrete | $\left(\frac{I_i}{q_{95}}\right)^2 \frac{\rho_{q2} I_i}{q_{min}}$ | 0.62 ± 0.04 |
| I_i^a / q_{95} | amoeba | $I_i^{1.09 \pm [0.16, 0.11]} / q_{95}$ | 0.61 ± 0.04 |
| [pressure profile] $r_{q2}^\alpha a^b \rho_{qmin}^c q_{min}^d \beta_N^e I_p ^f B_T ^g$ | discrete | $r_{q2}^3 a^{-2} q_{min}^{-1}$ | 0.66 ± 0.04 |
| $(a - I_i/q_{95})^b d_{edge}^c$ | amoeba | $(4.5 - I_i/q_{95})^{2.9} d_{edge}^{0.12}$ | 0.57 ± 0.04 |

Main Conclusions from Locked Mode Database, so far

- 1. Two parameters separate disruptive from non-disruptive IRLMs well:**
 1. I_i/q_{95} (might be a proxy for classical stability)
 2. d_{edge} (a small value also implies a short survival time)
- 2. The $n=1$ field grows ~exponentially within 50 ms of the disruption**
 1. Preliminary study suggests m is often even
- 3. The thermal quench might be triggered by a sudden widening of the T_e flattening at $q=2$**
 1. Qualitative result of tens of inspected discharges
- 4. IRLMs change the plasma equilibrium by**
 1. Peaking the current profile
 2. Degrading β_N

- **Prediction**

- Database of Locked Modes at DIII-D
 - Typical evolution, including deceleration, saturation, final growth
 - When do they cause disruptions?
 - How do they cause Thermal Quench?
- **When do they lock?**
 - Solve Eq. of Motion
 - Future work: couple with Modified Rutherford Eq.

- **Avoidance & Control**

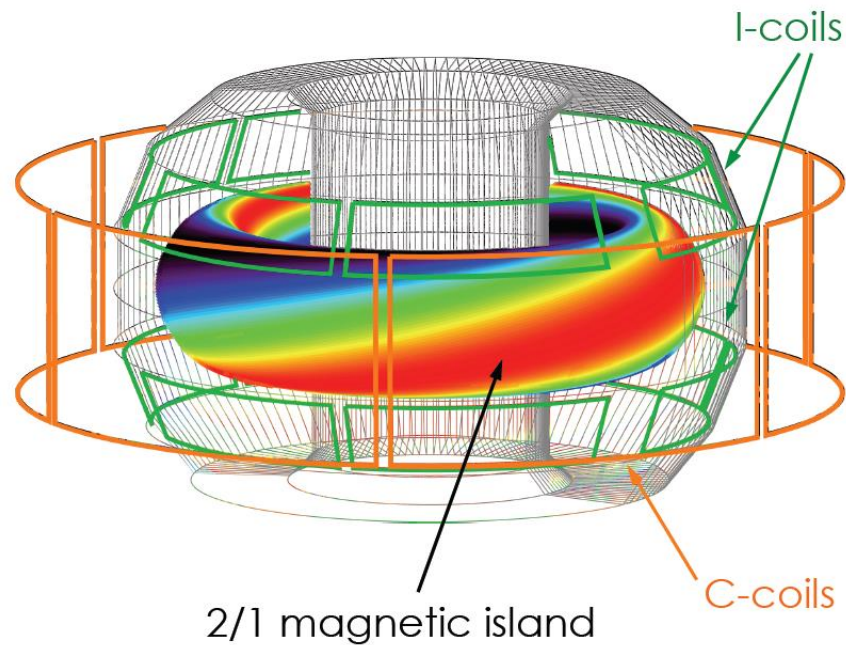
- Static or rotating RMPs + ECCD → disruption avoidance
- Preemptive entrainment → locking avoidance
- Feedback controller of locked mode phase
- Magnetic control in present devices (ITPA, WG-11)
- **Modeling for ITER**

Modeling effect of rotating RMPs on locked or nearly-locked mode

$$I \frac{d^2 \phi}{dt^2} = \boxed{T_{wall} + T_{EF} + T_{RMP} + T_{TM}} + \boxed{T_{visc} + T_{NBI}}$$

E.M. Torques on Island

Other Torques



Modeling effect of rotating RMPs on locked or nearly-locked mode

$$I \frac{d^2 \phi}{dt^2} = \boxed{T_{wall} + T_{EF} + T_{RMP} + T_{TM}} + \boxed{T_{visc} + T_{NBI}}$$

E.M. Torques on Island

Other Torques

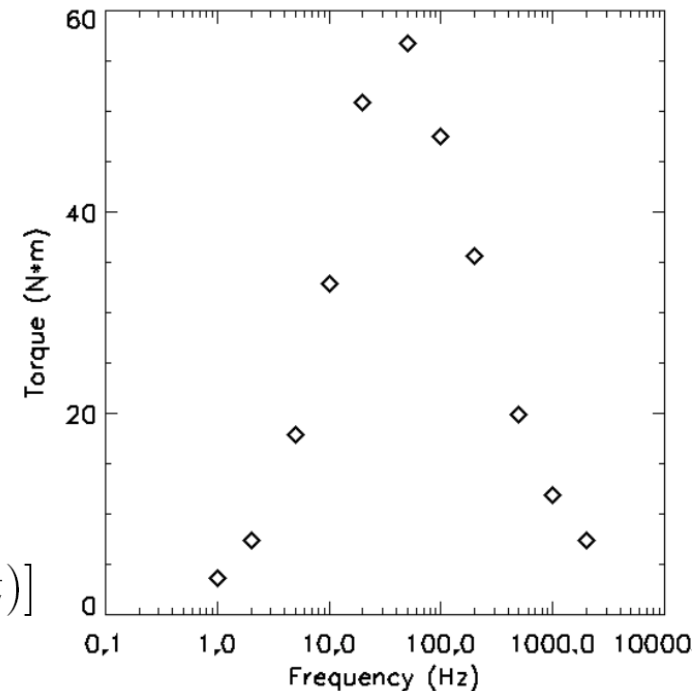
$$I_h = \pm 2 |B_R(b)| b \left(\frac{b}{r_{mn}} \right)^m \frac{1}{m \mu_0}$$

$$T_{wall} = - \frac{[2\pi R \boxed{B_R(b)} r_{mn}]^2}{\mu_0 b} \left[\frac{r_{mn}}{b} \right]^{2m-1} \frac{\boxed{\Omega \tau}}{1 + \boxed{(\Omega \tau)^2}}$$

$$T_{EF} = -\pi^2 R^2 m \frac{a}{r_{mn}} \boxed{I_{EF} B_R(a)} \sin[n\phi(t)]$$

$$T_{RMP} = -\pi^2 R^2 m \frac{b}{r_{mn}} \boxed{I_{RMP} B_R(b)} \sin[n\phi(t) - n\phi_{RMP}(t)]$$

$$T_{TM} = -\pi^2 R^2 m \sum_{m', n'} \frac{r_{m'n'}}{r_{mn}} \sin[n\phi(t)] I_{m'n'} B_R[r_{m'n'}]$$



Modeling effect of rotating RMPs on locked or nearly-locked mode

$$I \frac{d^2 \phi}{dt^2} = \boxed{T_{wall} + T_{EF} + T_{RMP} + T_{TM}} + \boxed{T_{visc} + T_{NBI}}$$

E.M. Torques on Island

Other Torques

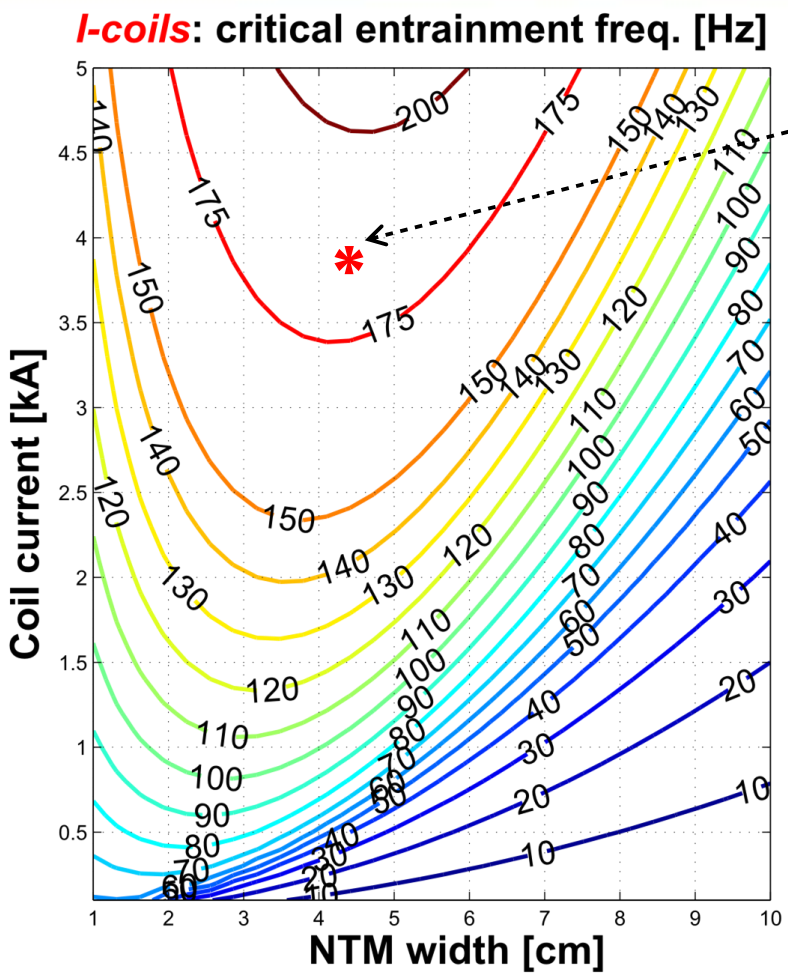
Simplified equation of motion (next slides)

$$I \frac{d^2 \phi}{dt^2} = T_{wall} + T_{EF} + T_{RMP}$$

Condition for smooth entrainment (next slides)

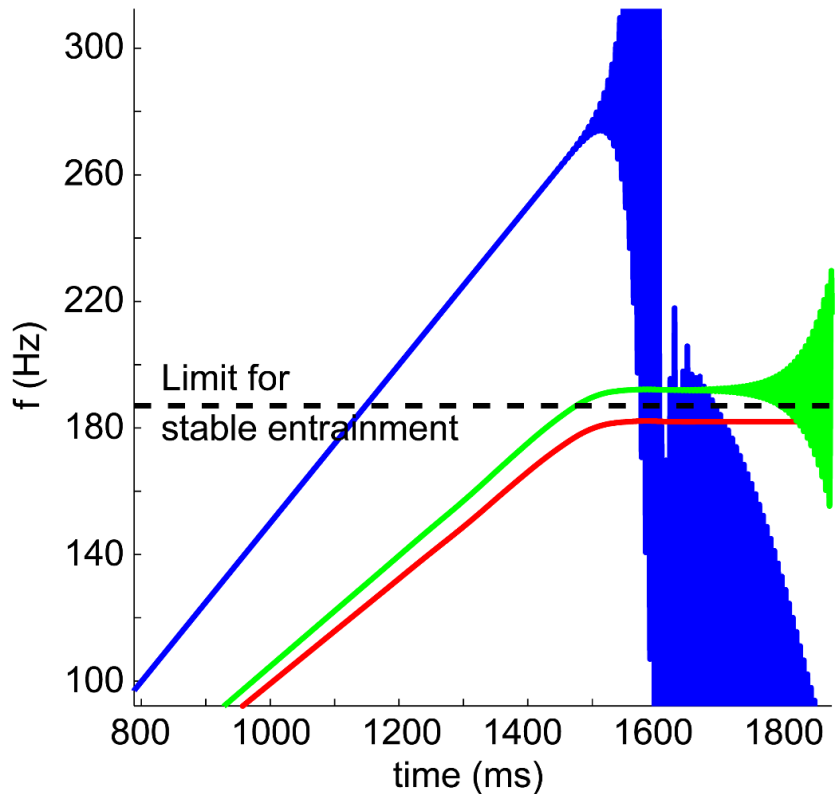
$$0 = T_{wall} + T_{RMP}$$

Entrainment can be lost due to failure of applied torque to counteract braking torque from the wall at high frequency



W = 4cm
I = 4 kA
I-coils

→ **SPEED LIMIT 187**

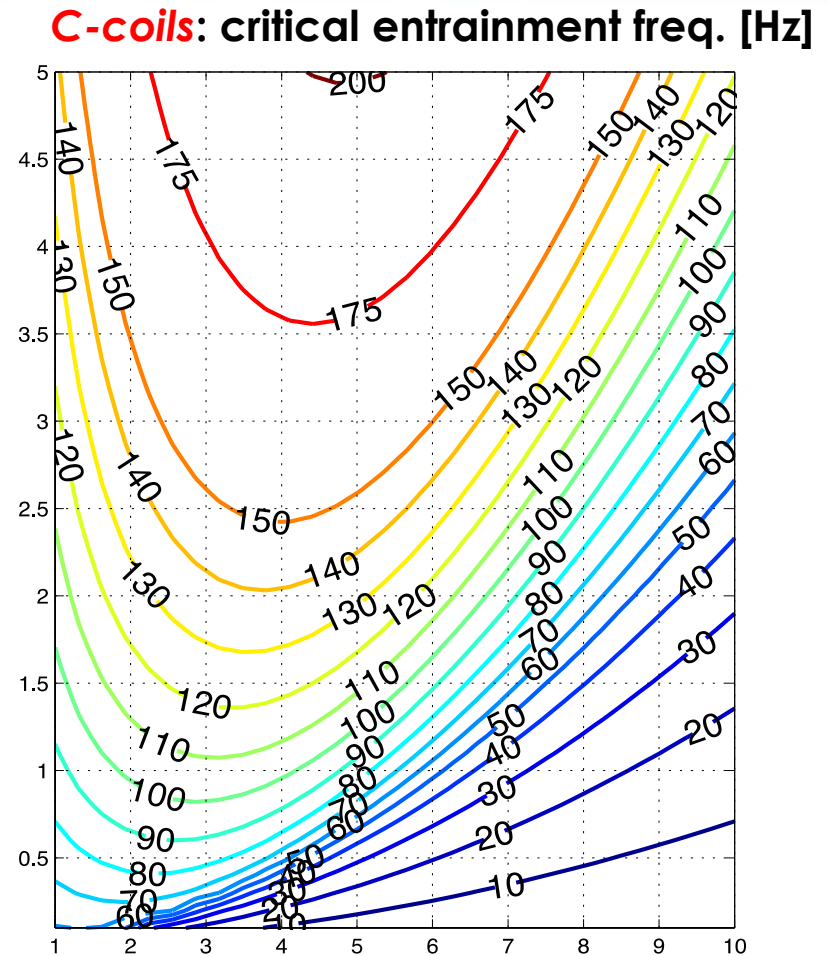
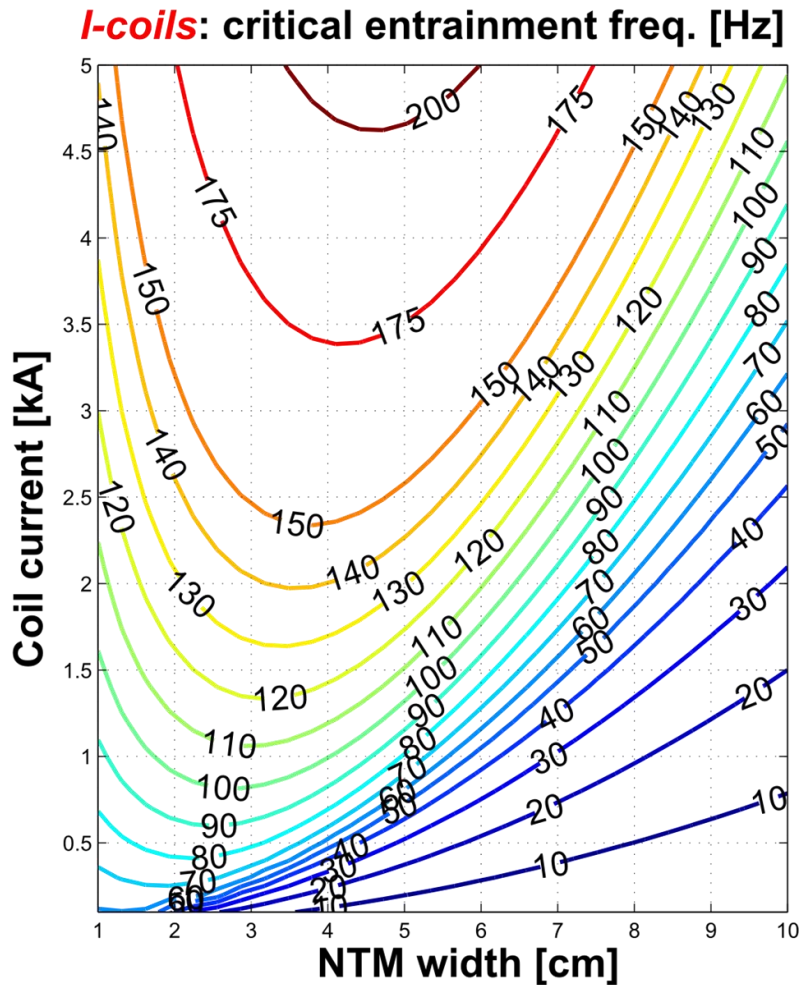


Max frequency increases with coil current and decreases with island width



K.E.J. Olofsson PPCF 2016

Entrainment with C-coils have lower critical frequency due to being external to the vessel

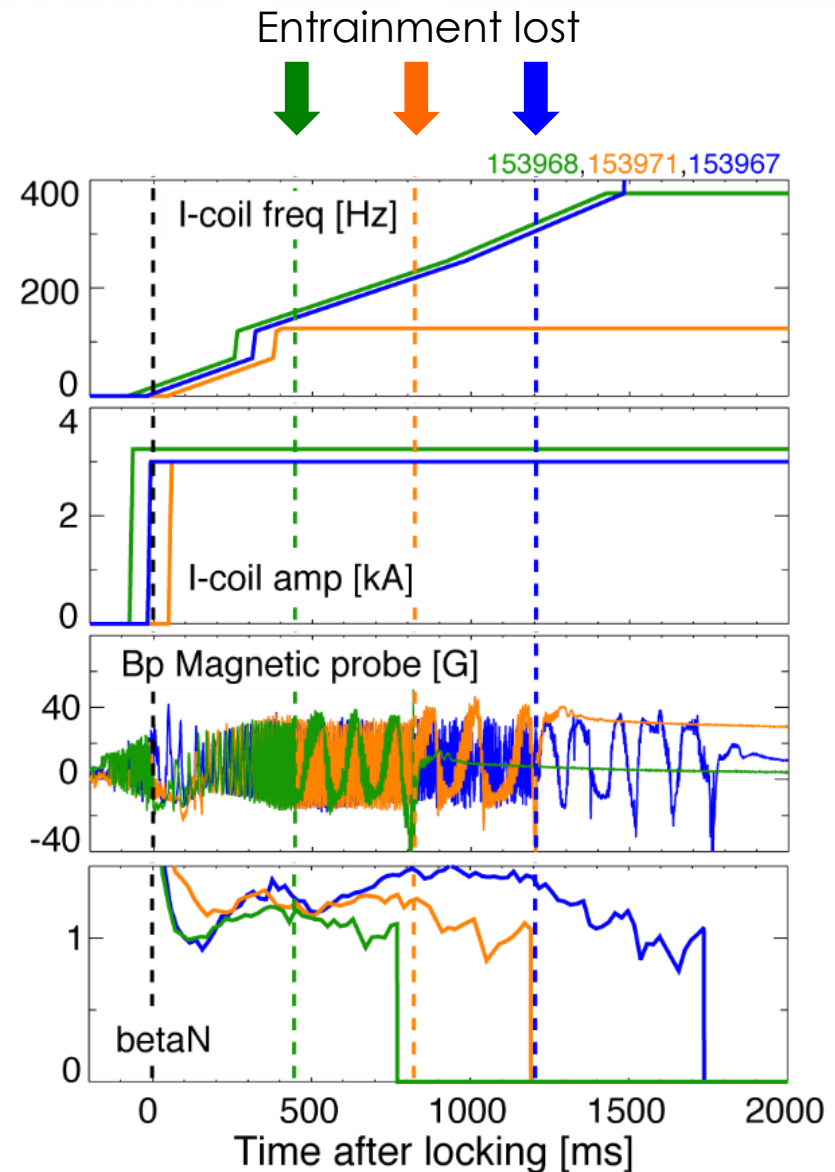


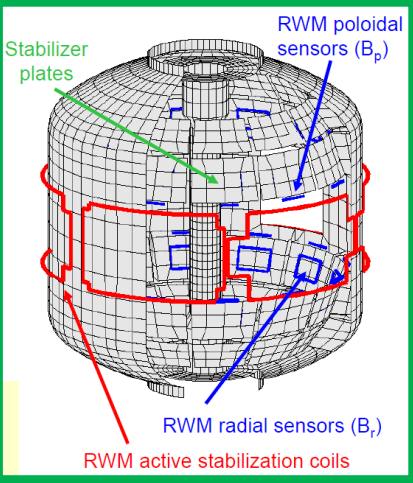
Max frequency increases with coil current and decreases with island width.

K.E.J. Olofsson PPCF
2016

Loss of entrainment is more complicated than a simple loss of torque balance

- Entrainment lost at different times and frequencies in similar discharges.
 - Possibly due to MHD events.
- Entrainment depends not just on coil currents/frequency

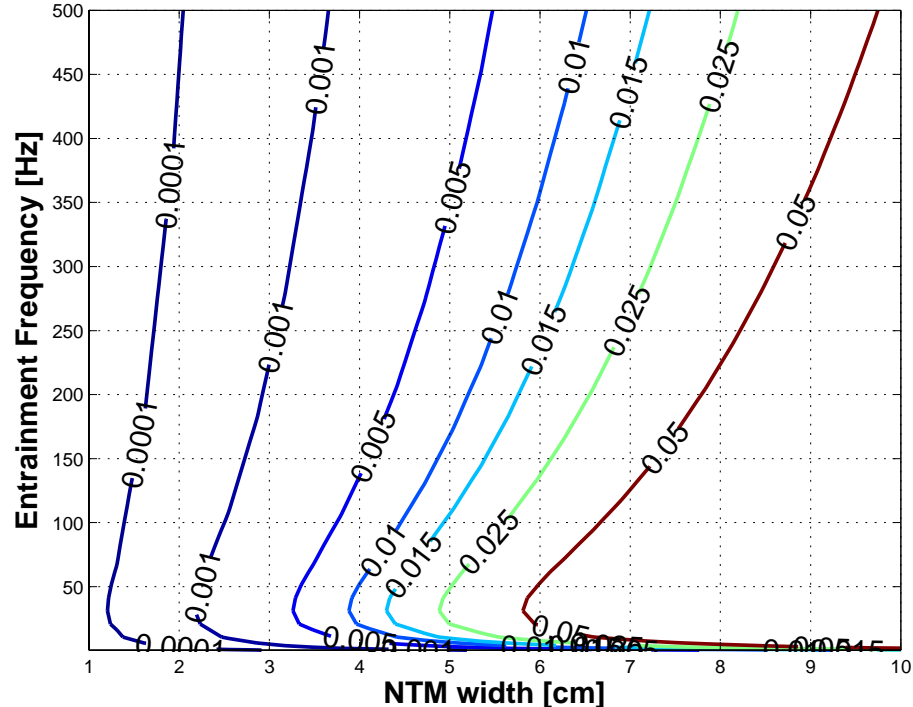




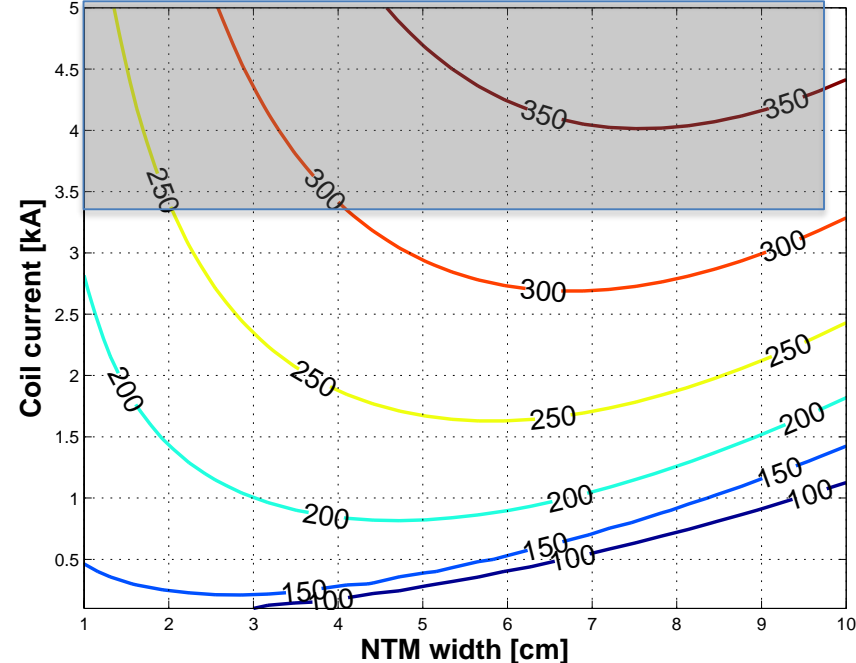
With available power supplies, NSTX-U 1x6 ext. coils could entrain modes at ~ 350 Hz ($\Omega\tau_w \approx 11$)

- major radius: 0.86 m
- wall time: 5 ms
- density: $3 \times 10^{19} \text{ m}^{-3}$
- B_T : 0.18 T

NSTX Steady State Wall Torque [Nm]



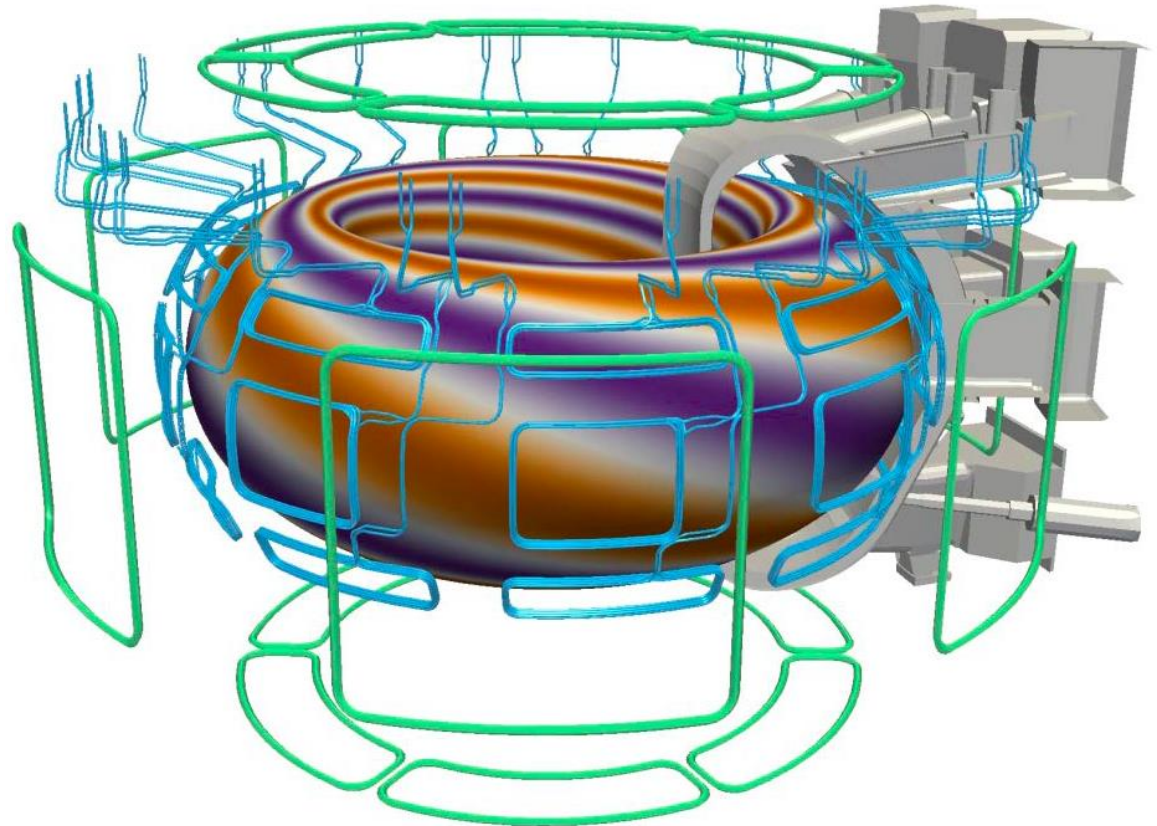
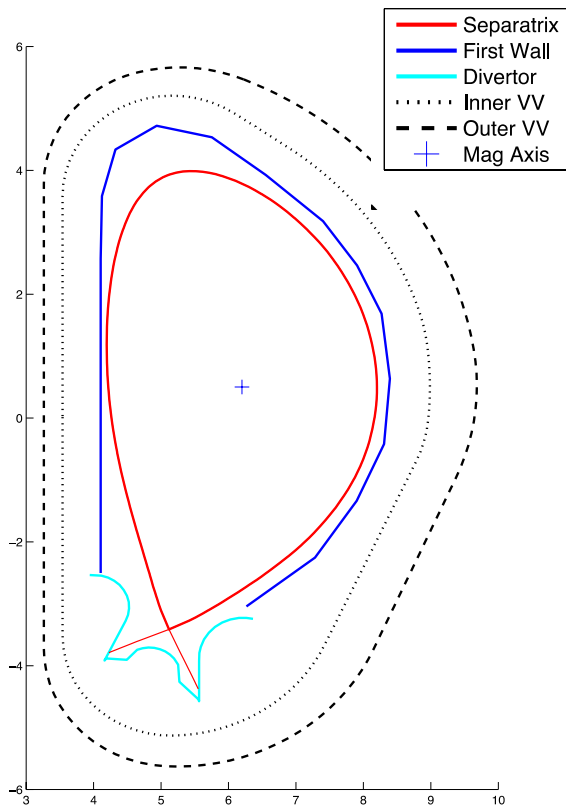
NSTX Critical entrainment frequency [Hz]



Low B_T and $R \rightarrow$ small $T_{wall} \rightarrow$ high entrainment frequency



ITER model – 3 sets of 6 external correction coils, 3 sets of 9 internal ELM coils

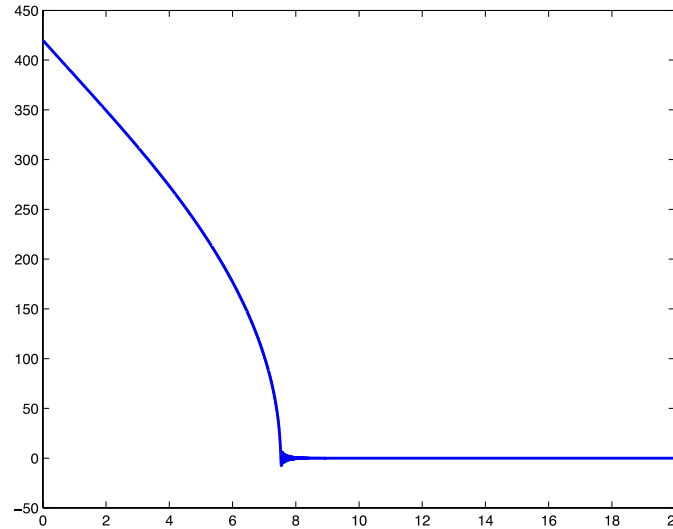
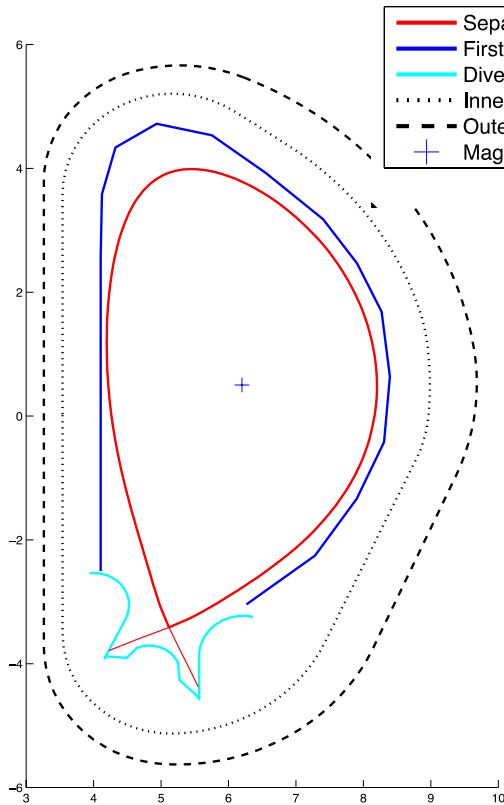


ITER treated with 2 walls:

- 1) vacuum vessels
- 2) tiled Be first wall

Image by Guido Huijsmans, ITER Org.

ITER model – NTM slows and locks in about 7 seconds

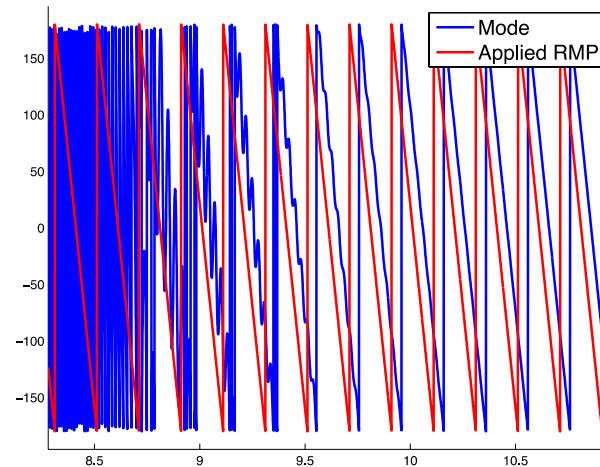


5 cm island slows from 420 Hz and locks in 7 seconds

matches well with previous predictions La Haye NF2009

ITER treated with 2 walls:

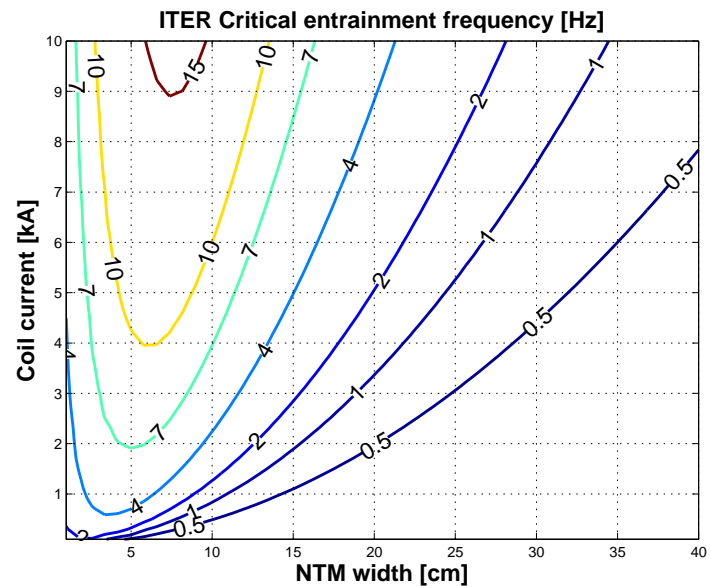
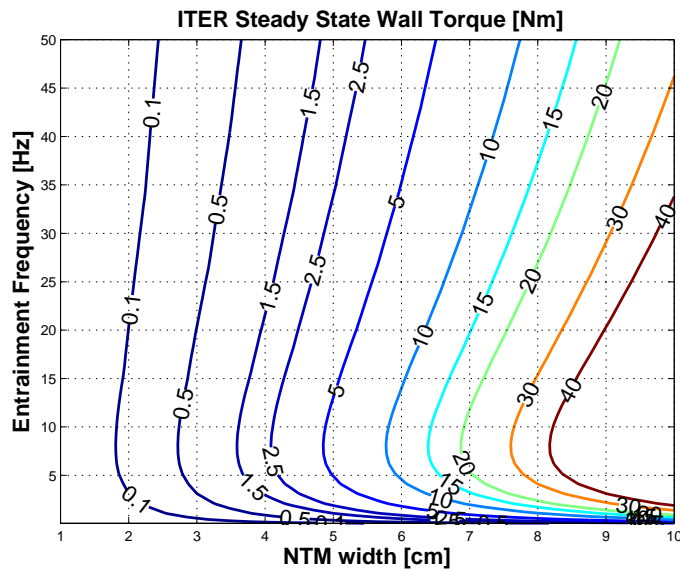
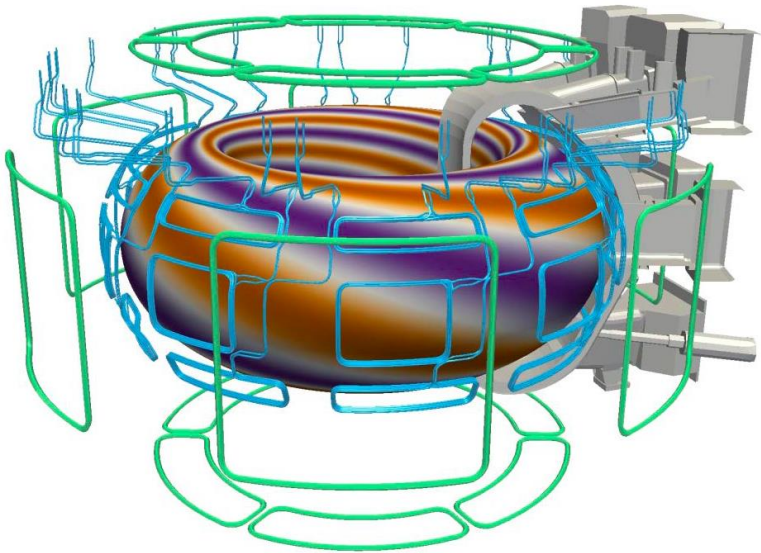
- 1) vacuum vessels
- 2) tiled Be first wall



5 Hz entrainment with 10 kA in correction (external) coils

ITER 2/1 mode entrained by external coils

- **coils:**
 - External coils: 3 sets of 6
 - Internal coils: 3 sets of 9
- **major radius: 6.2 m**
- **wall time: 188 ms**
- **density: $7.2 \times 10^{19} \text{ m}^{-3}$**
- **B_i : 5.3 T**



larger island results in stronger torque

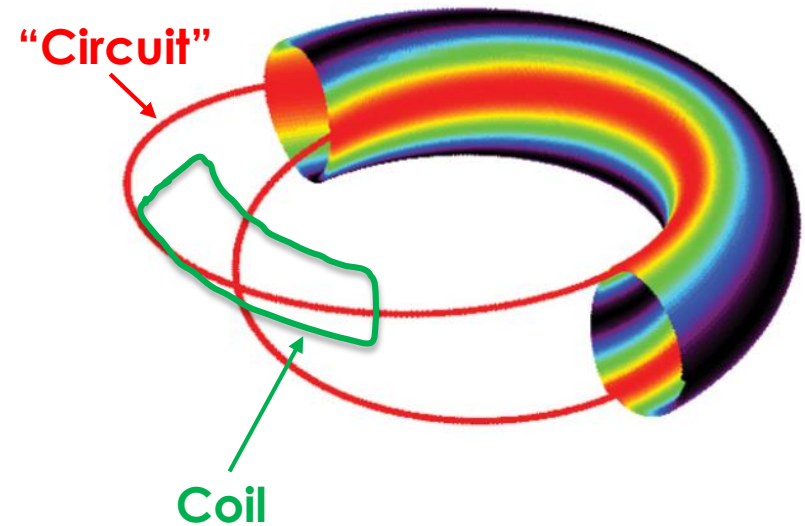
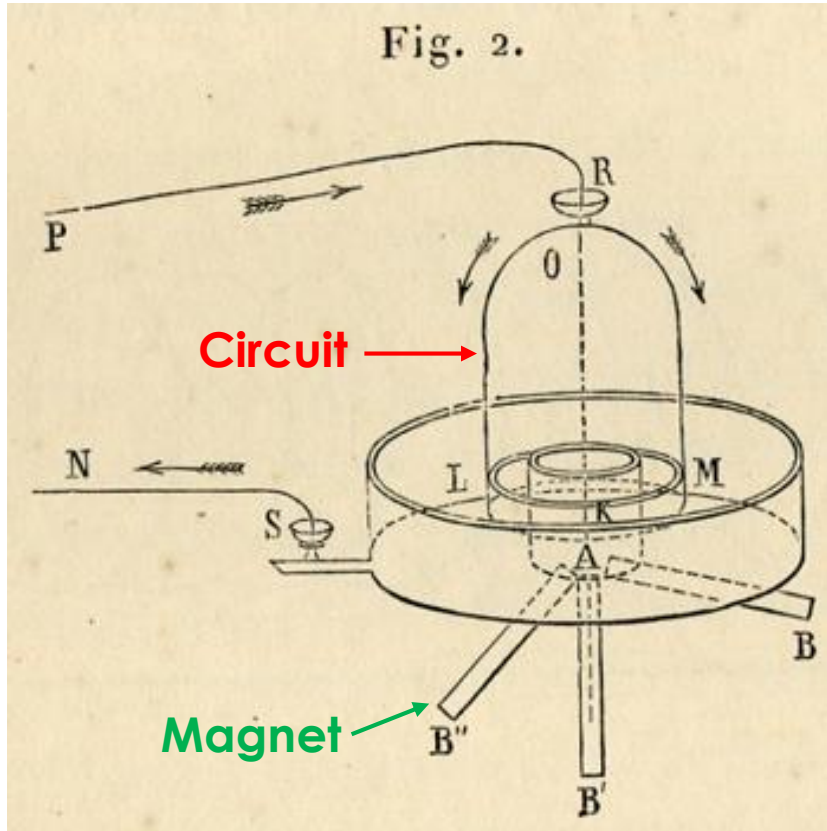
- **Prediction**

- Database of Locked Modes at DIII-D
 - Typical evolution, including deceleration, saturation, final growth
 - When do they cause disruptions?
 - How do they cause Thermal Quench?
- When do they lock?
 - Solve Eq. of Motion
 - Future work: couple with Modified Rutherford Eq.

- **Avoidance & Control**

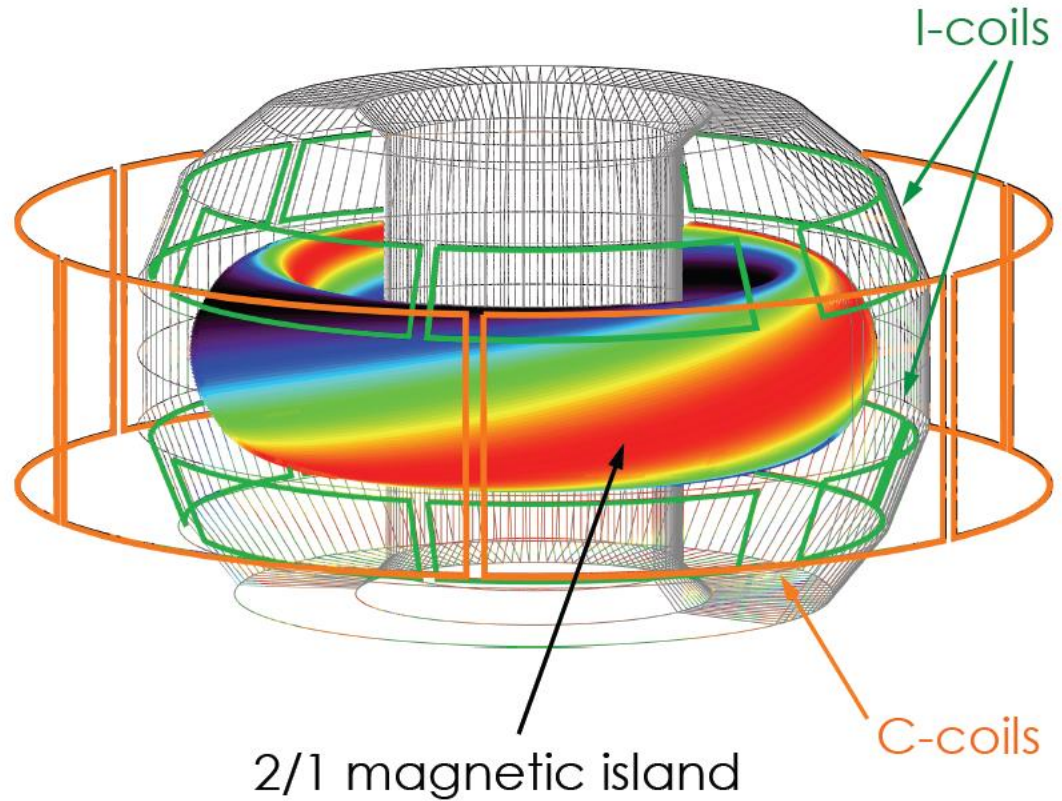
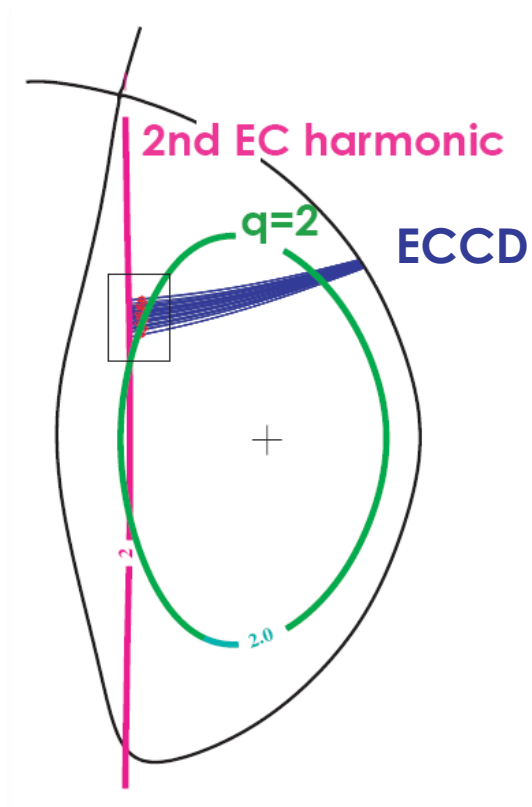
- Static or rotating RMPs + ECCD → disruption avoidance
- Preemptive entrainment → locking avoidance
- Feedback controller of locked mode phase
- Magnetic control in present devices (ITPA, WG-11)
- Modeling for ITER

Electrical circuits interact with magnetic fields (Ampere, 1822)

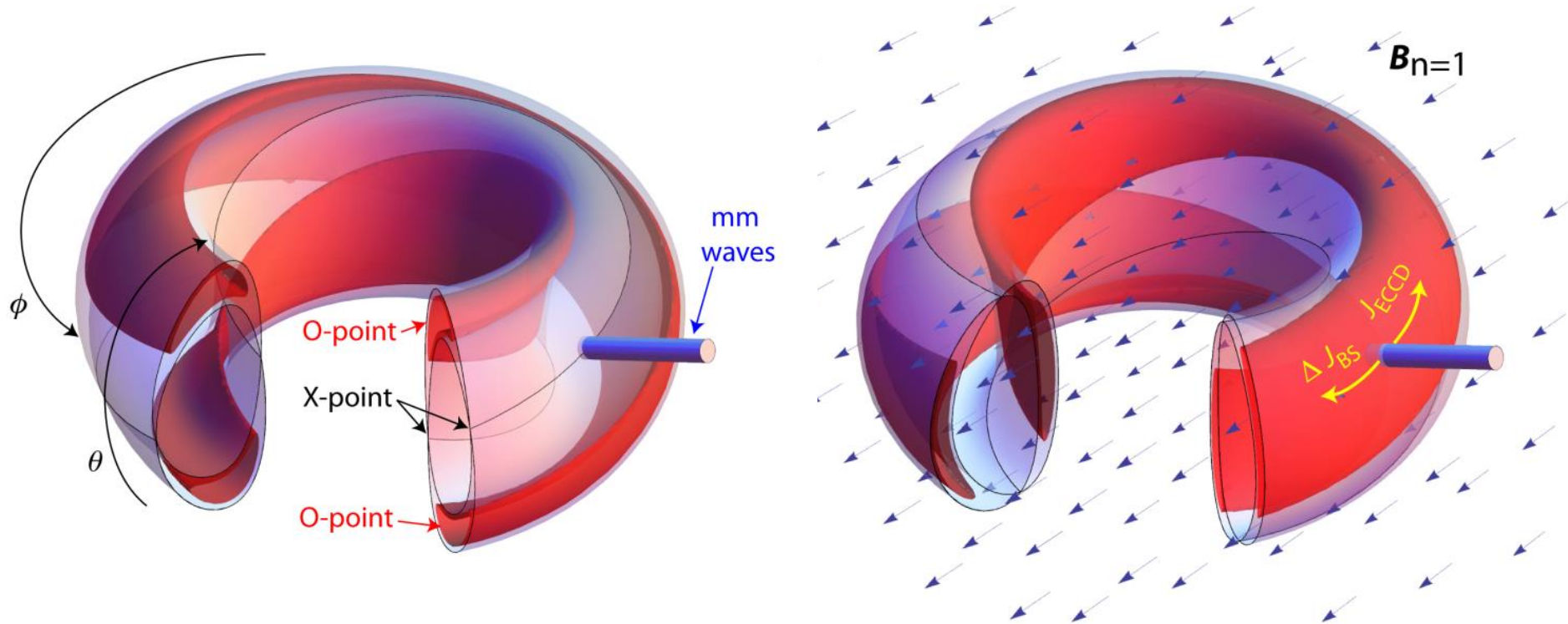


DITE [Morris 1990]
COMPASS-C [Hender 1992]
HBT-EP [Navratil 1998]
TEXTOR [Koslowski 2006]
DIII-D [Volpe 2009]
J-TEXT [Rao 2013]

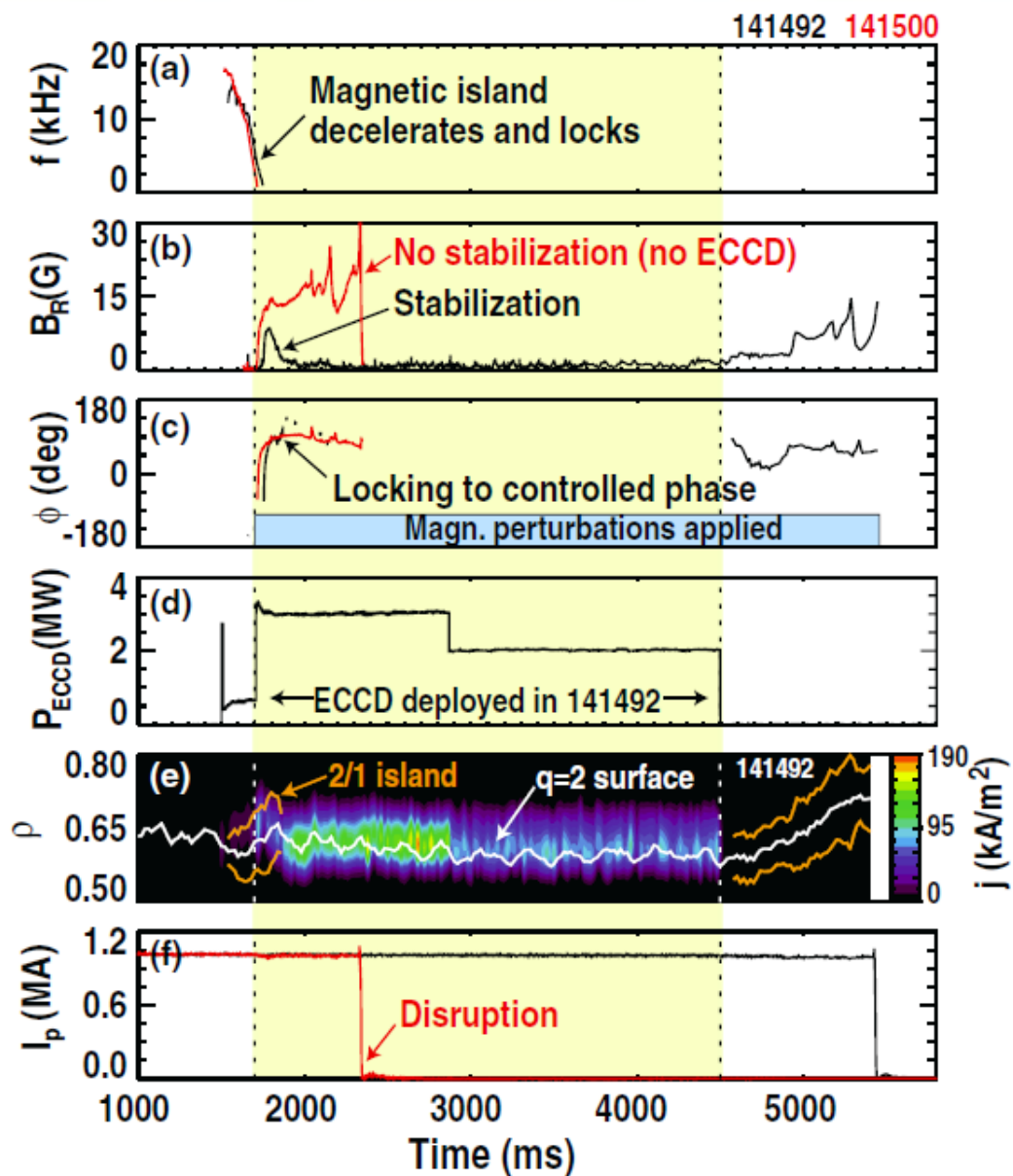
Control-coils, magnetic diagnostics and ~3MW of steerable Gyrotron power were used at DIII-D



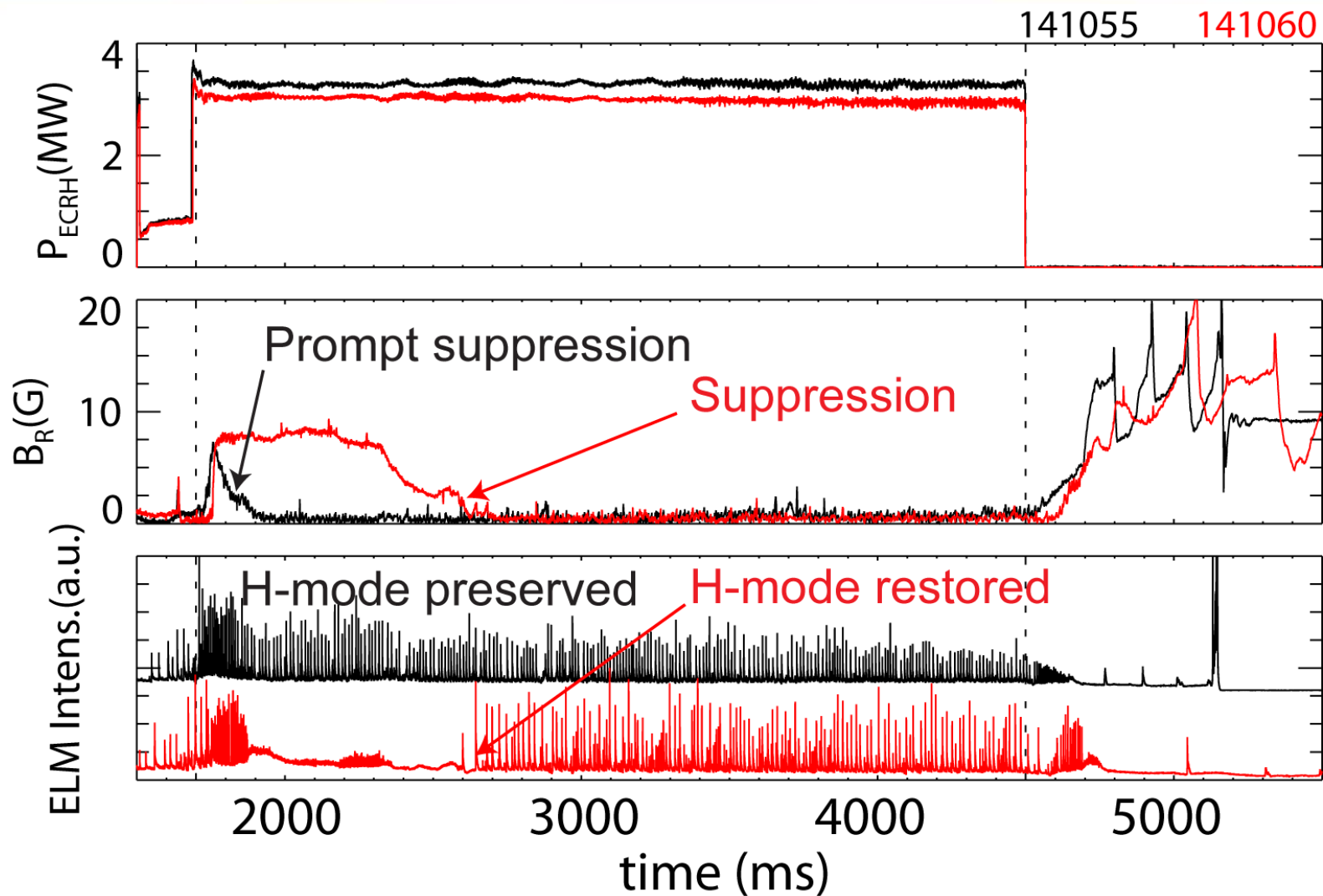
Magnetic steering aligns locked mode O-point to stabilizing ECCD



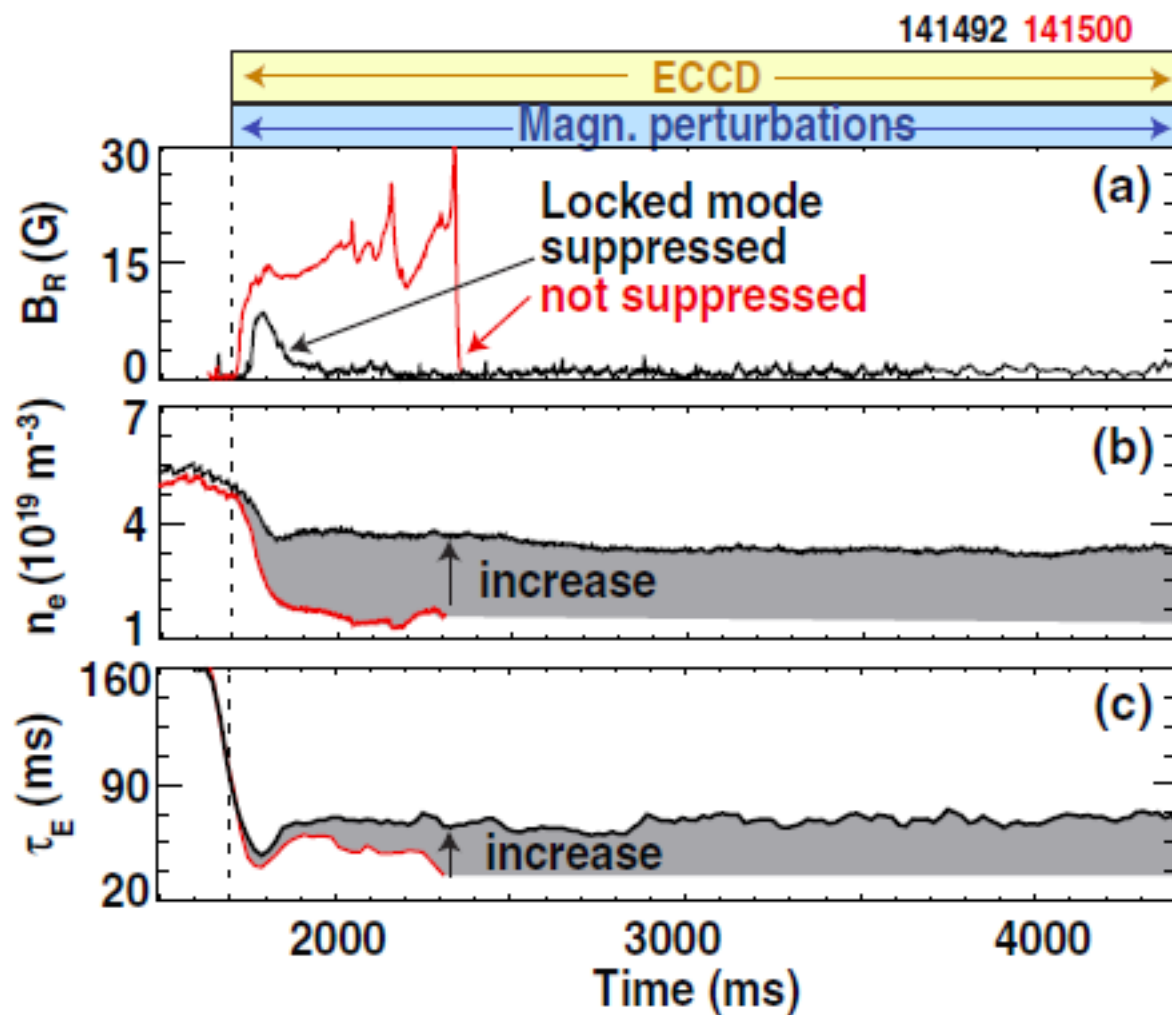
Static applied RMP make Locked Mode O-point accessible to stabilizing ECCD



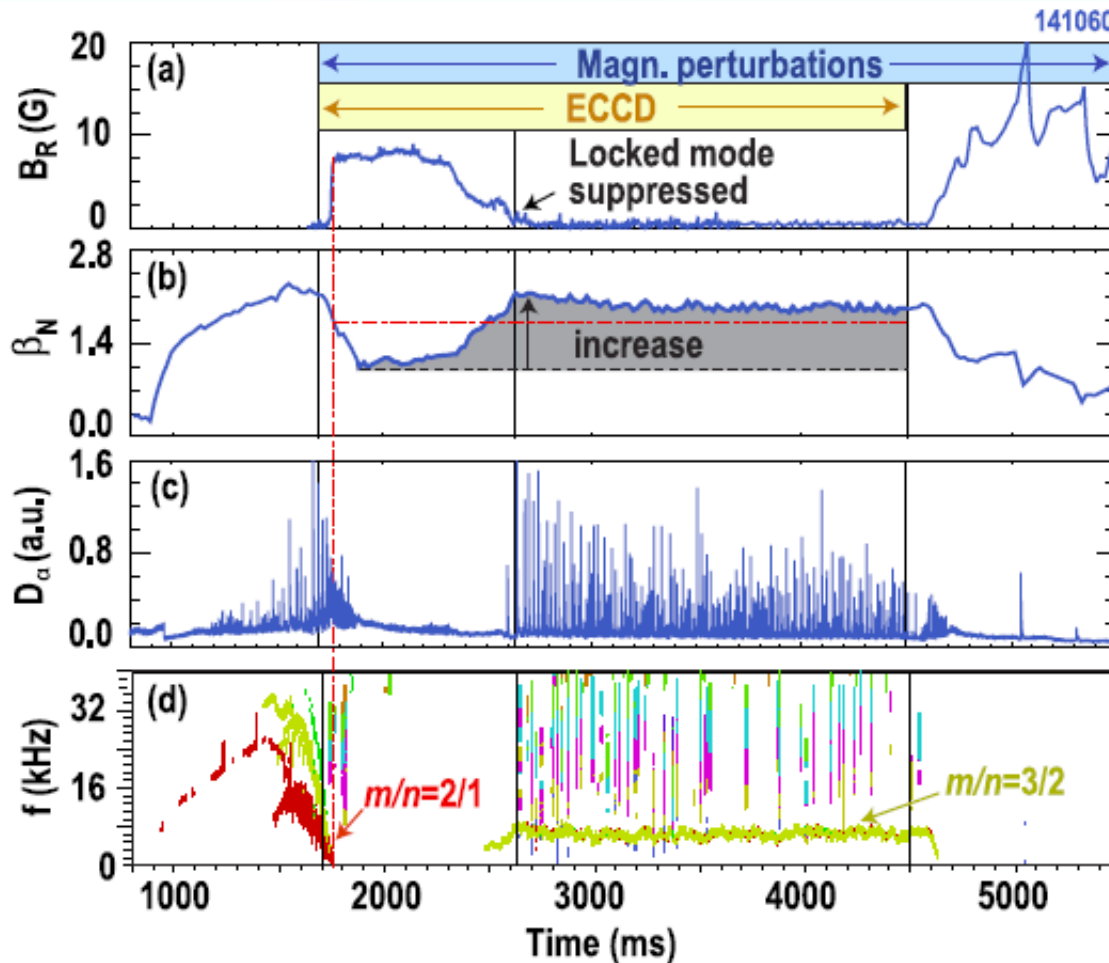
Locked-mode-controlled discharges do not lose H-mode, or rapidly recover it



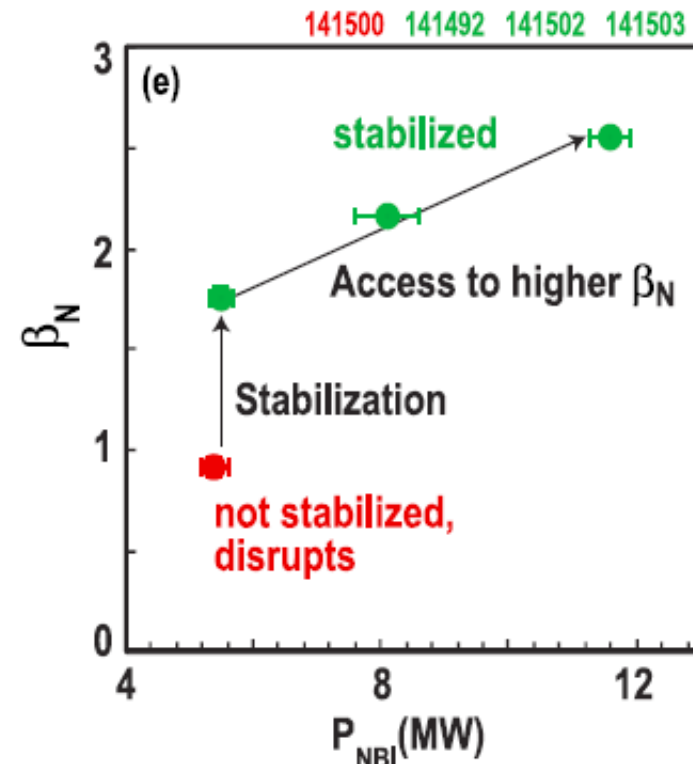
Incomplete recovery of pre-locking confinement is probably due to ECCD and RMPs still on



β_N is recovered after locked mode suppression



ECCD at $q=2$ prevents
reappearance of 2/1,
whether locked or rotating



Locked mode stabilized:

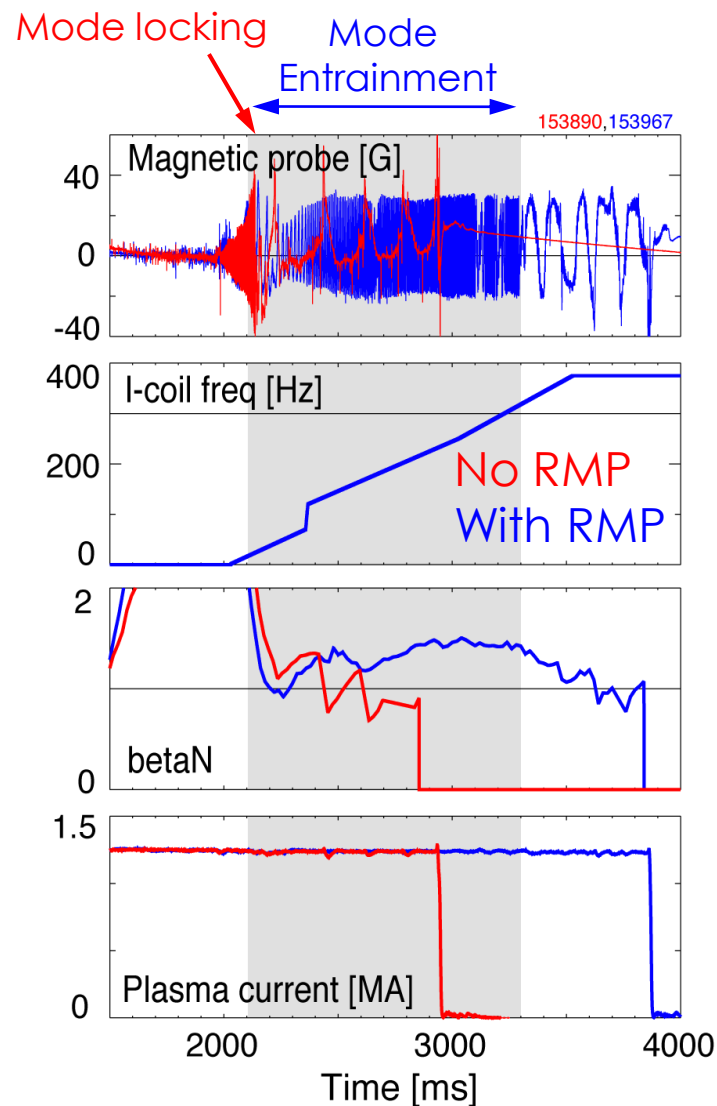
- High β and no disruption

Locked mode not stabilized:

- Disruption at $\beta \sim 1.7$

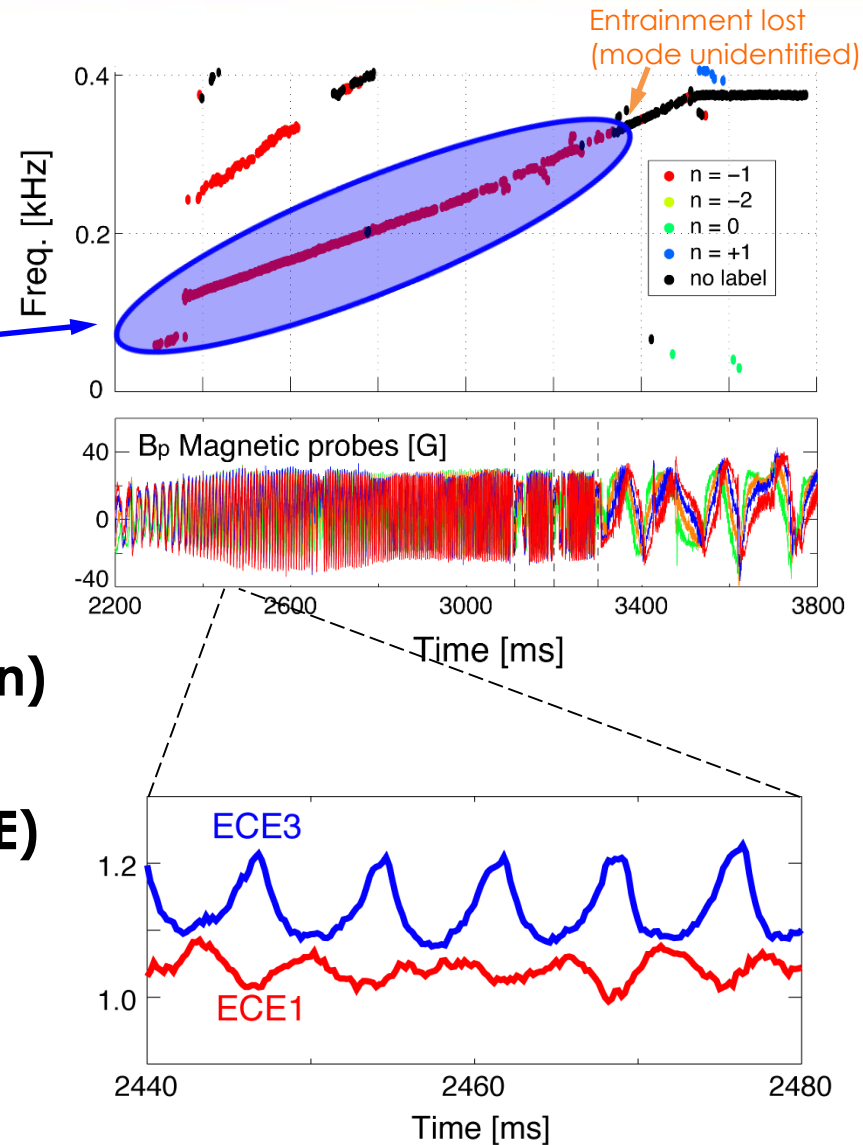
Rotating field sustains mode rotation up to 300 Hz ($\Omega\tau_w \approx 6$)

- **Without control:** 2/1 NTM grows and locks $\rightarrow \beta_N$ collapse and major disruption
- **Rotating $n=1$ I-coil field “entrains” slowing island**
 - Avoids disruption without using ECCD
- **Entrainment up to 300 Hz ($\Omega\tau_w \approx 6$)**



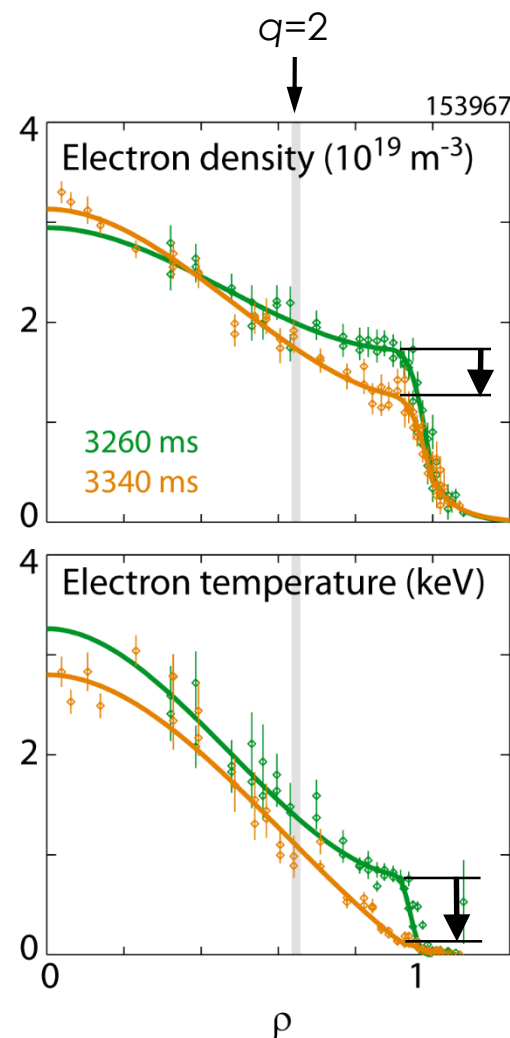
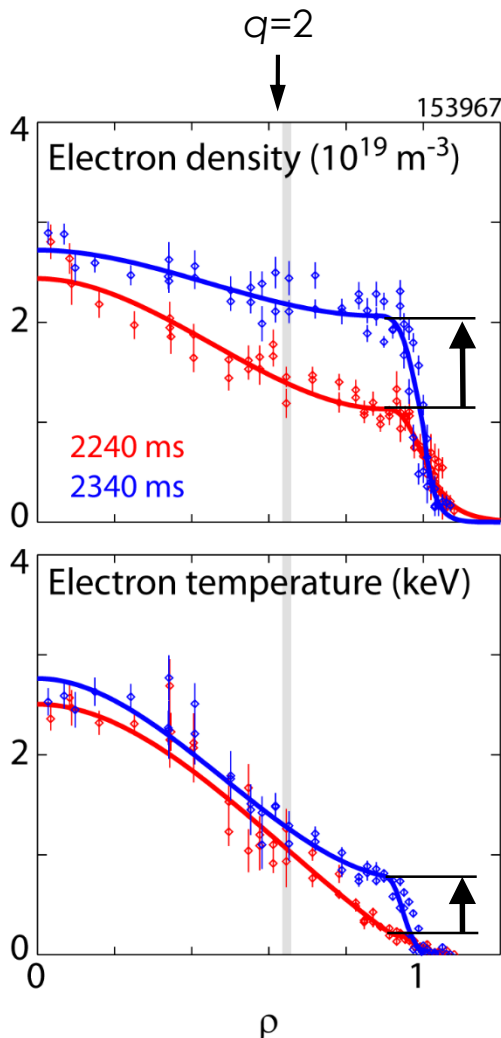
Magnetics array analysis and ECE diagnostic confirm entrainment and spin-up of 2/1 mode

- Magnetics arrays analyzed for modal shapes (eigspec code)
- $m/n=-2/-1$ mode tracks I-coil frequency
- Entrainment frequency is modulated by Error Field on sub-period timescale (not shown)
- Electron Cyclotron Emission (ECE) phase inversion across $q=2$ surface, synchronous with I-coil



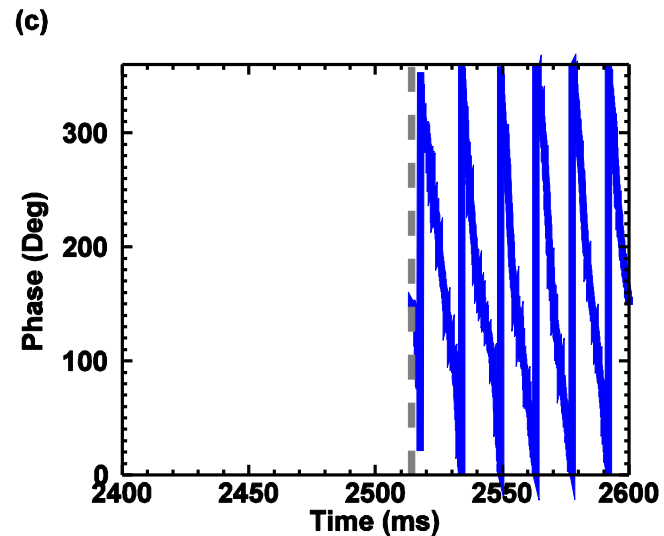
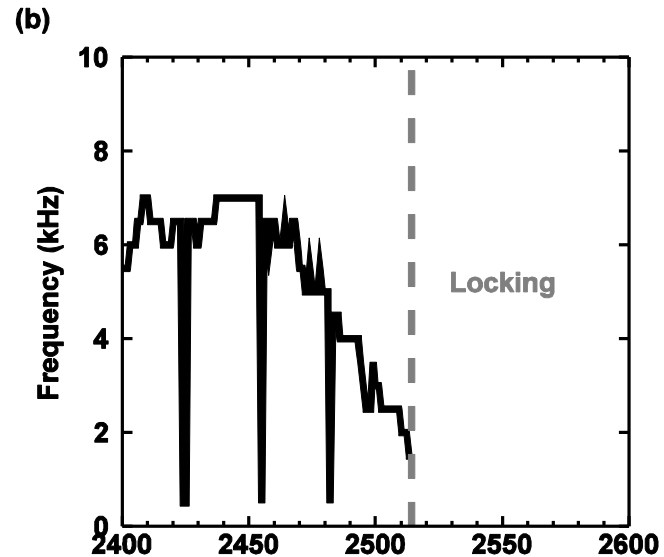
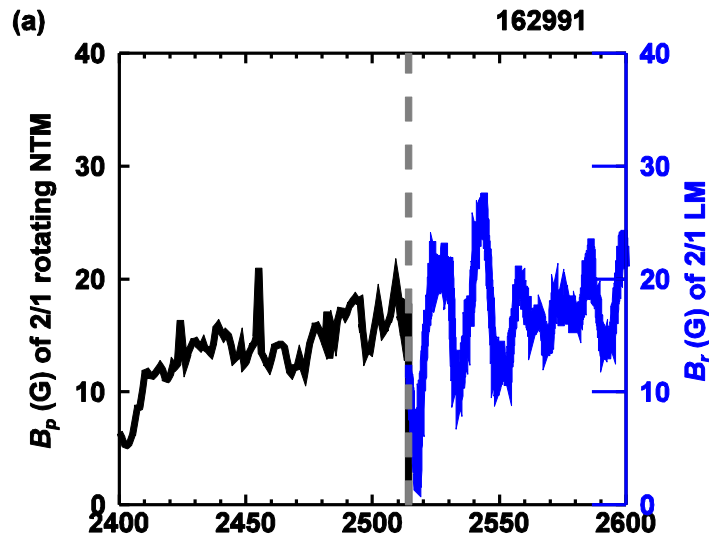
Improved confinement: edge pedestal forms during entrainment

At entrainment <



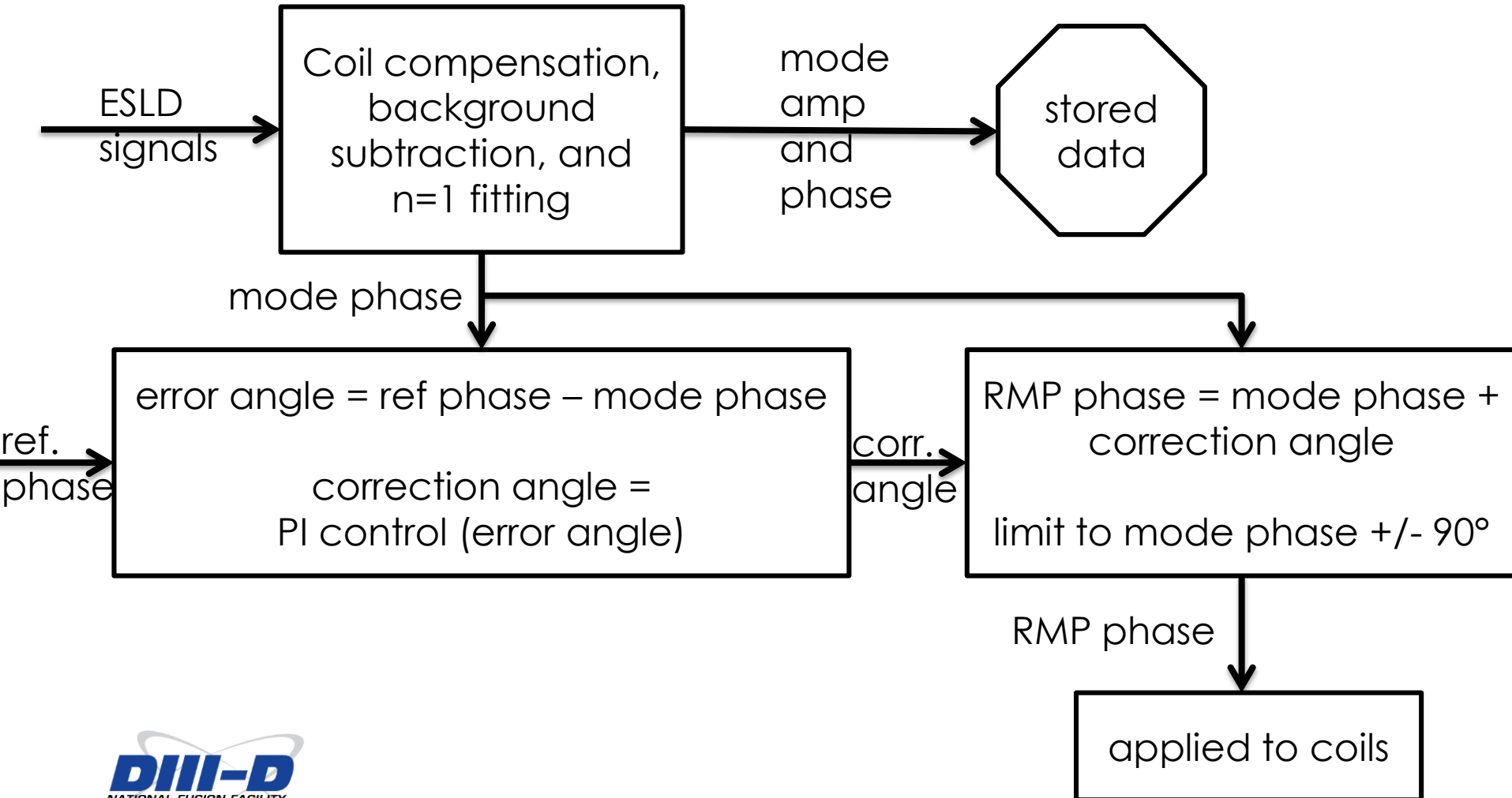
> At loss of entrainment

Pre-emptive entrainment



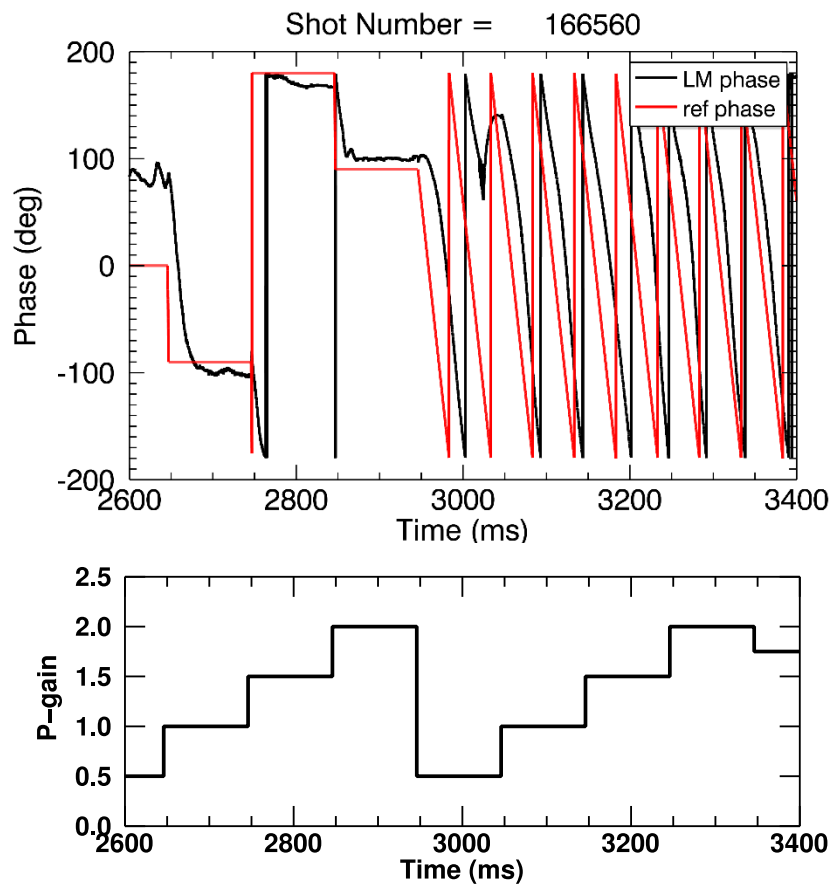
Features of phase controller

- A proportional-integral controller was implemented to control the phase of $n=1$ locked modes

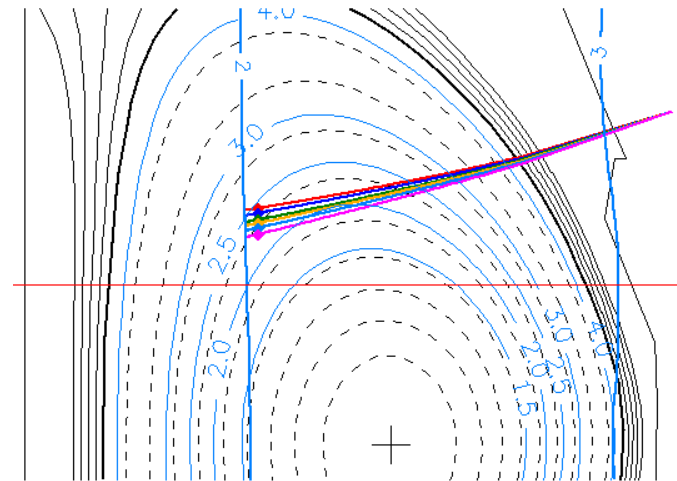
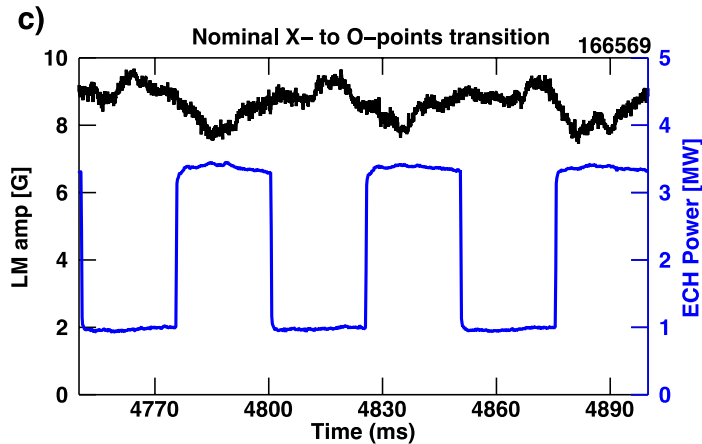
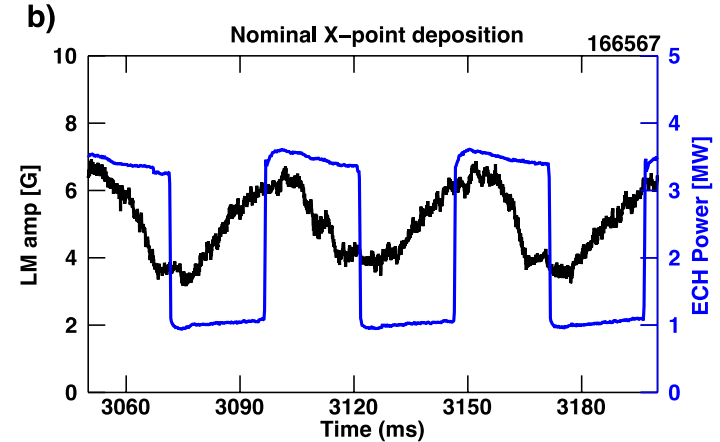
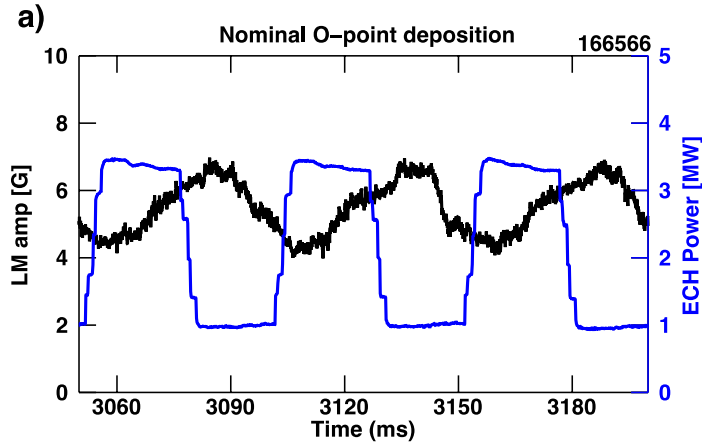


Phase controller behaved well during half-day

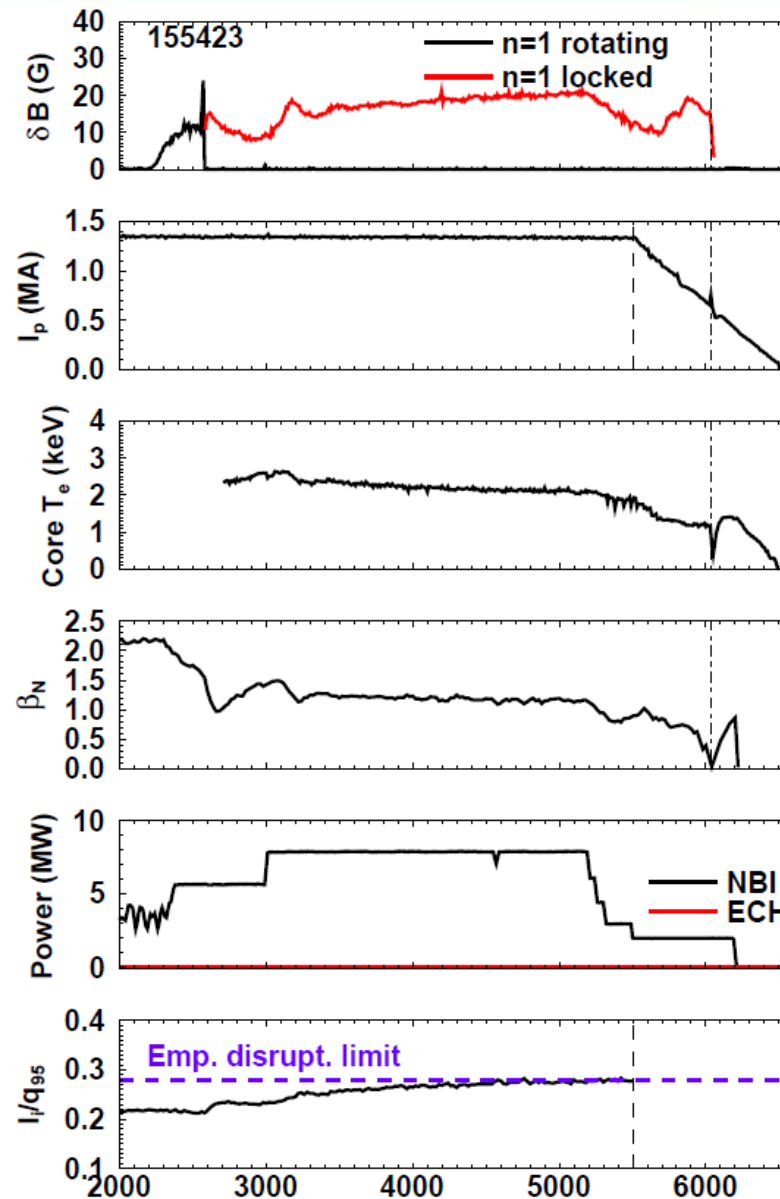
- When RMP was applied, successful demonstration of controller's ability to prescribe phase and entrain at 20 Hz



Different phasing gives different behavior. Deposition slightly outside $q=2$ location.



Long survival gives time to safely ramp discharge down



- **Prediction**

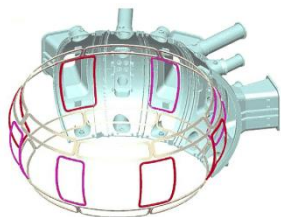
- Database of Locked Modes at DIII-D
 - Typical evolution, including deceleration, saturation, final growth
 - When do they cause disruptions?
 - How do they cause Thermal Quench?
- When do they lock?
 - Solve Eq. of Motion
 - Future work: couple with Modified Rutherford Eq.

- **Avoidance & Control**

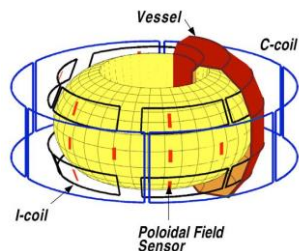
- Static or rotating RMPs + ECCD → disruption avoidance
- Preemptive entrainment → locking avoidance
- Feedback controller of locked mode phase
- **Magnetic control in present devices (ITPA, WG-11)**
- Modeling for ITER

5 tokamaks, 2 spherical tokamaks, 2 RFPs and a helical device are involved in WG-11

AUG



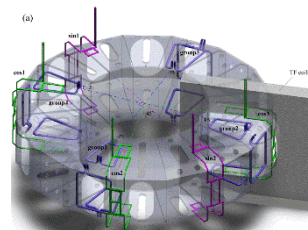
DIII-D



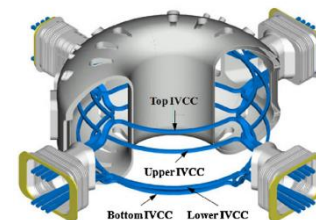
JET



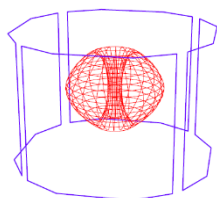
J-TEXT



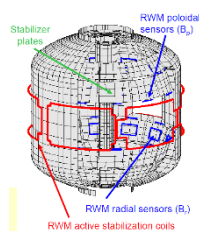
KSTAR



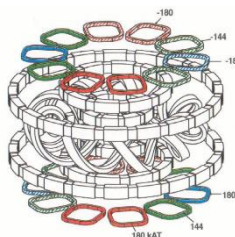
MAST



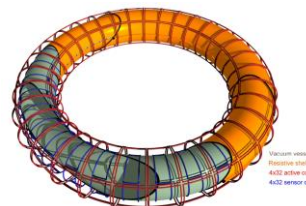
NSTX



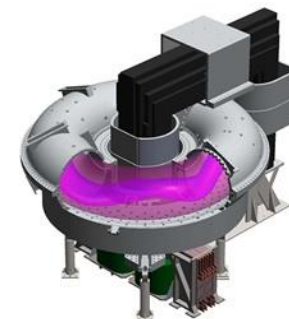
LHD



EXTRAP-T2R



MST



Different Machines

- Sizes
- Aspect ratios
- elongations
- wall times

Different Coil sets

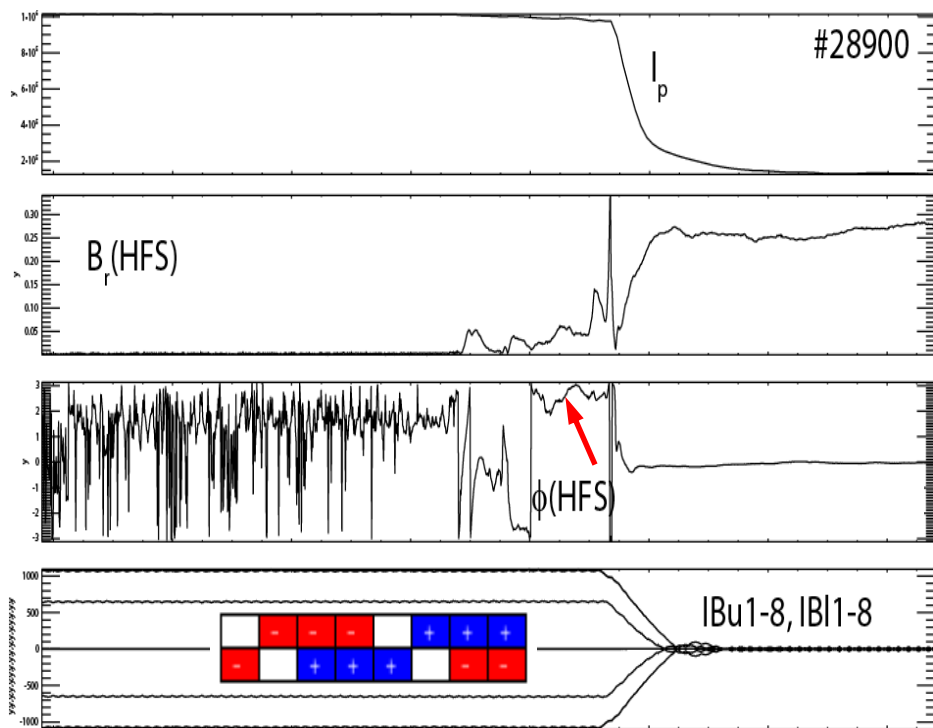
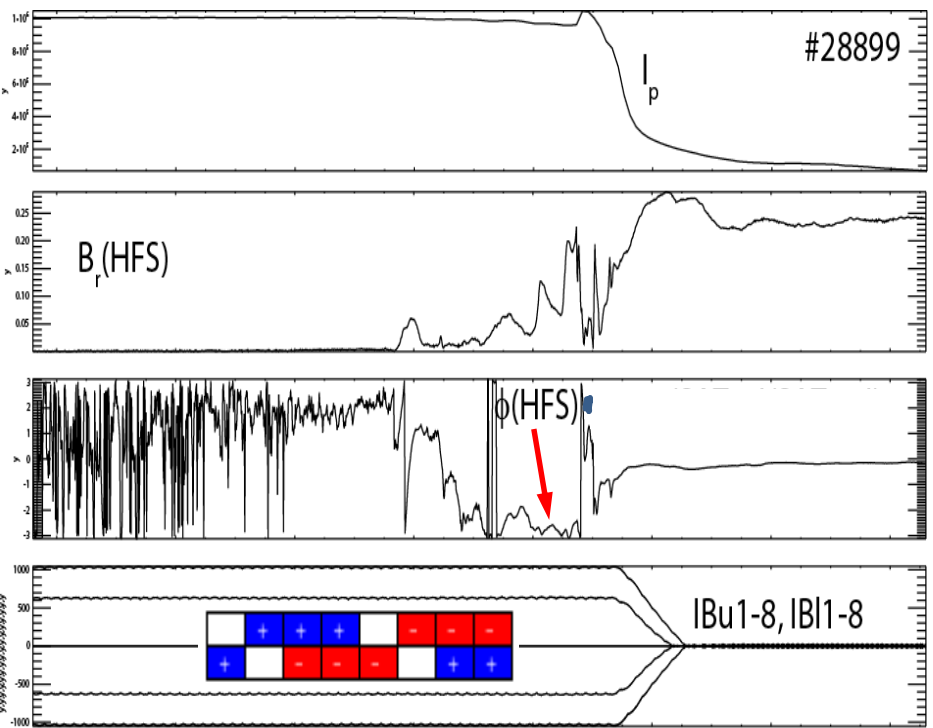
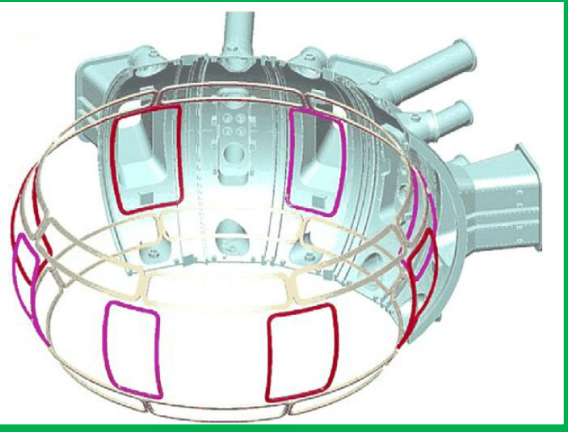
- Internal or external
- narrow or broad in angular spread
- dense or sparse arrays
- partial/full toroidal/poloidal coverage

Static applied RMPs control phase of locked modes

- **Born-locked $n=1$ modes (EF-penetration modes) in:**
 - AUG, DIII-D, JET, KSTAR, MAST, NSTX
- **$m/n = 2/1$ LMs with rotating precursors in:**
 - DIII-D, J-TEXT, KSTAR
- **$m/n = 1/-15$ LMs with rotating precursors in**
 - EXTRAP-T2R

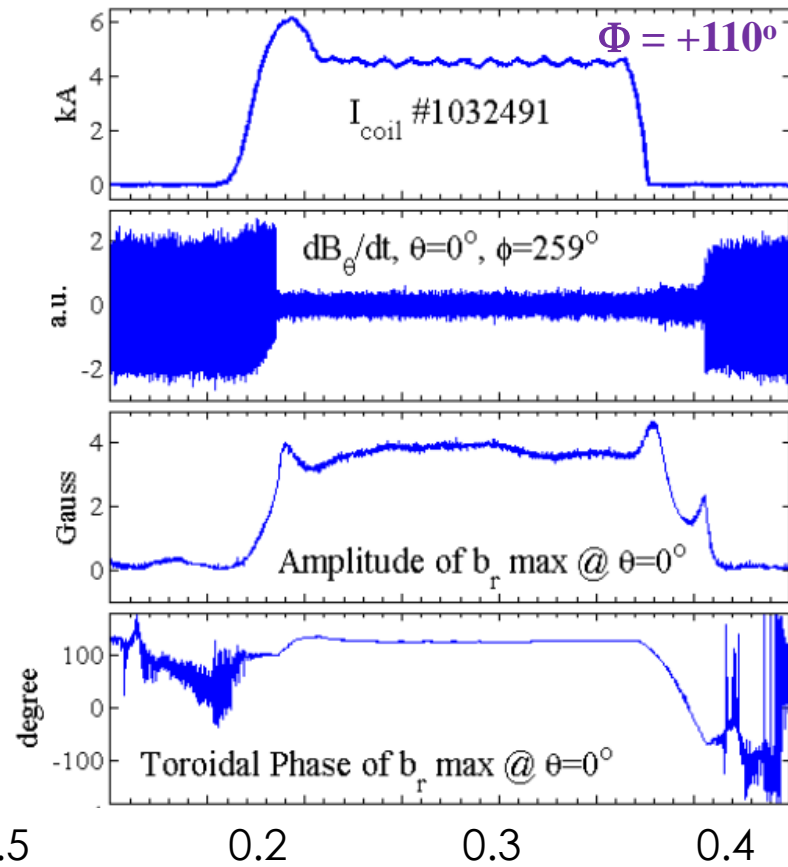
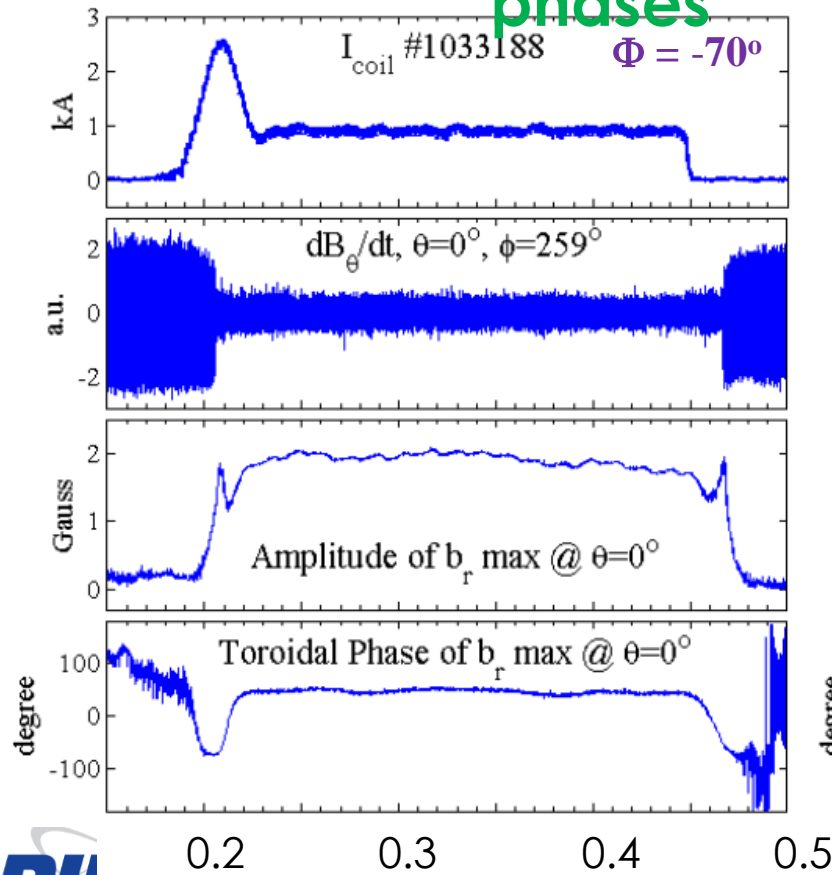
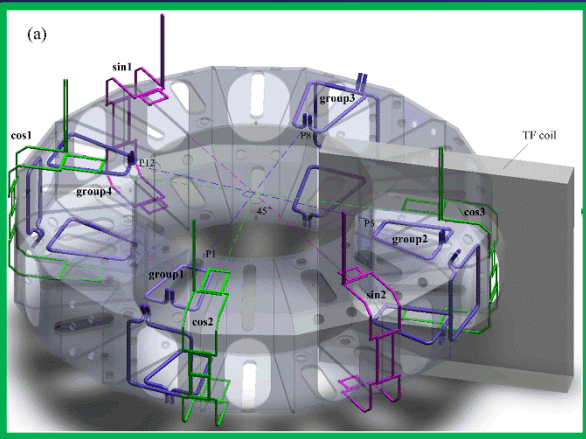
AUG (currently 2x8 internal coils)

Flipping $n=1$ RMP by 180°
changes $n=1$ LM phase by $\Delta\phi \neq 180^\circ$.

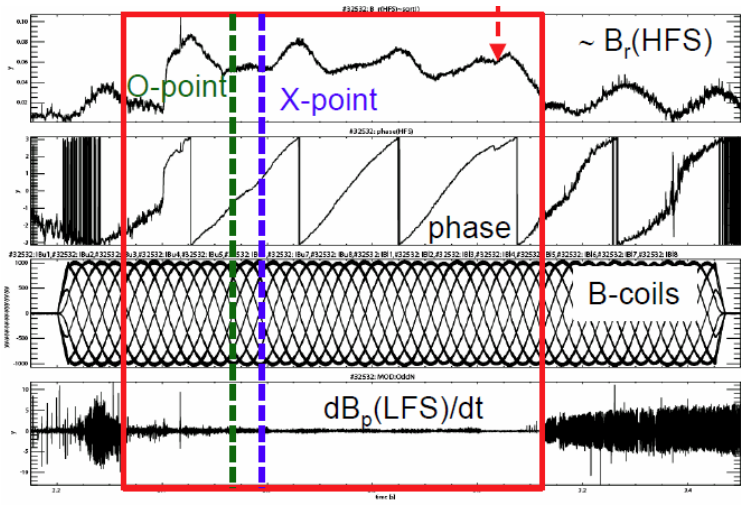


J-TEXT (3x4 internal + 1x2+1x3 ext. coils)

$n=1$ RMPs applied with different phases cause pre-existing rotating TM to lock with different phases

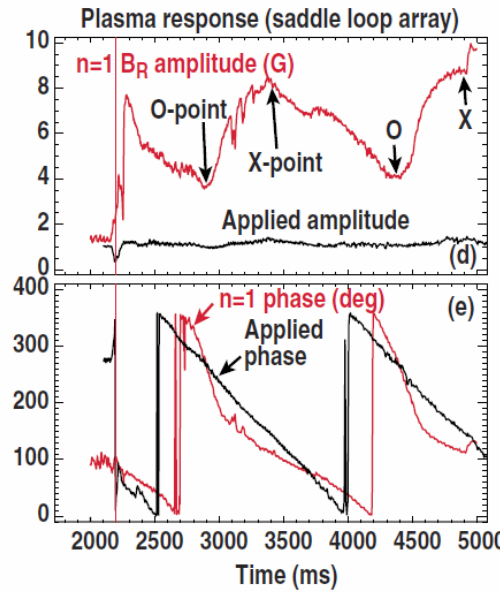


Initially locked islands were entrained by applied rotating RMPs at AUG, DIII-D, J-TEXT

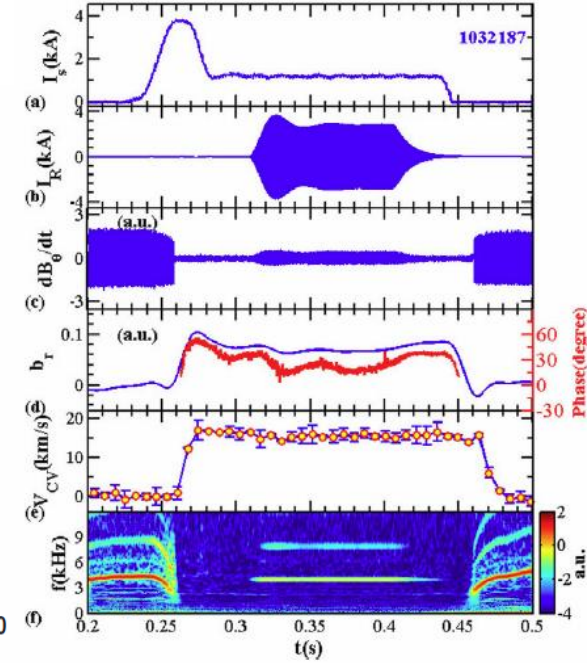


AUG, Maraschek *et al.*, this meeting

Paccagnella *et al.*, EPS 2016



DIII-D, Volpe *et al.*, PoP 2009; J-TEXT, Jin *et al.*, PPCF 2010



Earlier entrainment studies (of initially rotating or initially locked islands):
 DITE [Morris 1990], COMPASS-C [Hender 1992], HBT-EP [Navratil 1998], TEXTOR [Koslowski



Conclusions

- I_i/q_{95} (probably a proxy for Δ') predicts 94% of Locked Mode Disruptions at DIII-D, with warning time ≥ 100 ms
- Island proximity to plasma edge correlates with Thermal Quench onset
- Applied magnetic perturbations (static or rotating) and driven currents suppress Locked Modes and avoid disruptions
- Pre-emptive entrainment avoids locking
- f/back phase controller recently deployed at DIII-D
- Evidence of Locked Mode control in several other devices.
- ITER coil-currents will easily entrain islands which just locked. Only 0.5 Hz entrainment if fully grown.

Back-up Slides 1

on LM Database and its Interpretation

Decay-time used to differentiate disruptive from non-disruptive discharges

- Decay time = duration of current quench

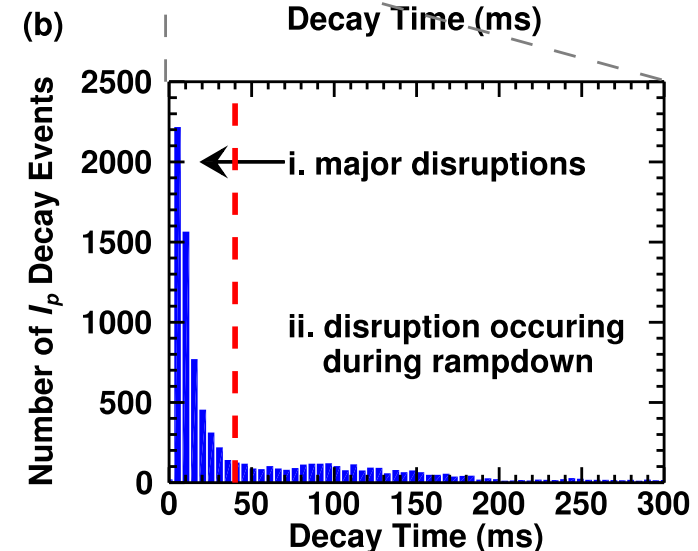
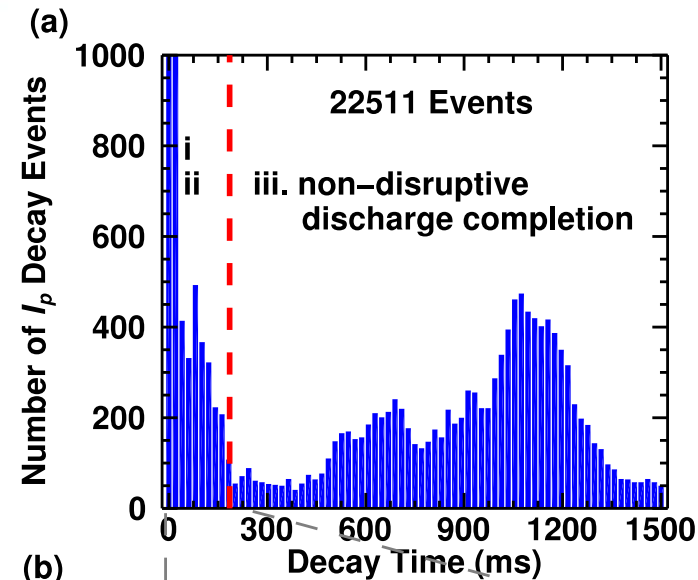
$$t_d = \frac{\text{time of } 80\% I_p - \text{time of } 20\% I_p}{0.6}$$

- Three groupings

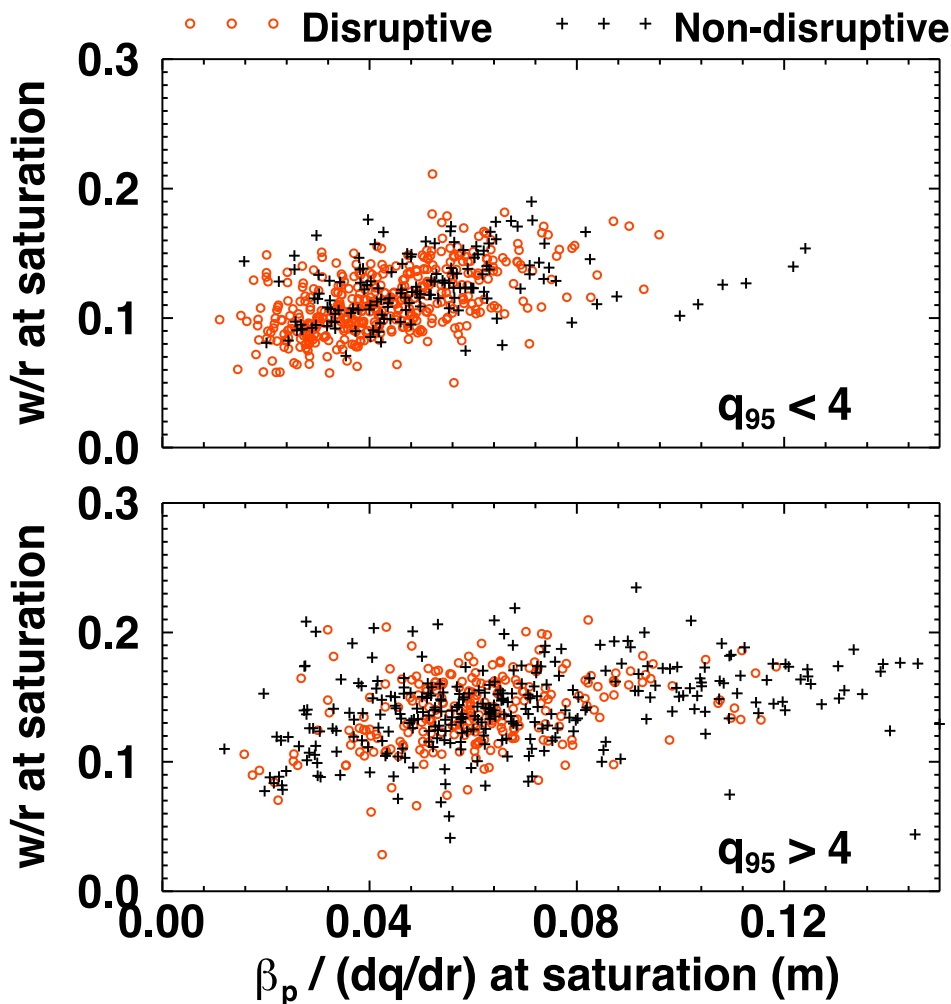
- i. $t_d < 40$ ms **Disruptive**
- ii. $40 \text{ ms} < t_d < 200$ ms **Intermediate**
- iii. $t_d > 200$ ms **Non-disruptive**

- 50 shots manually analyzed in populations *i* and *iii*, confirmed that:

- **No false positives** in major disruptions (i.e. calling non-disruptive shot disruptive)
- **No false negatives** in non-disruptions (i.e. calling disruptive shot non-disruptive)



Saturated width scales with $\beta_p/(dq/dr)$, indicating at least partial drive from bootstrap deficit



- Expected from steady-state Modified Rutherford Equation
- IRLMs occurring at low q_{95} (top) correlate better than those at high q_{95} (bottom)

Controlling the toroidal phase of locking, in f/fwd or f/back, has numerous applications

Locked Mode (LM) and NTM Control, Disruption Avoidance:

- In combination with Electron Cyclotron Current Drive (ECCD):
 - Re- or “pre”-position LM to assist its cw ECCD stabilization.
 - Controlled rotation, in synch with *modulated* ECCD.
- Without ECCD:
 - Unlock island and spin it by NBI or magnetically.
 - Rotational stabilization by conducting wall, flow and flow-shear.
- Avoid locking by entrainment.

Other:

- Spread heat during disruptions.
- Assist diagnosis of islands.
- Study radiation asymmetries in massive gas injection.

Controlling toroidal phase of magnetic islands has numerous applications

Locked Mode and NTM Control, Disruption Avoidance:

- In combination with ECCD:
 - Re- or “pre”-position LM, to assist its ECCD stabilization (cw).
 - Pace island rotation in synch with modulated ECCD.
- Without ECCD:
 - Unlock island and spin it by NBI or magnetically.
 - Rotational stabilization?
 - Stabilizing effect of conducting wall on rotating mode [Fitzpatrick].
 - Stabilizing effect of flow and flow-shear [Buttery, La Haye, Sen *et al.*].
- Avoid locking altogether by entraining island while still slowing down.

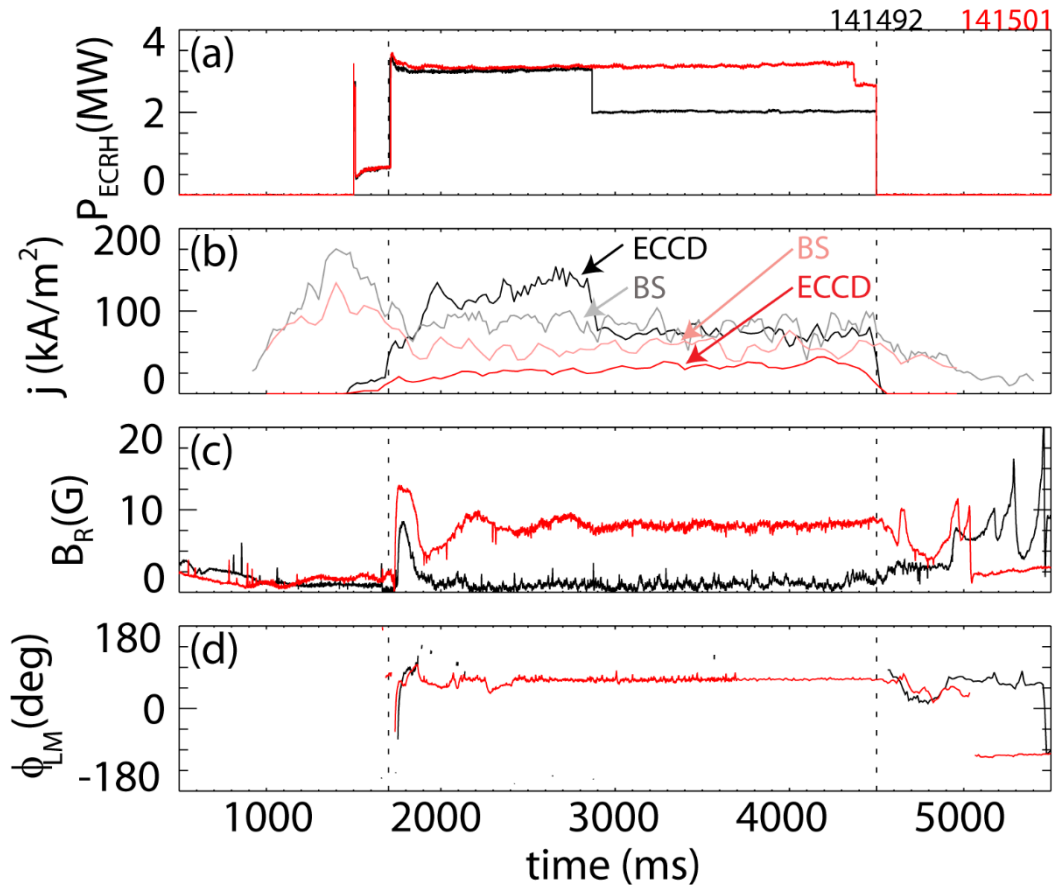
All of the above can be done in *f/back* or *f/fwd*.

- *f/back* can also directly reduce island width, not just its phase [Hender, Lazzaro, Morris *et al.*]. Not our scope.

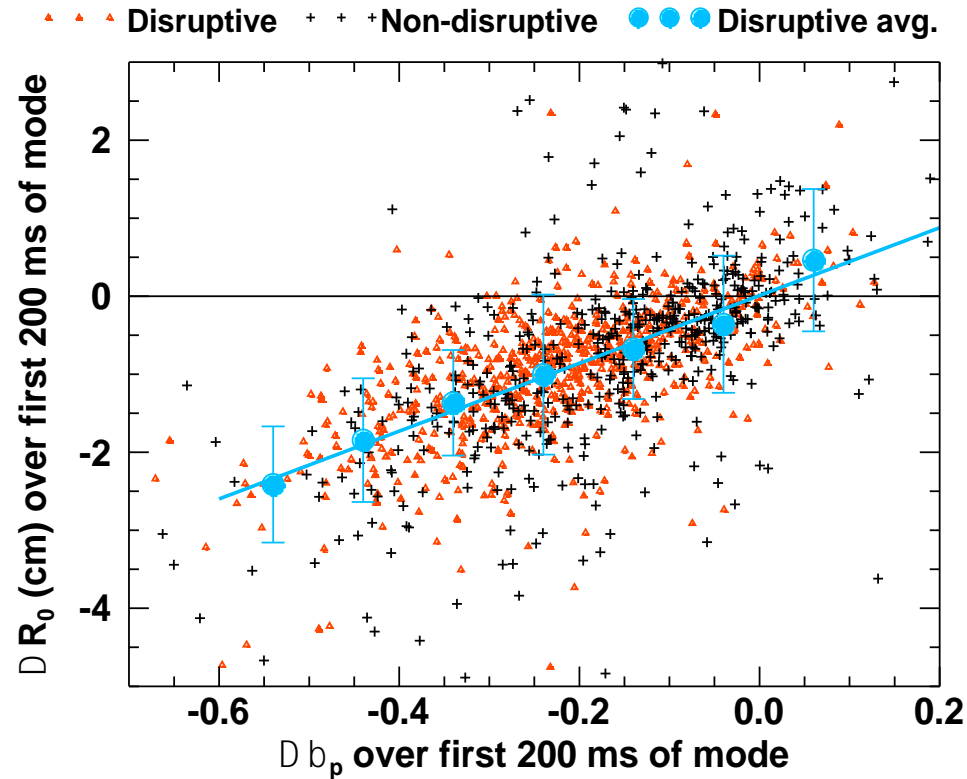
Other:

- Spatially spreading heat loads during disruptions.
- Assisting diagnosis of islands [Liang, Shaffer *et al.*].
- Disruption control (by massive gas injection) and disruption studies with controlled phase relative to mode [Pautasso, Izzo, Shiraki *et al.*].

EC current drive is more stabilizing than heating. Key is (over-)compensating for missing Bootstrap.

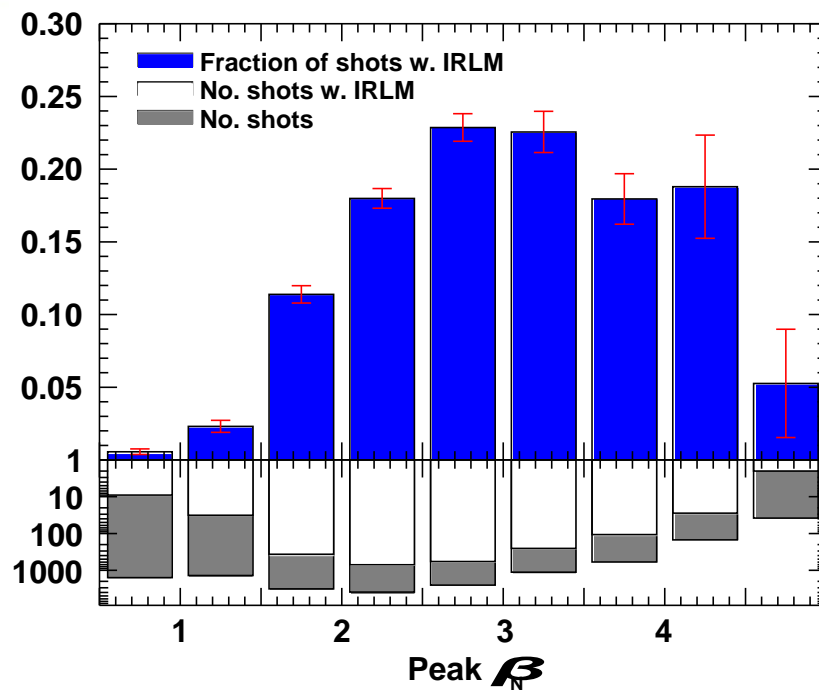


IRLMs change the 2D equilibrium shape by reducing the Shafranov shift



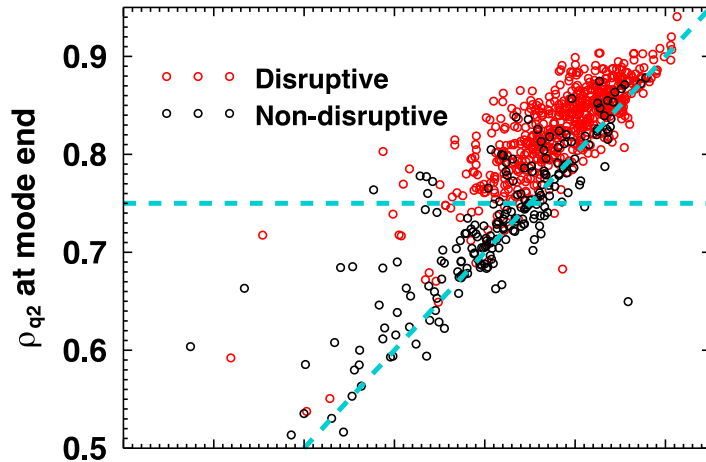
- $\Delta R_0 / \Delta \beta_p \approx 4 \text{ cm}$
- Decrease of $m/n=1/0$ shaping might affect toroidal coupling of $m/n=2/1$ with other $n=1$ perturbations

In a 1D study, IRLMs appear most often in intermediate β_N plasmas

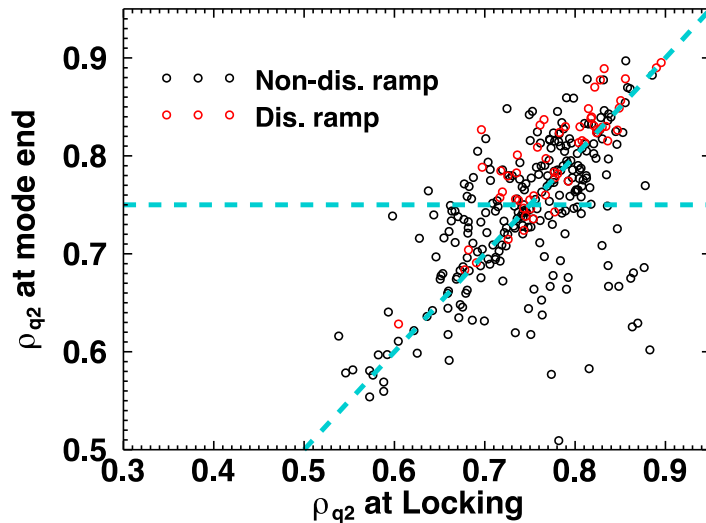


- Low occurrence at $\beta_N > 4.5$ might be explained by observed conditions of $q_{95} > 7$ and $T_{NBI} > 6$ NM in most of these shots
- 3D study of IRLM rate of occurrence vs. β_N , T_{NBI} , and ρ_{q2} might be more informative

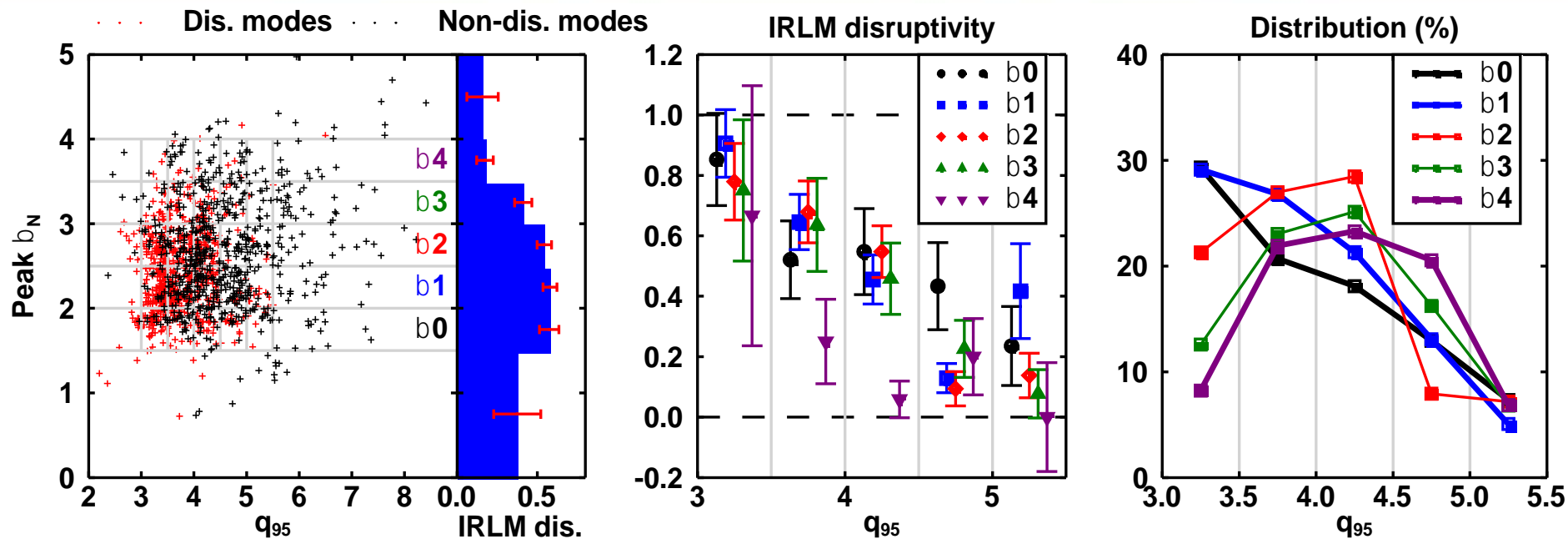
ρ_{q2} increases through lifetime of IRLM



- evolution of ρ_{q2} from locking to 100 ms before mode end
- majority of disruptive IRLM move outwards

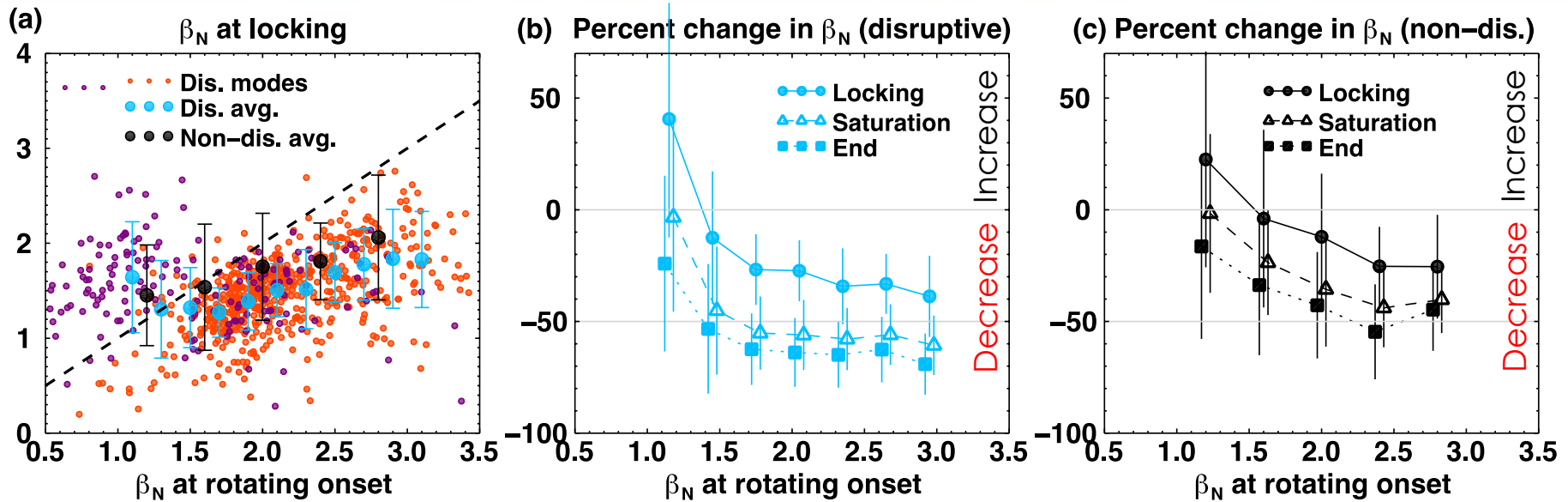


Decreasing IRLM disruptivity at high β_N observed in 1D, partially attributed to coincident high q_{95}



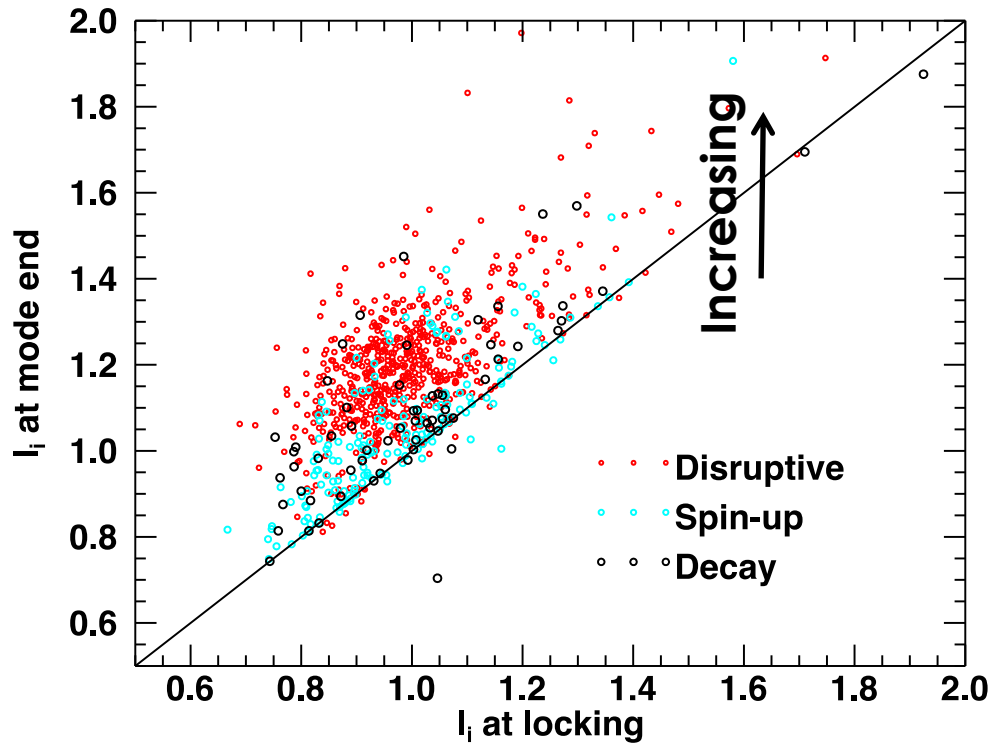
- (Left) 1D projection of IRLM disruptivity vs. β_N shows decreasing disruptivity with increasing β_N
- (Middle) IRLM disruptivity decreases with increasing q_{95}
- (Right) Percent distributions in q_{95} show high betaN bins (purple and green) have less low q_{95} discharges

On average, IRLMs continually decrease β_N



- (a) β_N tends to decrease between rotating onset and locking
 - Purple – preceded by former locked mode
- (b) Disruptive IRLMs decrease β_N by up to 80%
- (c) Non-disruptive IRLMs decrease β_N less

IRLMs cause the current profile to become more peaked



- On average, disruptive IRLMs increase I_i more
- q_{95} fixed via feedback, therefore I_i/q_{95} increases
- Classical stability (Δ') is a sensitive function of current profile

*Mode end here is 100 ms prior to mode termination

I_i/q_{95} might be related to the potential energy to drive nonlinear tearing growth

Assuming dj/dr monotonically decreasing, and q monotonically increasing, potential energy can be expressed as follows [Sykes PRL 80],

$$\delta W = - \int_0^{r_{q2-w/2}} \left| \frac{dj/dr}{(2-q)B_\theta} B_r^2 r \right| dr + \int_{r_{q2+w/2}}^a \left| \frac{dj/dr}{(2-q)B_\theta} B_r^2 r \right| dr$$

- Recall $I_i/q_{95} \approx \alpha \rho_{q2} + c$, and therefore I_i/q_{95} determine limits of integration
- As I_i determines profile peaking, and $q_{95} \sim 1/I_p$, dj/dr is expected to depend on I_i/q_{95}

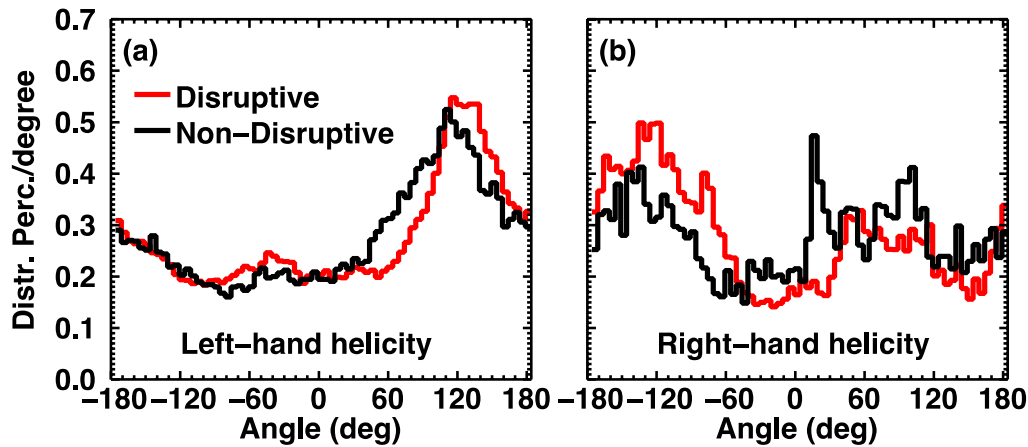
d_{edge} might be related to the physics of the thermal quench; other works that have also observed this...

- Experimental results from Compass-C find locked mode disruptions occur when inequality that is similar to d_{edge} is satisfied [*Hender NF 92*]

$$w/(a - r_{q2}) > 0.7$$

- Massive gas injection simulations using NIMROD find the thermal quench is triggered when $m/n=2/1$ island intersects the radiating edge [*Izzo NF 06*]
- Stochastic layer exists inside the unperturbed LCFS [*Evans PoP 02, Izzo NF 08*], which could stochastize the $m/n=2/1$ island when d_{edge} sufficiently small

For a given field helicity, IRLMs tend to rest at certain phases, suggesting the existence of residual error fields (EF)



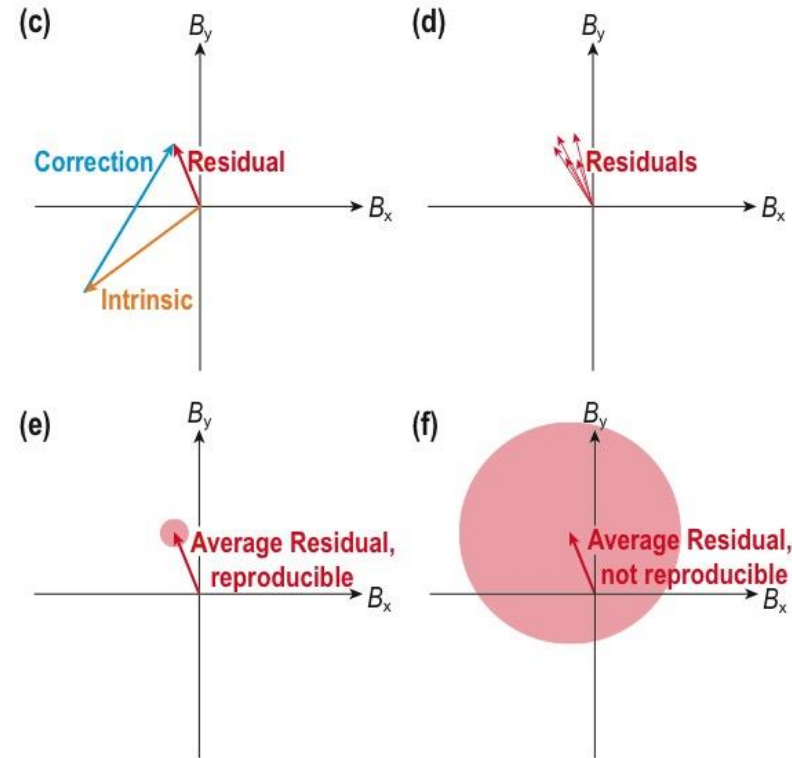
(a) Strong $n=1$ distribution

(b) Both $n=1$, and apparent $n=2$ components. Might be due to over/under correction of intrinsic EF

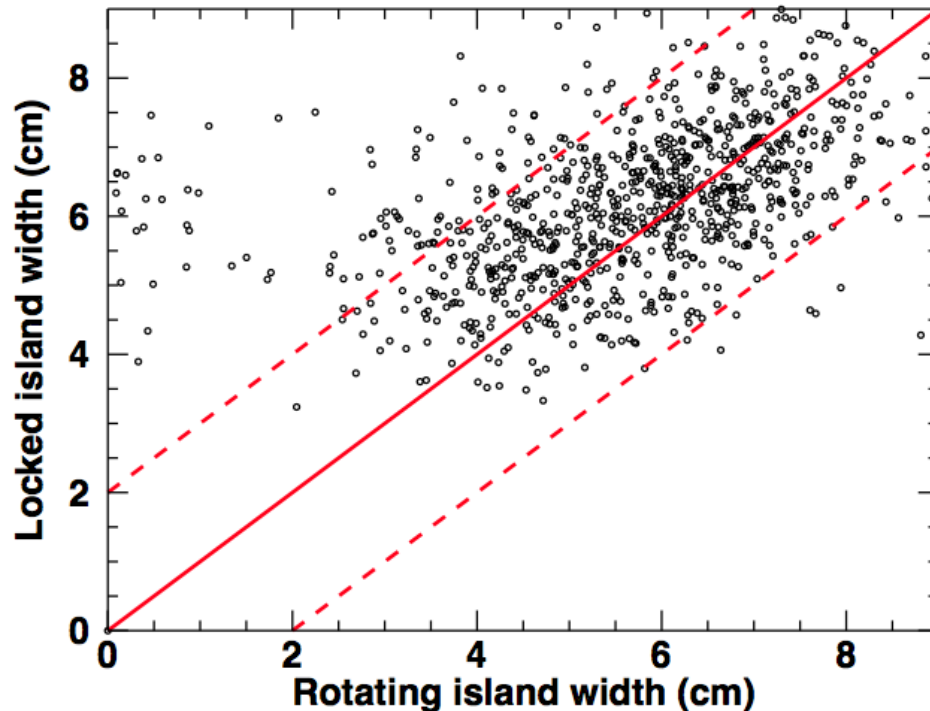
(c) Residual EFs result from imperfect correction

(d) Residual varies as intrinsic and correction vary

(e,f) Narrow or broad distributions result from variance in residual



From rotation at 2 kHz to 50 ms post locking, the island width usually does not change within error



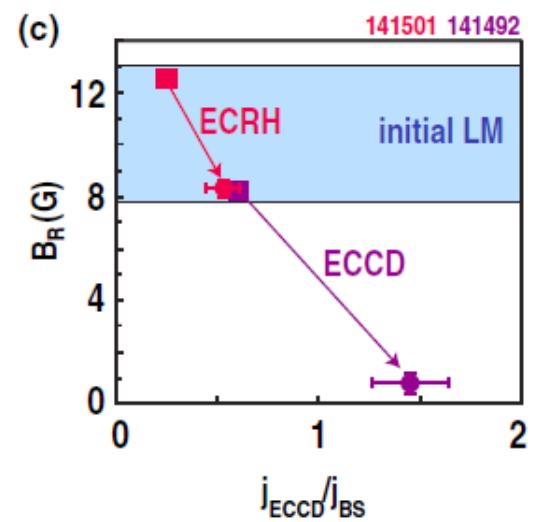
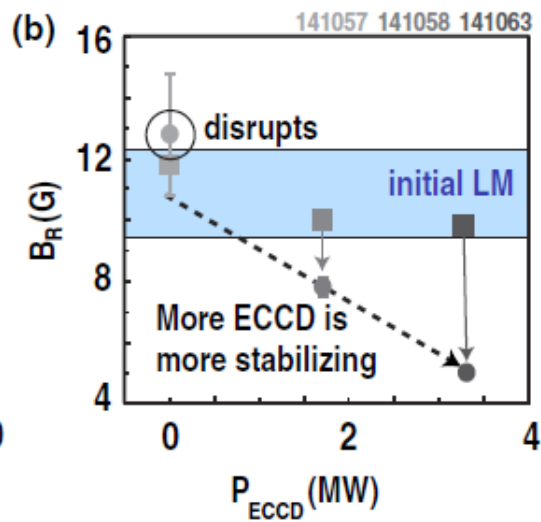
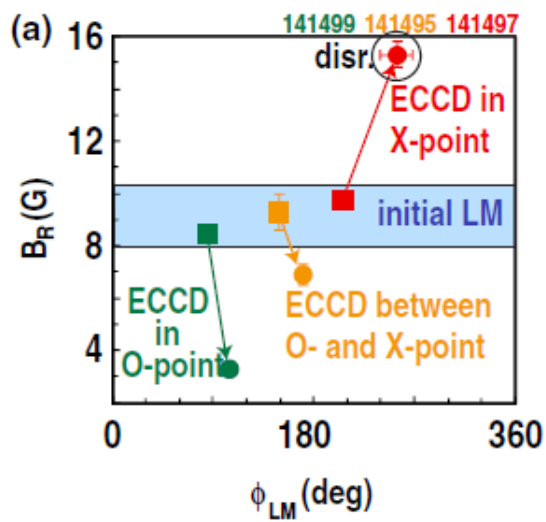
- Island widths not validated to better than ± 2 cm (conservative error bar)
- ~30 small rotating islands grow significantly

Other effects of disruptive locked modes

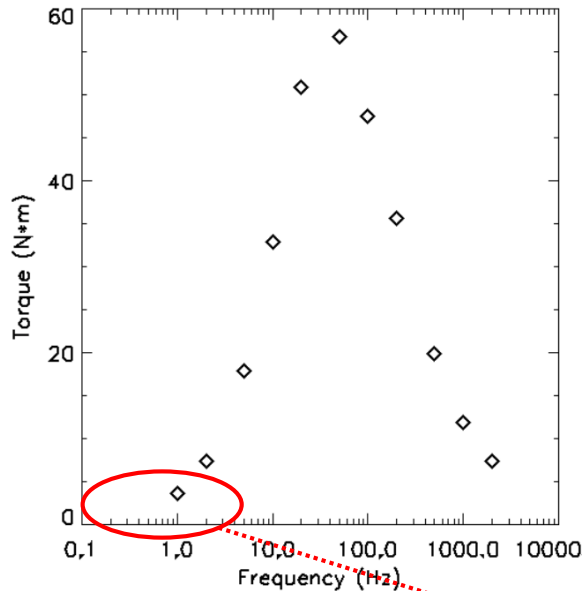
- ρ_{q2} increases
- I_i increases more than for non-disruptive modes
- β_N decreases more than for non-disruptive modes

Back-up Slides 2

on Magnetic Control of LMs +ECCD at DIII-D



Slowly accelerated LM always in torque balance. Unknown **EF torque** inferred from others, if known.



Calculated wall torque
 $\tau_w = 3\text{ms}$

No other NTM

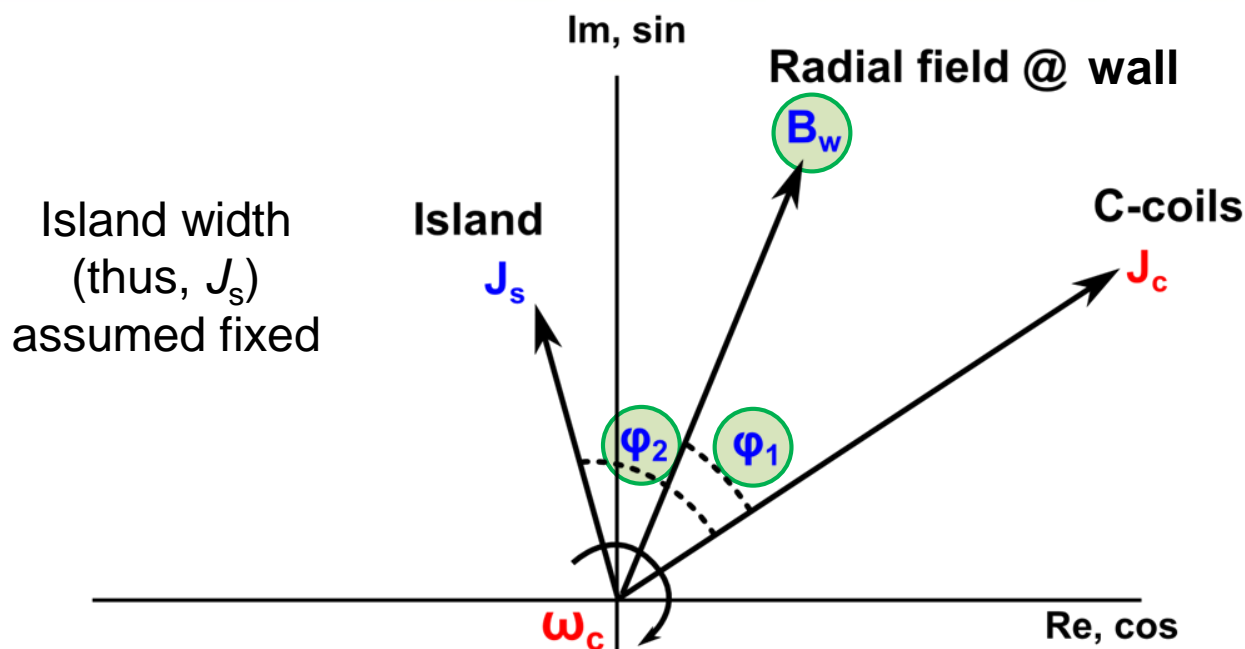
Balanced injection,
Low rotation

$$\cancel{I\dot{\phi}} = T_{EF} + T_{MP} + \cancel{T_{wall}} + \cancel{T_{NTM}} + \cancel{T_{NBI}} + \cancel{T_{disc}}$$

$$0 = T_{EF} + T_{MP}$$

Rotating RMP and static EFC
from I-coils and C-coils

Island dynamics (including entrainment stability) modeled by 3 differential equations in 3 unknowns



Island width
(thus, J_s)
assumed fixed

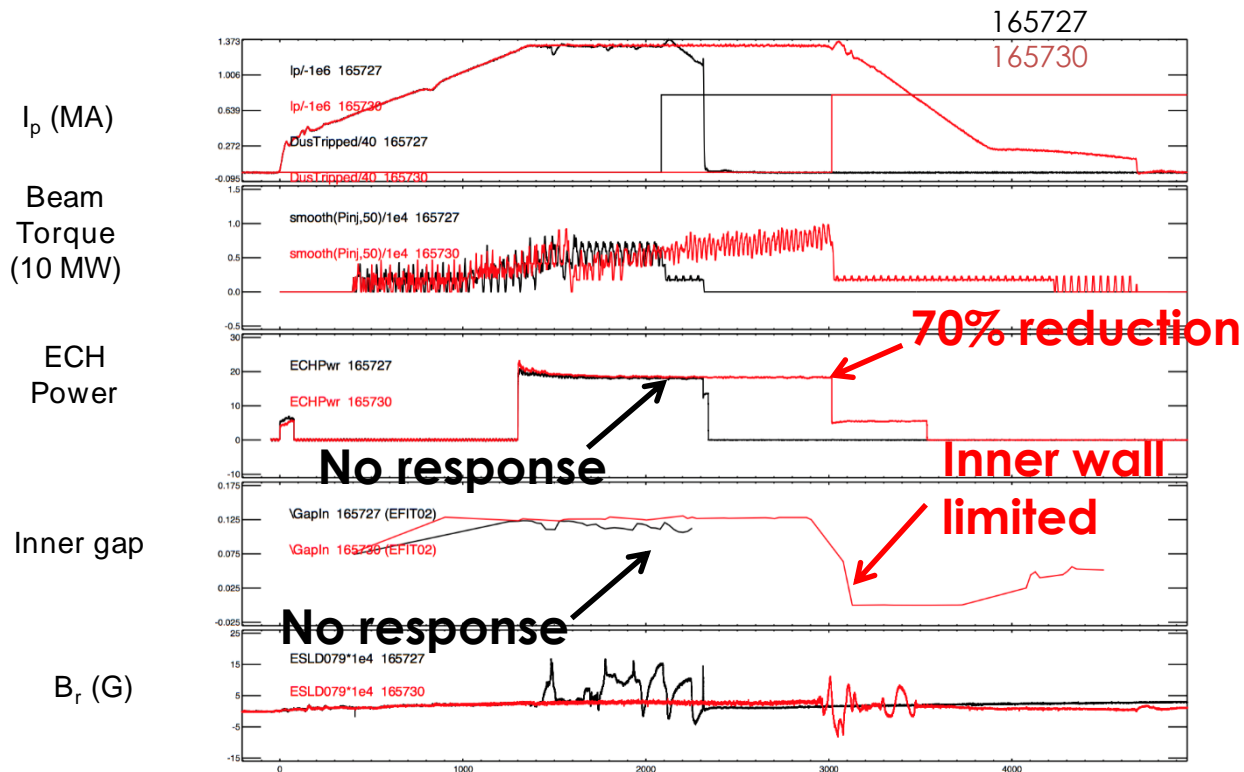
Synchronous frame
(co-moving with J_c)

$$\begin{aligned} \tau \dot{B}_w &= -B_w + \alpha_s J_s \cos(\varphi_2 - \varphi_1) + \alpha_c J_c \cos(\varphi_1) \\ \tau B_w \dot{\varphi}_1 &= -\tau B_w \omega_c + \alpha_s J_s \sin(\varphi_2 - \varphi_1) - \alpha_c J_c \sin(\varphi_1) \\ \ddot{\varphi}_2 &= -n\beta_1 \gamma_1 B_w J_s \sin(\varphi_2 - \varphi_1) \end{aligned}$$

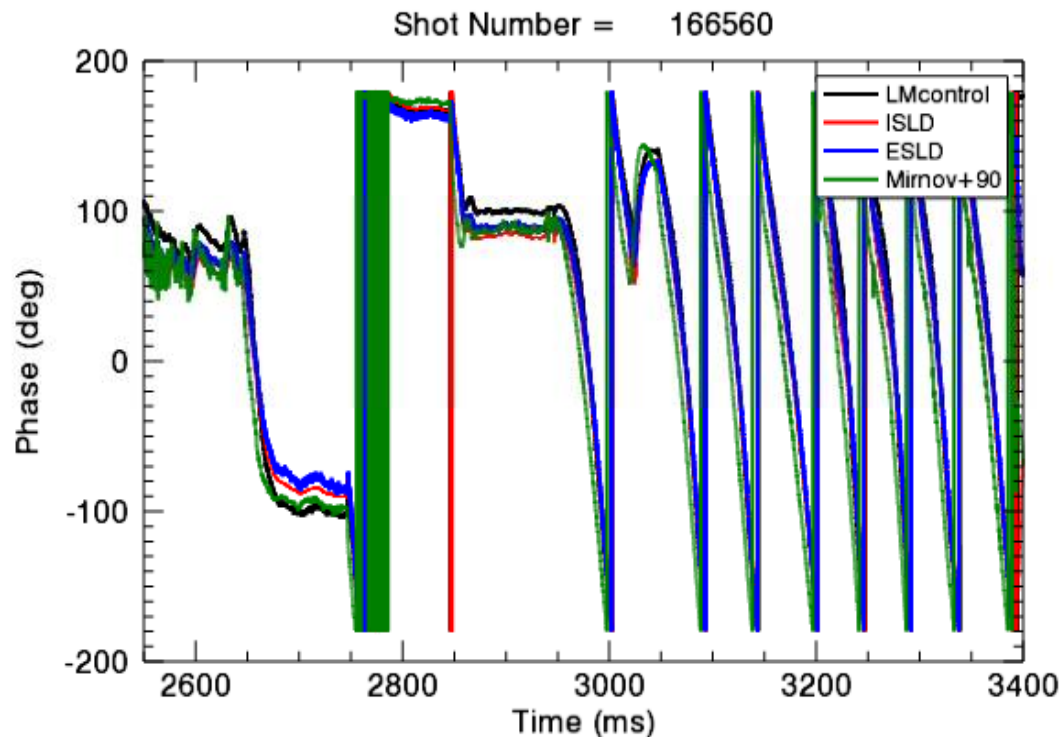
- (i) Find fixed points (torque balance)
- (ii) Evaluate stability of points (i)

Other, non-magnetic locked mode control?

- Drop in power (NBI and ECH), I_p ramp down, and smooth change in shape



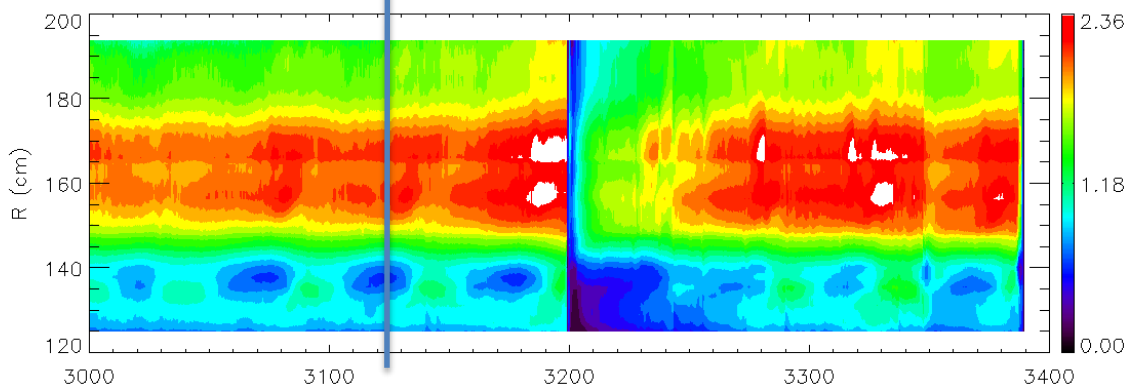
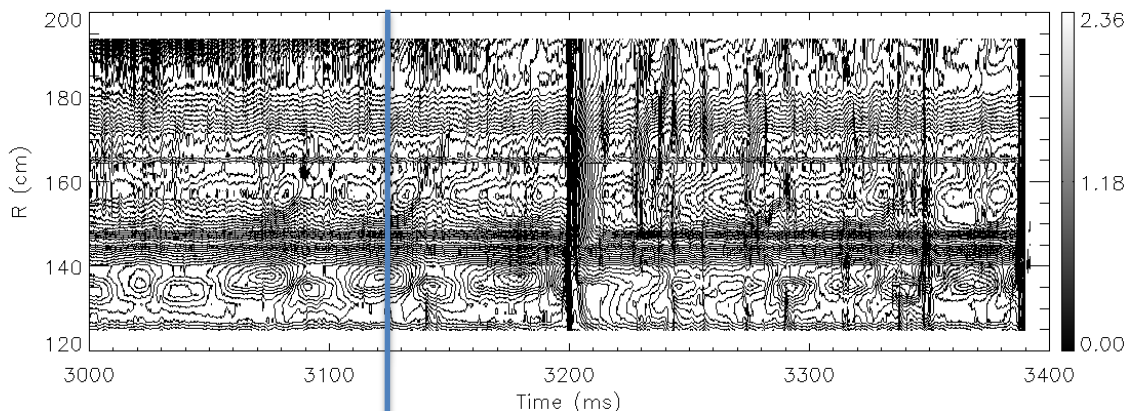
Real time calculations of mode phase from magnetic sensors matches well with post-experiment analysis



- Φ_{LM} defined as max B_R at outboard mid-plane
- Greatest angular difference $\sim 25^\circ$
- Post analysis done with SLContour: toroidal Fourier analysis
 - compensated for I-coils, early baseline 100 ms, no smoothing

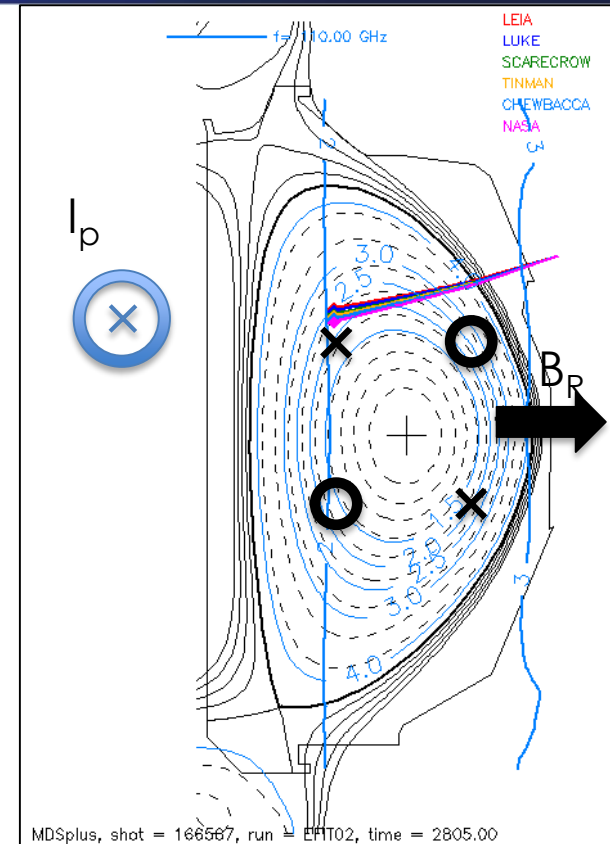
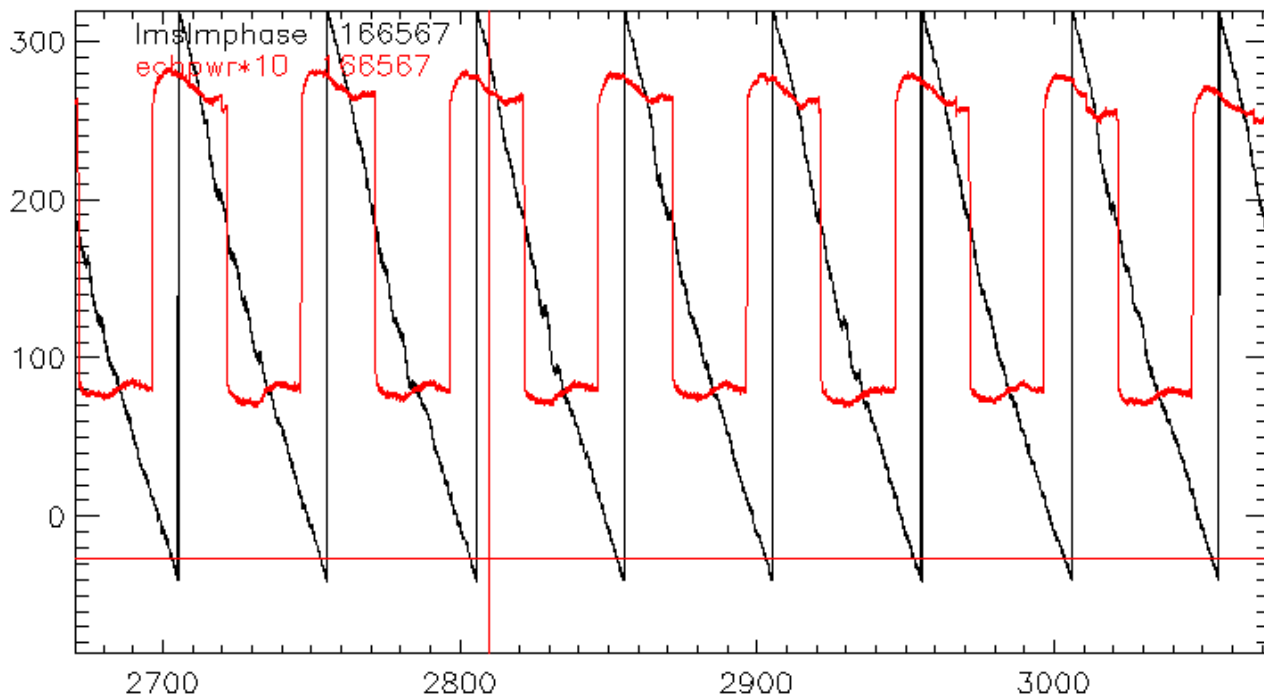
Mode phase calculated from magnetics also matches well with ECE contour

shot 166560



- at 3122 ± 2 ms, O-point at $\Phi = 81^\circ$, $\theta = 180^\circ$
- which expect max B_R at outboard mid-plane to be at -9°
- Imphase at this time is $+8 \pm 10^\circ$
- A lag in measured phase of 22° is expected for mode rotating at 20 Hz

Verifying ECCD deposition timing and location



- at 2810 ms, $\Phi_{LM} = 285^\circ$ (peak B_R at outboard mid-plane)
- at same time, at poloidal angle of 135° , X-point is also at $\sim 285^\circ$
- Toroidal deposition of ECH power is between 251° to 299°
- $\Phi_{LM} = \Phi_{ECCD}$ implies X-point deposition

Improvements to controller

- **Better control needs more accurate phase measurement**
 - Real-time AC compensation
- **Low-pass filter output to give realistic commands to power supplies**
 - only affects when shot first duds into control phase
- **Want to entrain at higher frequencies (~100 Hz) to better stabilize mode**
 - extend controller to be able to account for phase shift due to wall shielding
 - requires real-time frequency calculation
- **Want smoother entrainment**
 - Feed-back on frequency, instead of phase
 - easier control

Back-up Slides 3 on Magnetic Control of LMs in various Devices

WG-11 tests robustness of magnetic control of LMs in different devices, for different coil geometries → Extrapolation to ITER

Table 1. Geometry of devices considered and their control coils.

| | AUG | DIII-D | EXTRAP-T2R | JET | J-TEXT | KSTAR | LHD | MAST | NSTX |
|-------------------------------|------|--------|------------|------|---------|-------|------|------|------|
| <i>Coil geometry:</i> | | | | | | | | | |
| No.internal coils (pol.×tor.) | 3×8 | 2×6 | none | none | 3×4 | 3×4 | none | 2×6 | none |
| No.turns per internal coil | | 1 | - | - | 1 | 2 | - | | - |
| No.external coils (pol.×tor.) | none | 1×6 | 4×32 | 1×4 | 1×2+1×3 | none | 2×10 | 1×4 | 1×6 |
| No.turns per external coil | - | 4 | 40 | 16 | 1 | - | | | 2 |
| <i>Device:</i> | | | | | | | | | |
| Major radius R (m) | 1.65 | 1.66 | 1.24 | 2.96 | 1.05 | 1.8 | 3.9 | 0.85 | 0.86 |
| Aspect ratio A | 3.3 | 2.5 | 6.7 | 2.96 | 3.96 | 3.6 | 8.3 | 1.3 | 1.3 |
| Elongation κ | | | 1 | | 1 | | | | |

- **Internal/external coils**
- **Angularly narrow/broad coils**
- **Dense/sparse arrays of coils**
- **Partial/full toroidal/poloidal coverage**
- **Different sizes, aspect ratios, elongations**

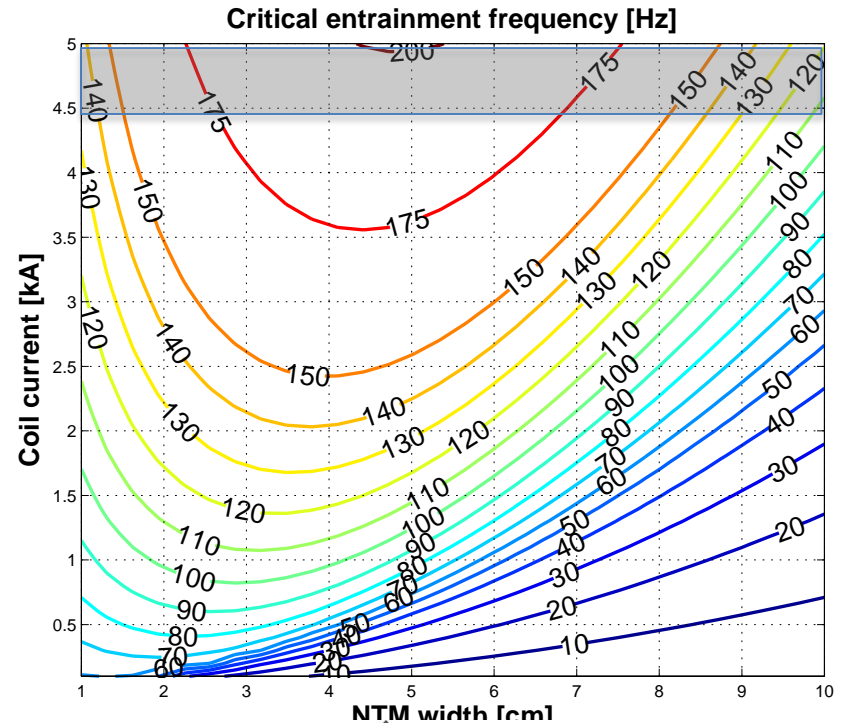
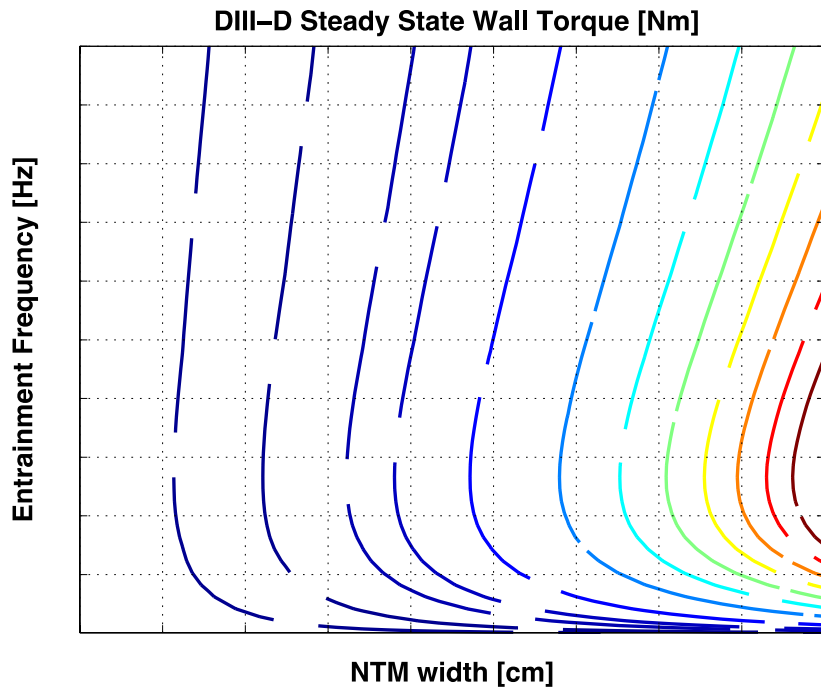
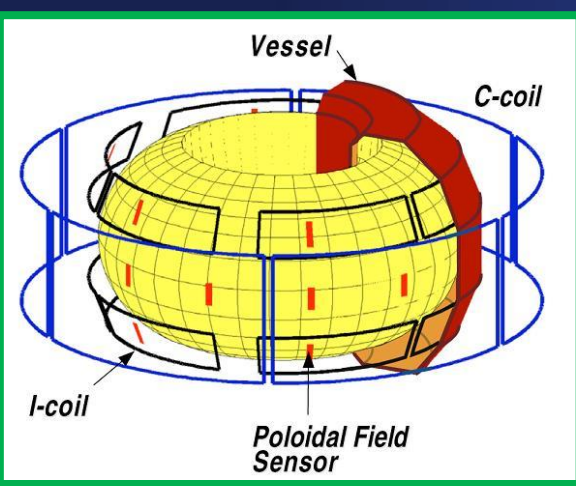
Electrical engineering and physics are also different and will improve our understanding and predictive capabilities

| | AUG | DIII-D | EXTRAP-T2R | JET | J-TEXT | KSTAR | LHD | MAST | NSTX |
|---|-----|-----------------------|------------|-----|-----------------------|-------|------|------|------|
| <i>Power supply limits:</i> | | | | | | | | | |
| Max coil current I (kA) | 1.2 | 4.5 (SPA) 1.5 (AA) | 0.02 | 6 | 6 (int.) 8 (ext.) | 5 | 1.92 | | 3.3 |
| Max B_r (G) at plasma edge | | | 30 | | | 22 | | | 61 |
| Max frequency f (kHz) | | 1 | | | 6 (int.) dc (ext.) | 0.01 | | | 7 |
| <i>Other frequency limits</i> | | | | | | | | | |
| Coil inductance limit (kHz) | | | | | 10 | | | | |
| Wall shielding limit (kHz) | | | 0.25-0.5 | | | | | | |
| <i>Typical $n=1$ EFC settings:</i> | | | | | | | | | |
| Amplitude (kA) | 0 | | 0.02-0.04 | | | 0 | 0.1 | | |
| Tor. phase ϕ (deg) | - | | | | | - | -126 | | 300 |
| Estimated intrinsic EF (G) | | | 1-5 | | | | 6 | | <6 |
| Max B_T (T) on axis | 3.1 | 2 | 0.2 | 3.4 | 2.2 | 3.5 | 3 | 0.55 | 0.45 |
| τ_W (ms) | | 2.5-3 | 10 | | 3.1 | 20 | 15 | | 5 |

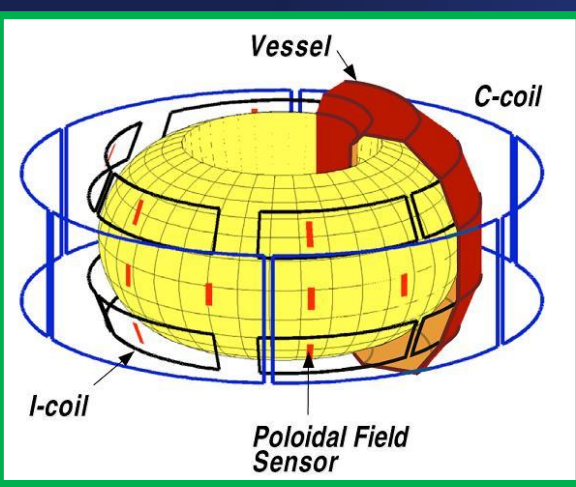
- **Rapidly/slowly varying or rotating MPs**
- **Strong/weak Magnetic Perturbations (MPs). Requirement: $MP \geq EF$**
- **Different τ_W**
- **KSTAR has very small EF**
- **Disturbance in LHD is interchange mode, not NTM**

RMPs in DIII-D can entrain >100 Hz

- coils: using 1x6 external coils (C-coils)
- major radius: 1.72 m
- wall time: 3 ms
- density: $2.2 \times 10^{19} \text{ m}^{-3}$
- B_{\parallel} : 1.86 T

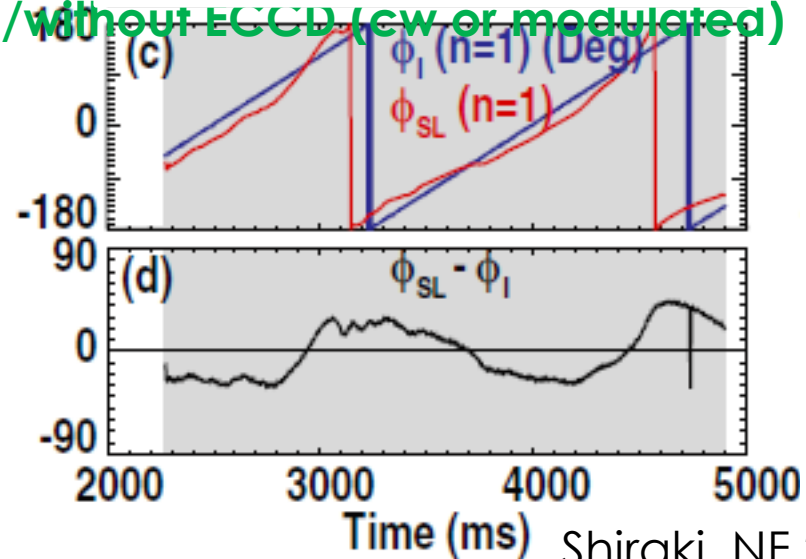
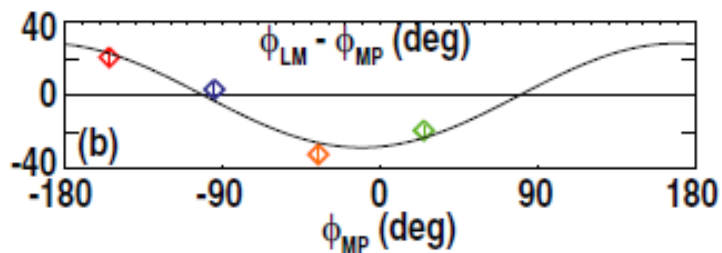
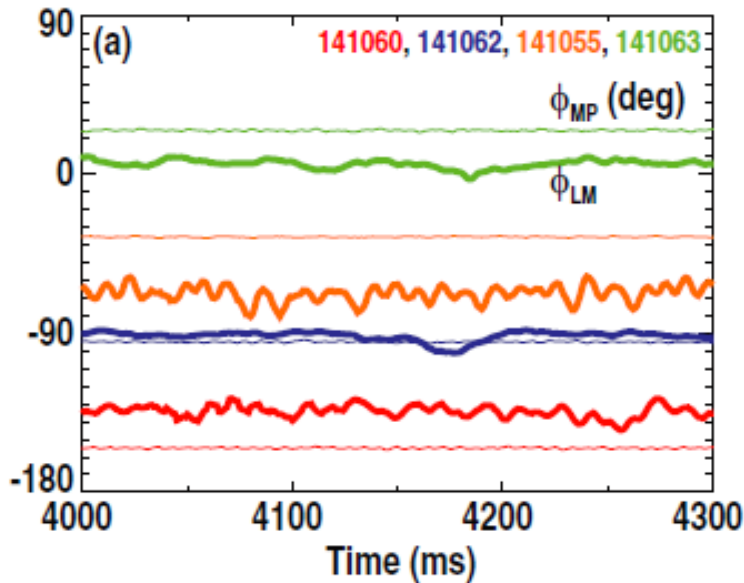


DIII-D (2x6 internal + 1x6 ext. coils)



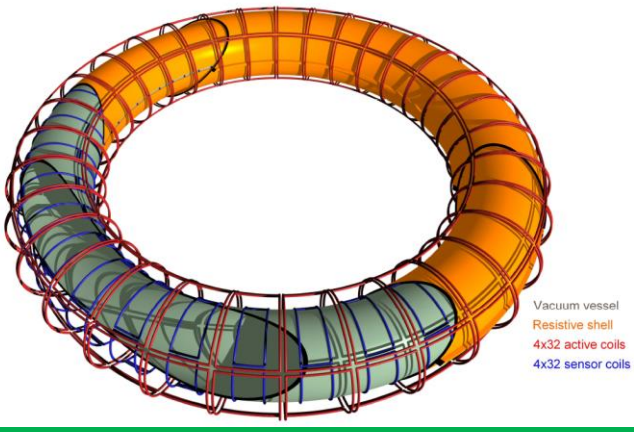
Locked mode phase is controlled at DIII-D for ECCD stabilization & EFC studies.

- On LM with/without rot. precursor
- Int./Ext. coils
- Static/rotating MPs (up to 300 Hz)
- Preprogrammed/feedback
- With/without ECCD (cw or modulated)



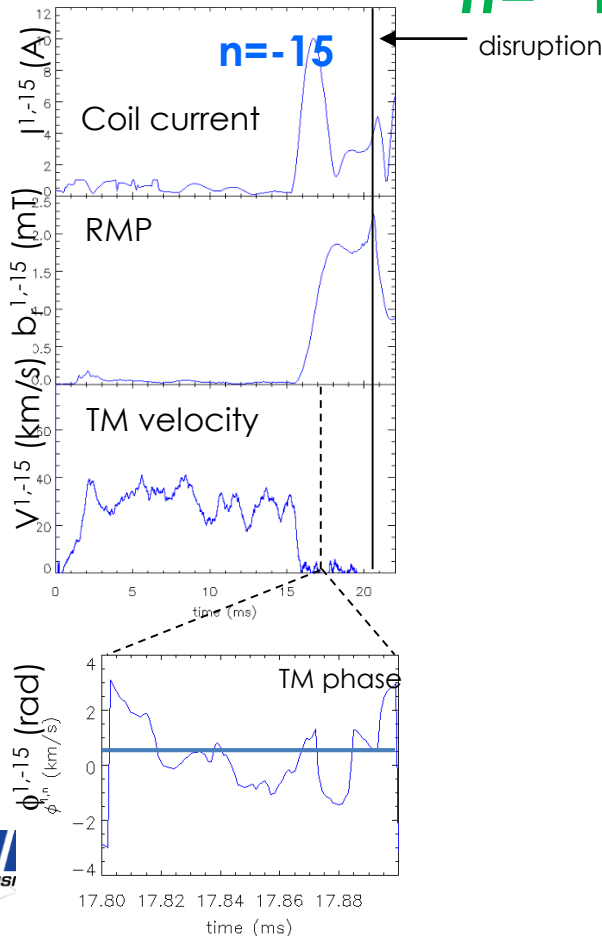
Shiraki, NF 2014
 Strait, NF 2014
 Volpe, PoP 2009

EXTRAP-T2R (4x32 external coils)

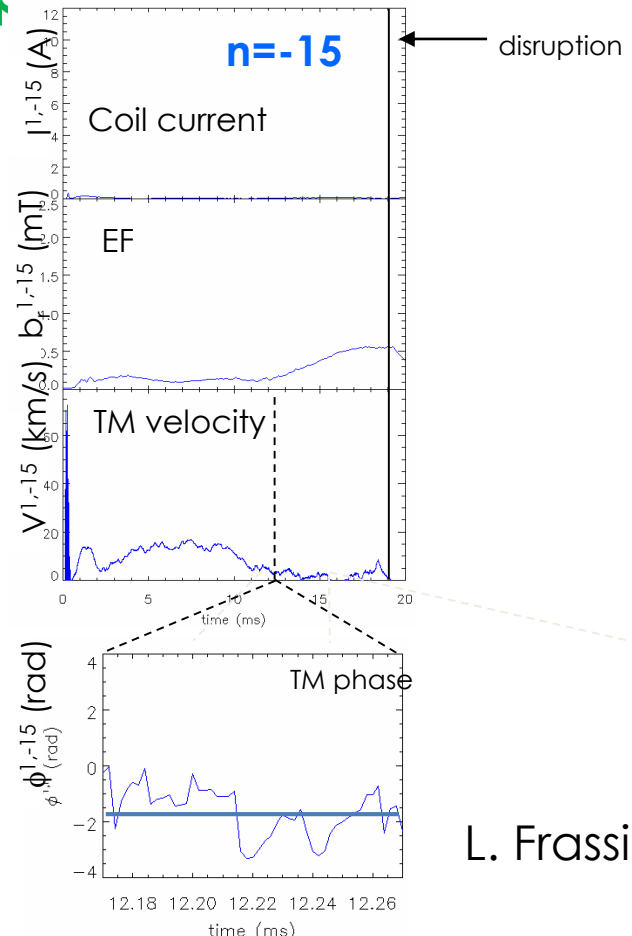


$n = -15$ TM locks with different phases if $n = -15$ RMP is applied, with $\phi_{RMP} = 0^\circ$ (left) or only intrinsic $n = -15$ EF is present (right)

shot 24776

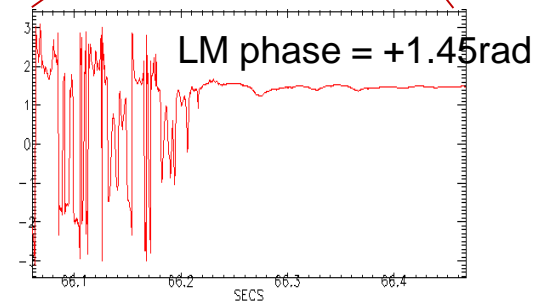
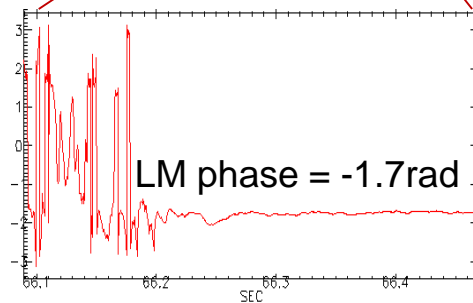
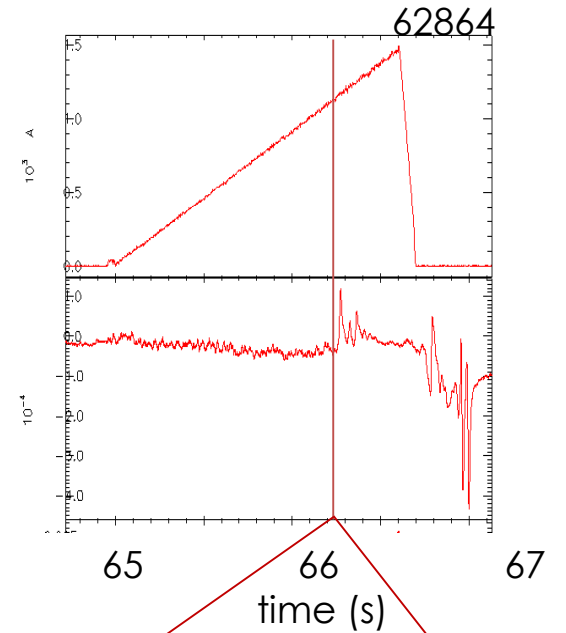
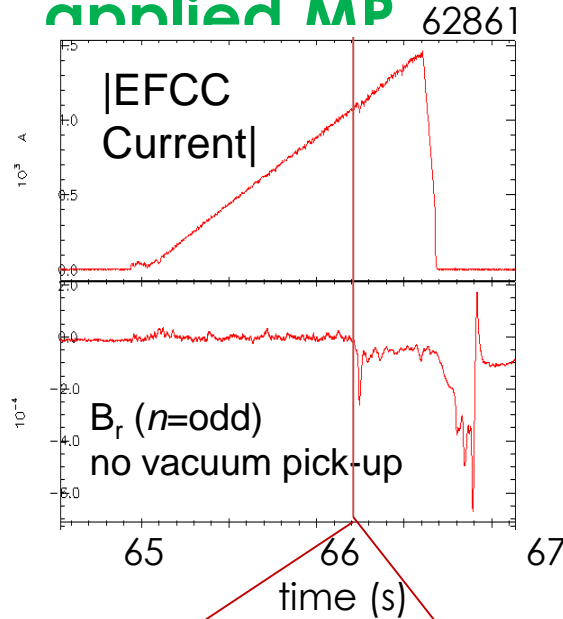


shot 21604



JET (1x4 external coils)

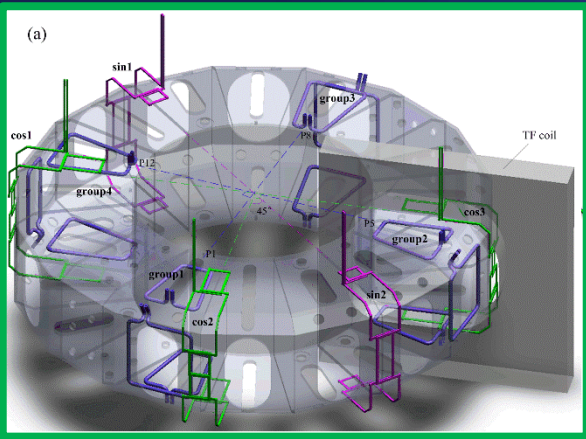
Error-field penetration Locked Modes form at phase of strong applied MP



T. Hender

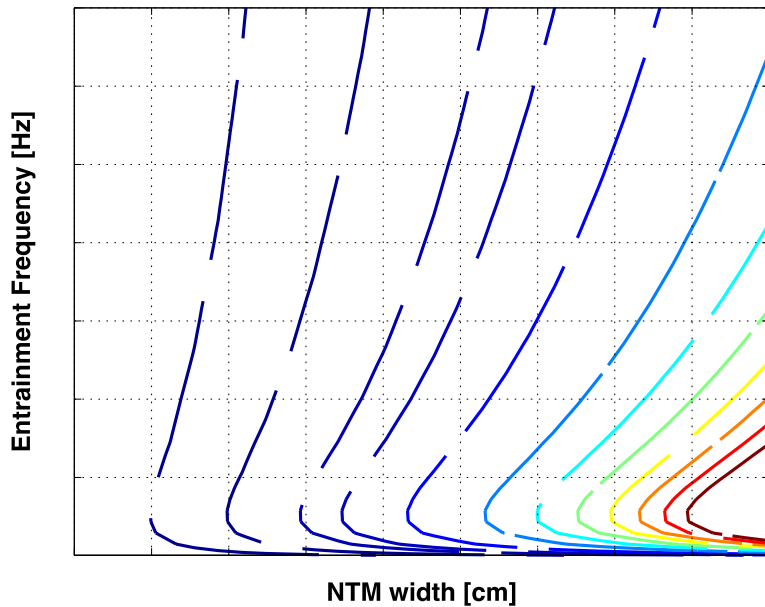


J-TEXT internal coils expected to entrain 2/1 modes at >600 Hz

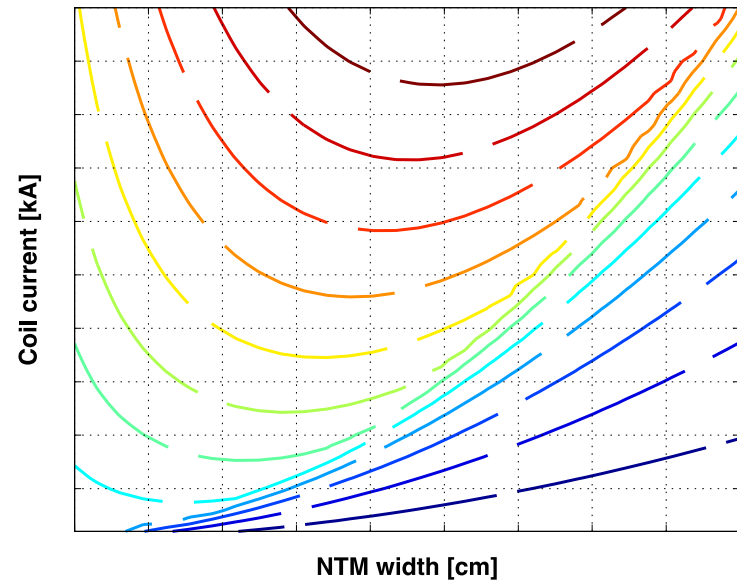


- 3 sets of 4 internal coils treated as one set
- external coils ignored: DC only
- major radius: 1.05 m
- wall time: 3.1 ms
- density: $1 \times 10^{20} \text{ m}^{-3}$
- **B.: 3.5 T**

J-TEXT Steady State Wall Torque [Nm]



J-TEXT Critical entrainment frequency [Hz]



slightly smaller wall torque, higher entrainment frequency

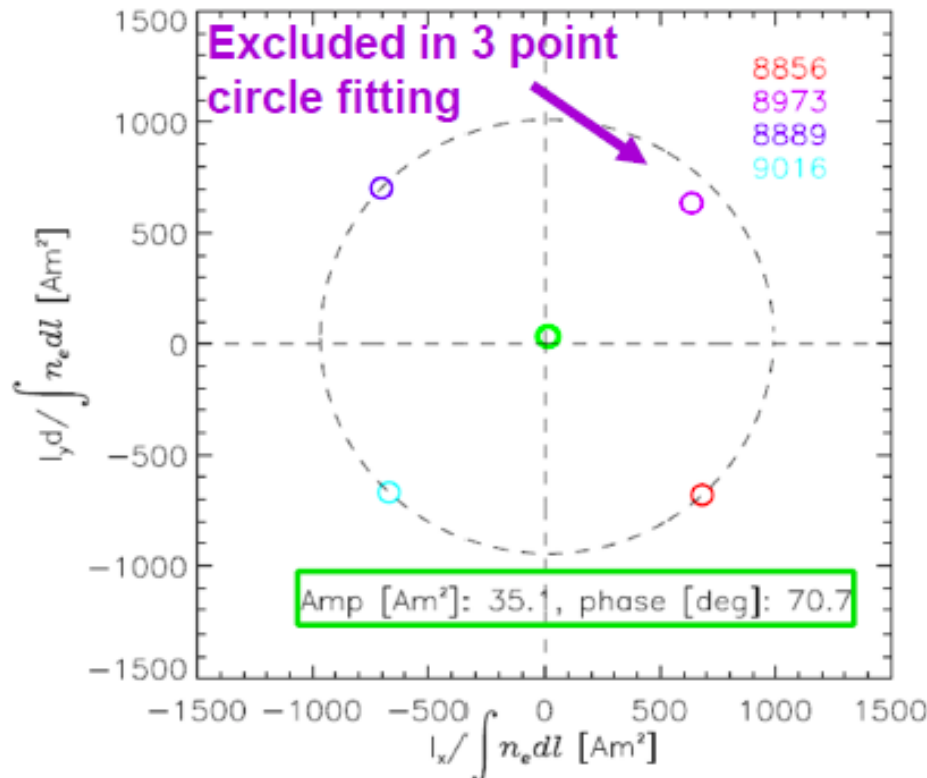
KSTAR (3x4 internal coils)

Rotating NTMs rarely observed to lock.

Ascribed to very small EF and wall

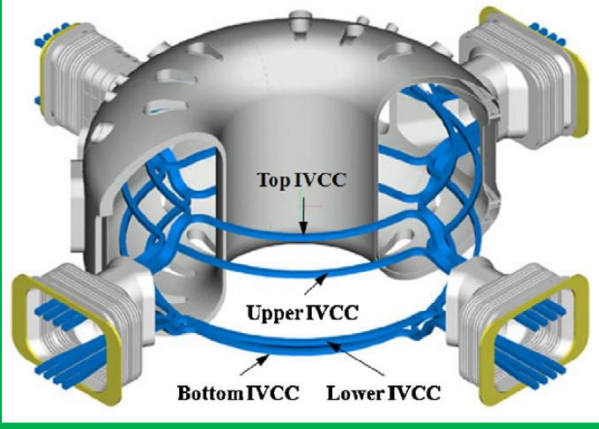
Error Field Compass Scan
with MID-RMP coils only
(density normalized)

plied



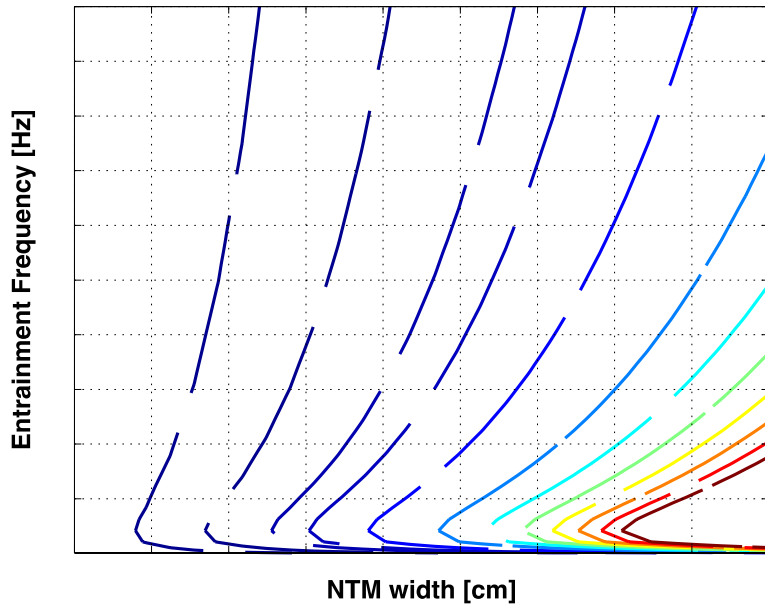
Y. In

KSTAR 2/1 mode – still needs work

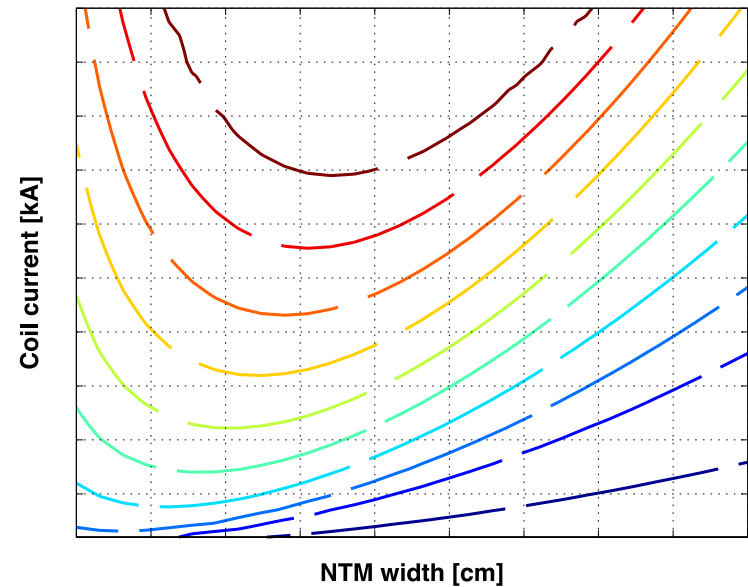


- coils: internal 3 sets (upper, mid-plane, lower) of 4 coils
- major radius: 1.8 m
- wall time: 20 ms
- density: $1 \times 10^{20} \text{ m}^{-3}$
- B_z : 3.5 T

K-STAR Steady State Wall Torque [Nm]

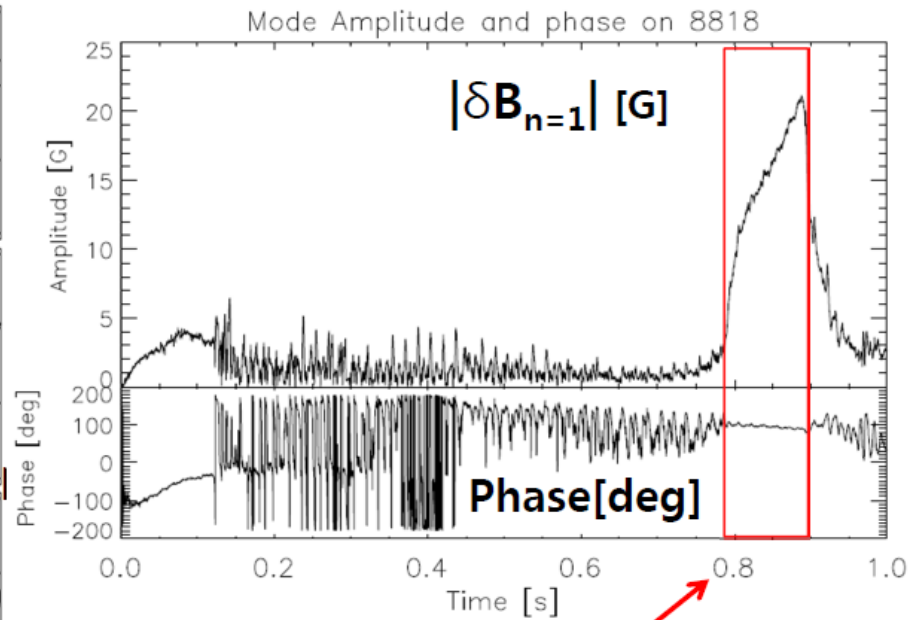
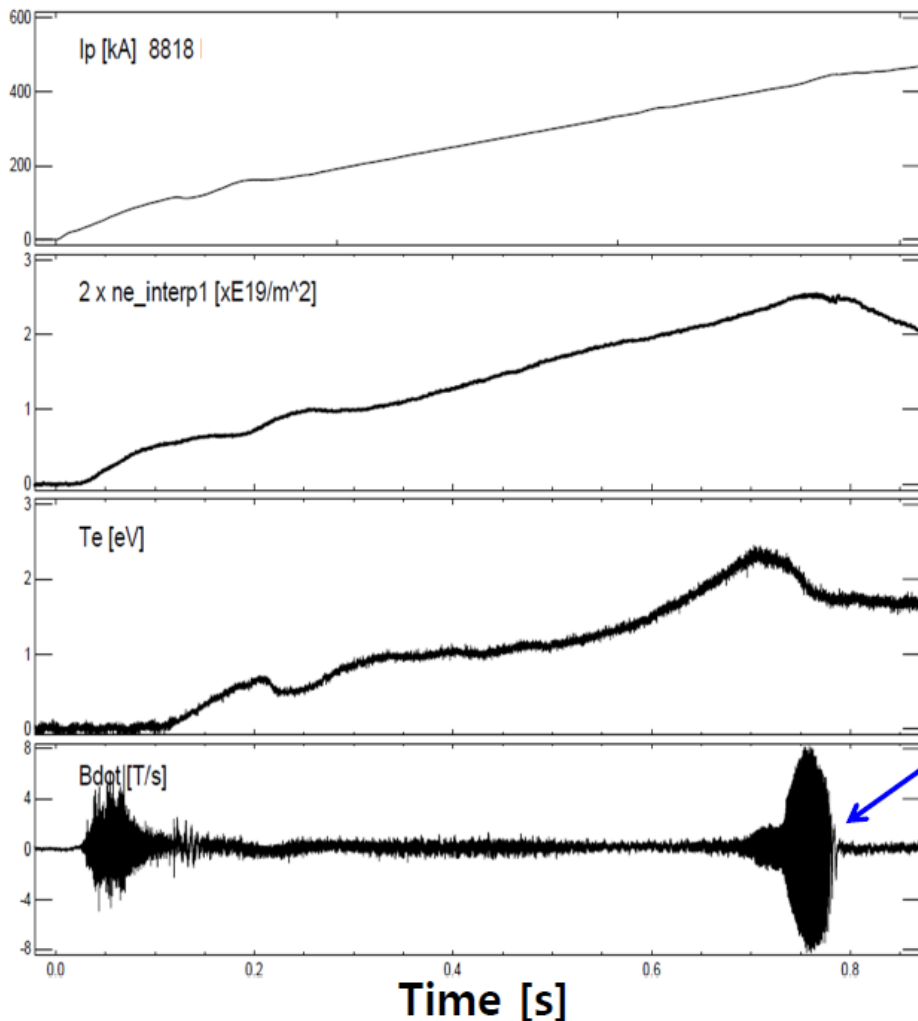


K-STAR Critical entrainment frequency [Hz]



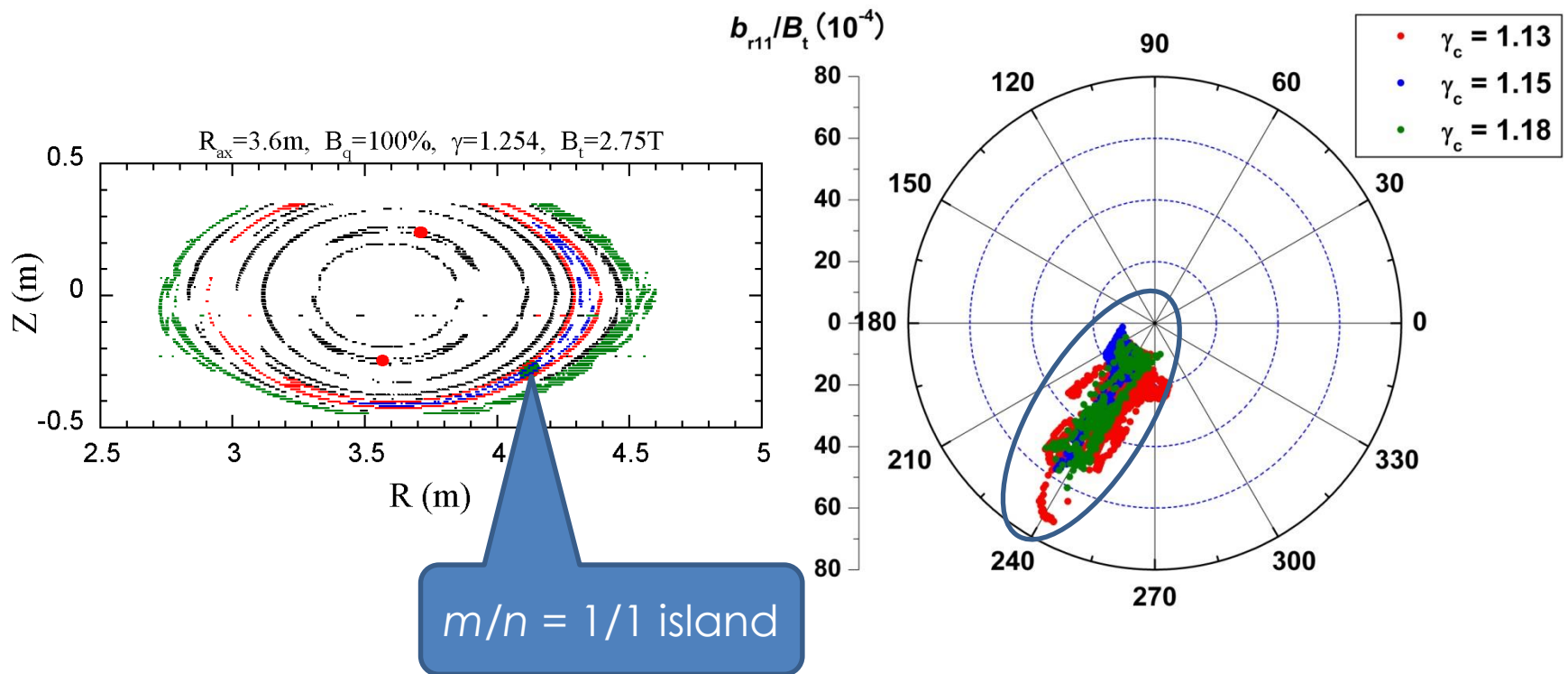
Wall torque peaks at lower frequency

A locked mode in KSTAR is not frequently observed, likely thanks to a very low intrinsic error field



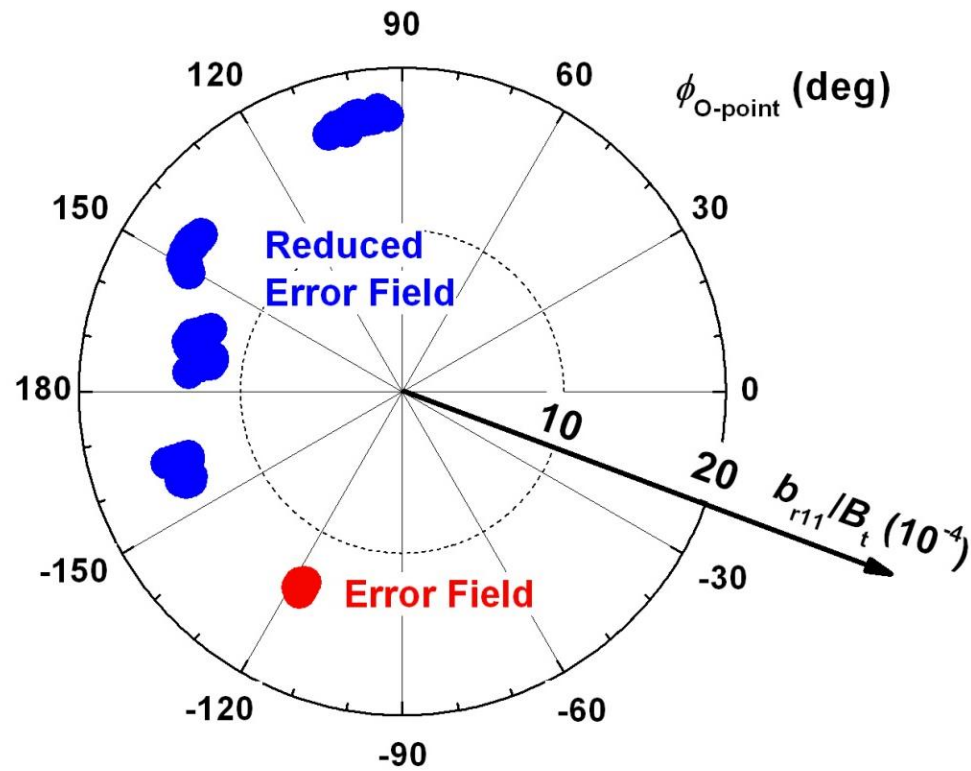
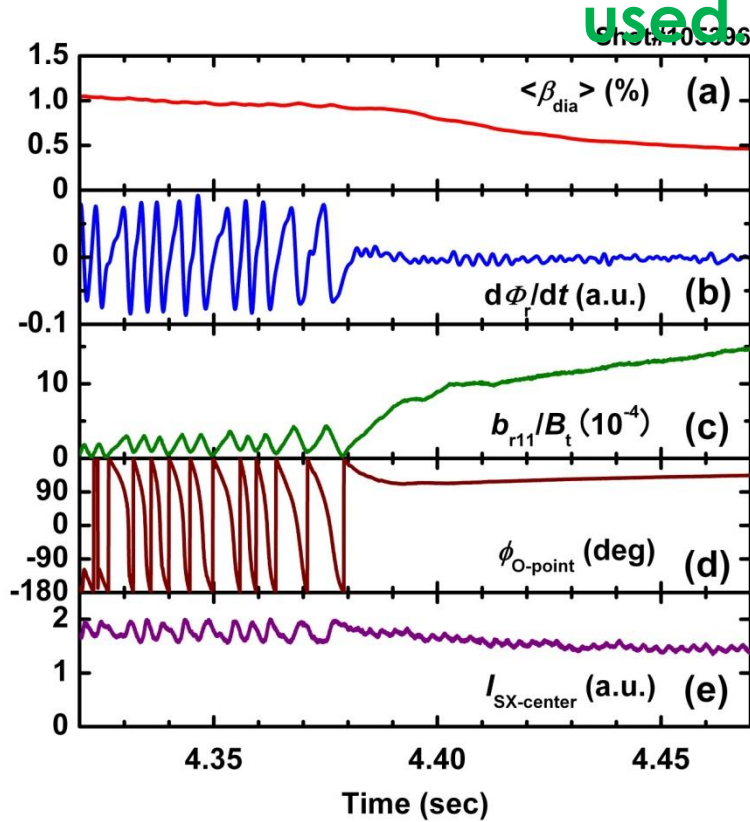
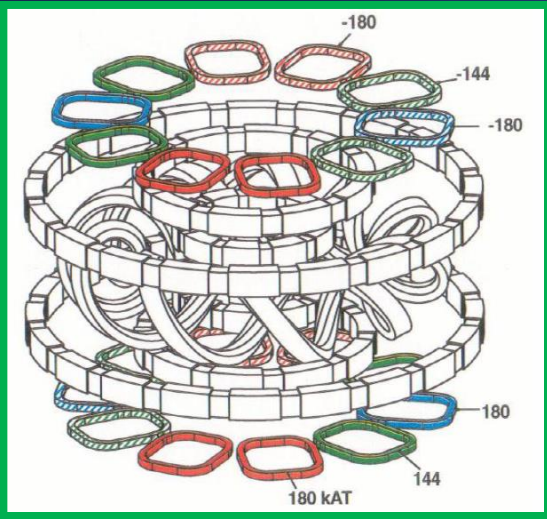
- **Rotating mode** leads to a **locked mode** near $t=0.8$ sec, which is one of the rare events in KSTAR
- AC power supply to be installed from 2015

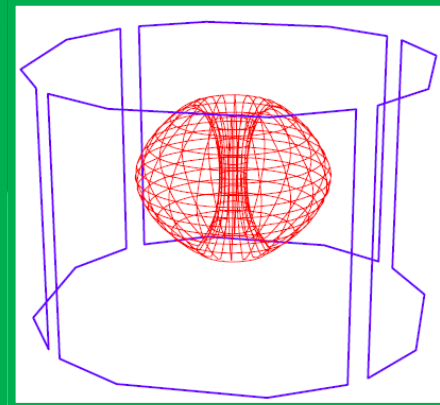
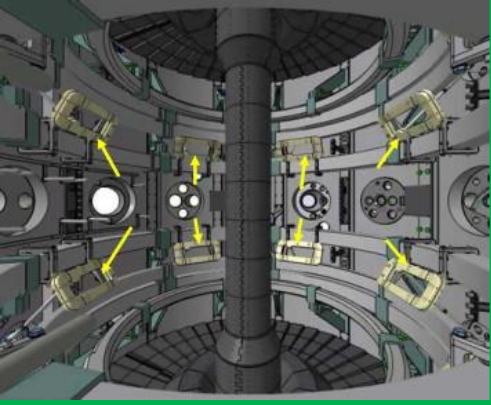
LHD detected $n=1$ EF by electron-beam mapping of vacuum flux surfaces



LHD (2x10 external coils)

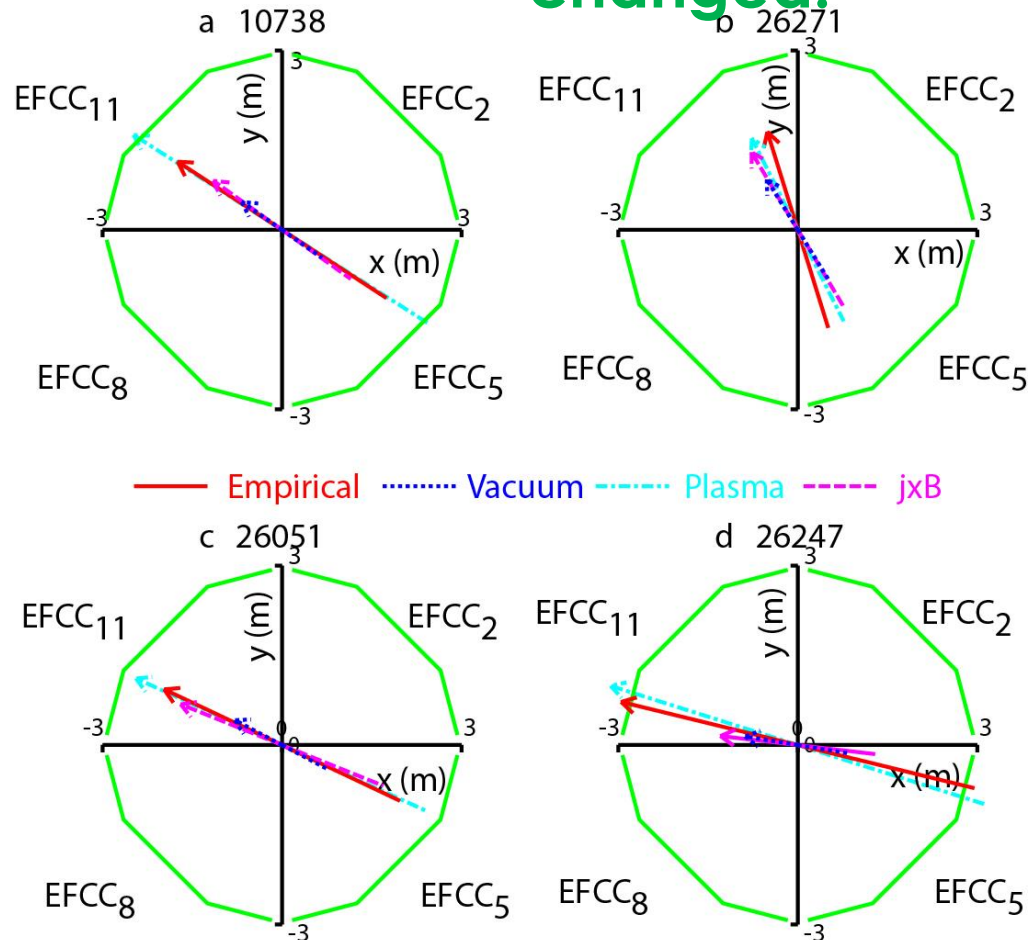
Rotating 1/1 interchange island locks to EF, or to different positions if different EF corrections are used



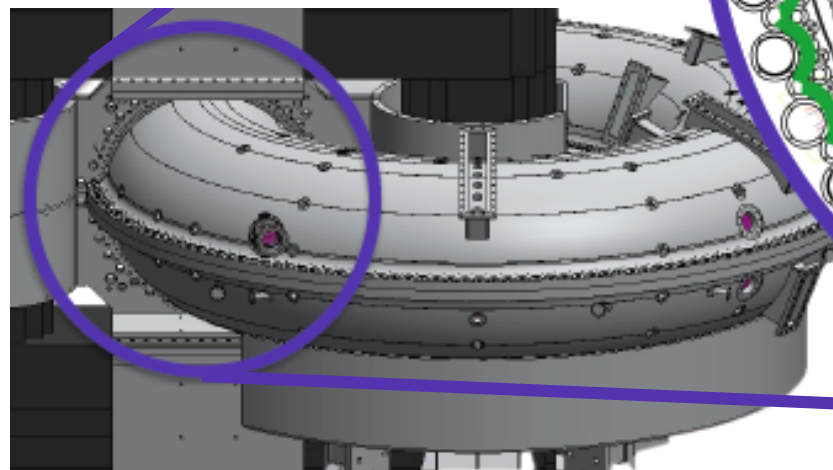
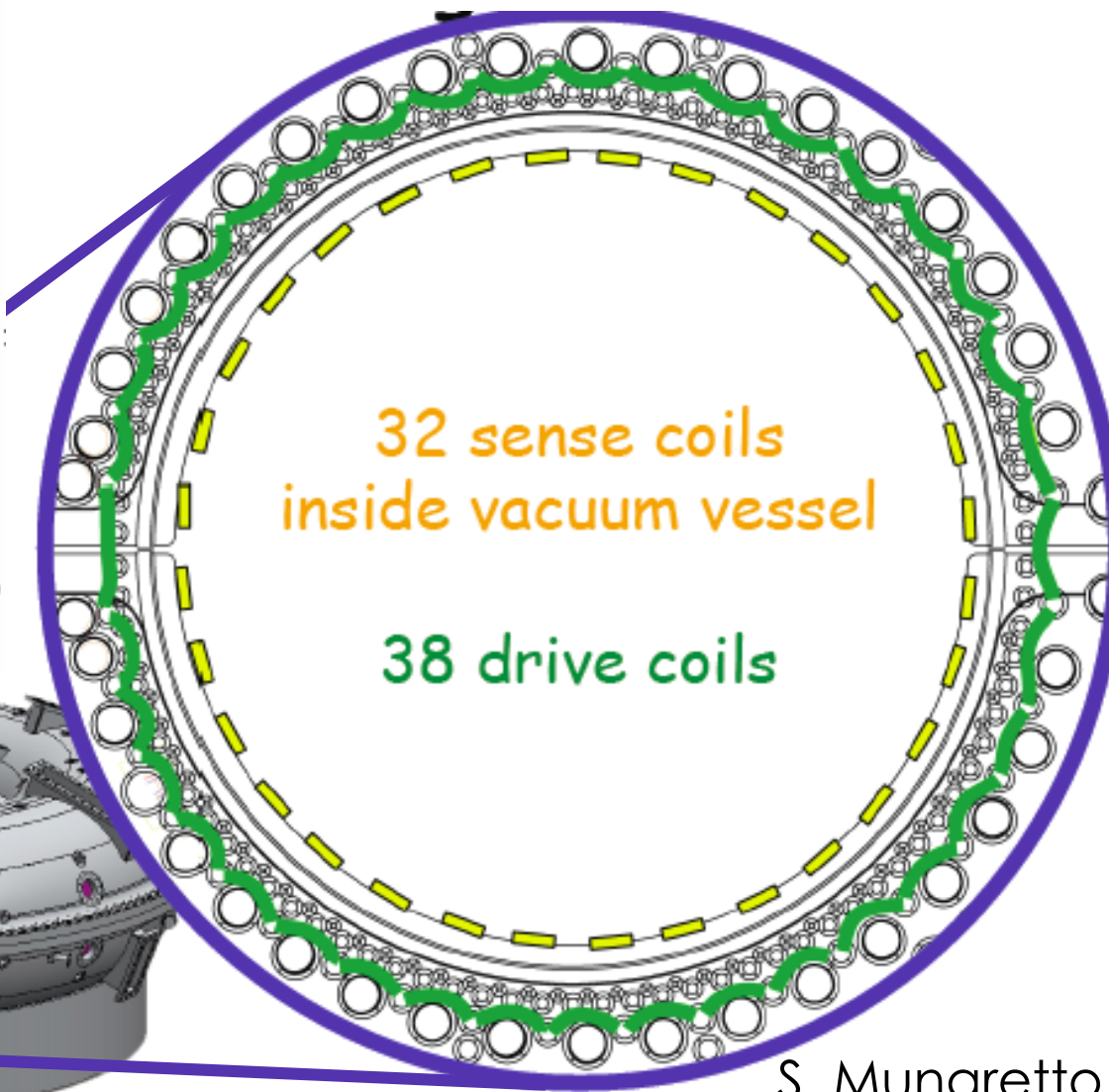
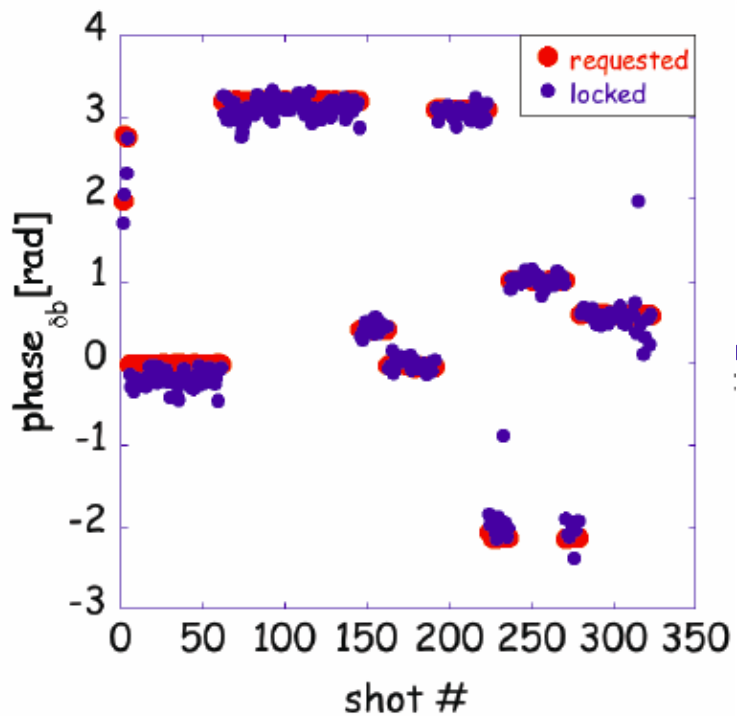


MAST (2x6 internal, 1x4 ext. coils)

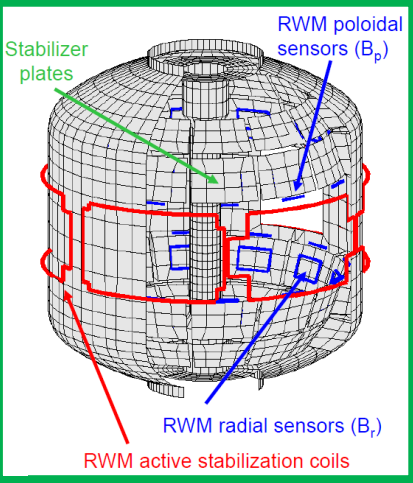
Locked mode phase observed to change when EFC phase is changed.



At MST, 38 external coils align dominant $m=1$, $n=5$ mode (Quasi Single Helicity) to any phase of choice

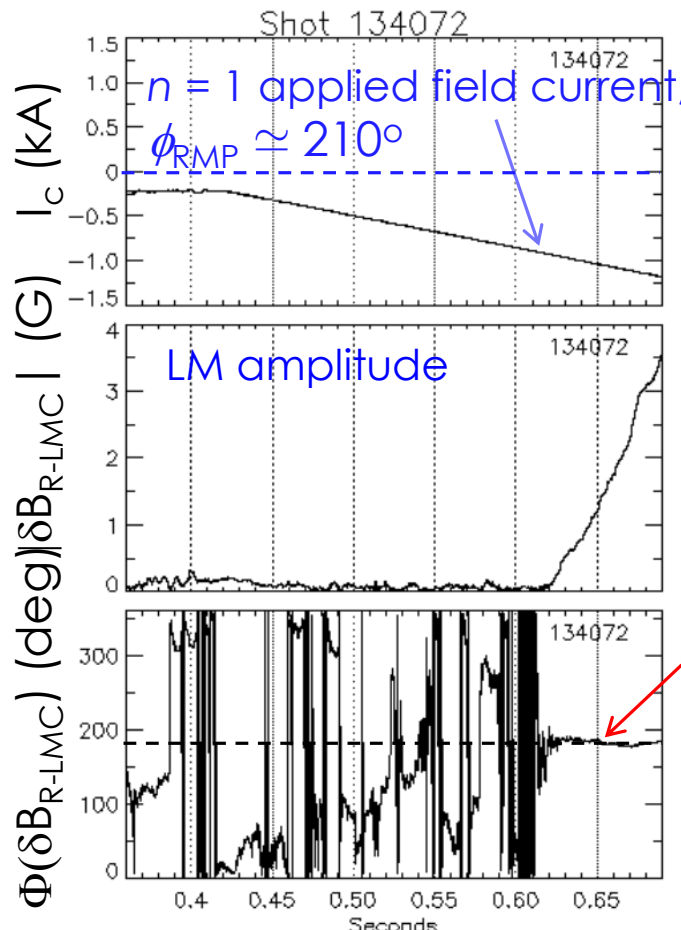
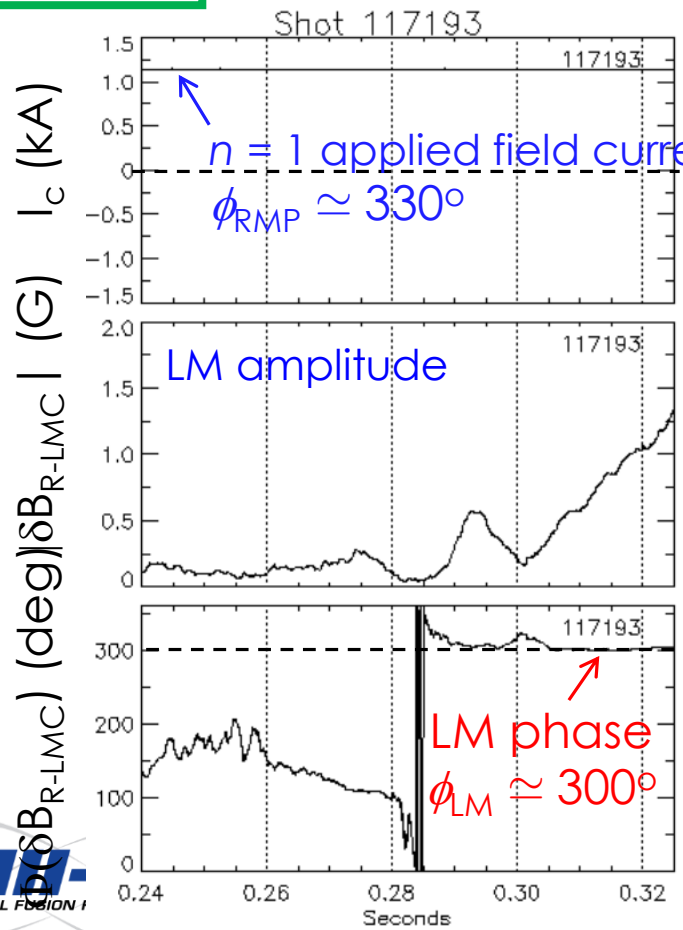


S. Munaretto
See poster PP8.022



NSTX (1x6 external coils)

When $n = 1$ fields are applied with different phases, $n = 1$ modes lock with different phases.



S. Sabbag